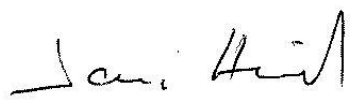




# **OPERATIONS REPORT**

**Issue 1/2024 rev. 3**

**Reporting period: January – June 2024**

Authors			
Prepared by			
NAME		INSTITUTE	
Jari Hovila		FMI	
Contributions			
NAME		INSTITUTE	
Jari Hovila, Jukka Kujanpää, Kaisa Lakkala		FMI	
Axel Schmidt, Matthias Hofmann, Birgit Wunschheim		DLR	
Olaf Tuinder, Robert van Versendaal		KNMI	
Helge Jønch-Sørensen		DMI	
Katerina Garane, MariLiza Koukouli, Konstantinos Michailidis		AUTH	
Jeroen van Gent, José Granville, François Hendrick, Jean-Christopher Lambert, Bavo Langerock, Gaia Pinardi, Tijl Verhoelst		BIRA-IASB	
Andy Delcloo		KMI	
Peggy Tesche-Achtert		DWD	
Anne Boynard, Cathy Clerbaux, Maya George, Camille Viatte		LATMOS	
Rosa Astoreca, Pierre-François Coheur, Daniel Hurtmans, Catherine Wespes		ULB	
Carlos Vicente		EUMETSAT	
Approved by			
AC SAF Technical Manager	Jari Hovila / FMI	28/01/2025	 Signature

## Document change log

Revision	Date	Description of change
1	06/11/2024	Initial revision
2	09/12/2024	Section 7.1.1.2: Added statement about investigation concerning the radiometric drift of GOME-2B L1b data
3	28/01/2025	<p>List of abbreviations: updated</p> <p>Section 1.2: Table 1.2 filled completely</p> <p>Section 3.2: Added description of anomaly ID 1 in Table 3.7 to Table 3.6 with status update</p> <p>Section 4.2: Information of KNMI software update added to Table 4.8</p> <p>Sections 7.1 – 7.6: ‘GOME-2’ added to the section titles</p> <p>Section 7.1.1.2: The last three paragraphs on page 43 updated</p> <p>Section 7.2: Reference to GOME-2A removed. Time period Jan 2021 – Dec 2022 corrected to Jan 2022 – Dec 2023 both in text and in Table 7.8.</p> <p>Section 7.3: Time periods corrected for the Kinshasa and IUP Bremen etc. data</p> <p>Section 7.7: Time period for correlation plots in Figure 7.47 corrected. Figures 7.39 – 7.43 updated.</p> <p>Section 9.1: Information of KNMI software update added</p>

## List of abbreviations

AC SAF	Satellite Application Facility on Atmospheric Composition Monitoring
ARP	Absorbing Aerosol Index from PMDs data product
ARP-A	Absorbing Aerosol Index from PMDs data product from Metop-A
ARP-B	Absorbing Aerosol Index from PMDs data product from Metop-B
ARP-C	Absorbing Aerosol Index from PMDs data product from Metop-C
ARS	Absorbing Aerosol Height data product
ARS-A	Absorbing Aerosol Height data product from Metop-A
ARS-B	Absorbing Aerosol Height data product from Metop-B
ARS-C	Absorbing Aerosol Height data product from Metop-C
ATMOS	Atmospheric Parameters Measured by in-Orbit Spectroscopy (DLR data service)
ATO	Assimilated Total Ozone
AUTH	Aristotle University of Thessaloniki
BIRA-IASB	Belgian Institute for Space Aeronomy
BrO	Bromine Oxide
CDOP	Continuous Development and Operations phase
CO	Carbon Monoxide
DLR	German Aerospace Center
DMI	Danish Meteorological Institute
DWD	German Weather Service
ECMWF	European Centre for Medium-Range Weather Forecasts
EDC	EUMETSAT Data Centre
EDD	Erythematous Daily Dose
EUMETCast	EUMETSAT's primary dissemination mechanism for the near real-time delivery of satellite data and products
EUMETSAT	European Organisation for the Exploitation of Meteorological Satellites
EUV	European UV product/data record
FMI	Finnish Meteorological Institute
GOME	Global Ozone Monitoring Experiment
H <sub>2</sub> O	Water Vapour
HCHO	Formaldehyde
HNO <sub>3</sub>	Nitric acid
HR	High resolution
KMI	Royal Meteorological Institute of Belgium
KNMI	Royal Netherlands Meteorological Institute
L1b	Level 1b data product
L1c	Level 1c data product
L2	Level 2 data product
L3	Level 3 data product



LATMOS	Laboratoire Atmosphères, Milieux, Observations Spatiales
LER	Lambertian-equivalent reflectivity data record
NHP	Near Real-time High-resolution Ozone Profile data product
NO2	Nitrogen Dioxide
NRT	Near Real-time
NTO	Near Real-time Total Column data product
NUV	Near Real-time UV index data product
O3	Ozone
O3M SAF	Satellite Application Facility on Ozone and Atmospheric Chemistry Monitoring
OHP	Offline High-resolution Ozone Profile data product
OHP-A	Offline High-resolution Ozone Profile data product from Metop-A
OHP-B	Offline High-resolution Ozone Profile data product from Metop-B
OHP-C	Offline High-resolution Ozone Profile data product from Metop-C
OEM	Optimal Estimation Method
OPERA	Ozone Profile Retrieval Algorithm
OTO	Offline Total Column data product
OUV	Offline Surface UV data product
OUV-A	Offline Surface UV data product from Metop-A
OUV-AB	Offline Surface UV data product from Metop-A and Metop-B
OUV-B	Offline Surface UV data product from Metop-B
OUV-BC	Offline Surface UV data product from Metop-B and Metop-C
PDU	Product Dissemination Unit
PGE	Product Generation Element
PMD	Polarisation Measurement Device
RD	Reference Document
RMS	Root Mean Square
RMSE	Root Mean Square Error
SACS	Support to Aviation Control Service
SCD	Slant Column Density
SO2	Sulphur Dioxide
TOC	Total Ozone Column data product
TrOC	Global Tropospheric Ozone Column data product
TTrOC	Tropical Tropospheric Ozone Column data product
ULB	Université libre de Bruxelles
UTC	Coordinated Universal Time

## TABLE OF CONTENTS

<b>1.</b>	<b>INTRODUCTION .....</b>	<b>8</b>
1.1.	Scope .....	8
1.2.	Reporting period .....	8
1.2.1.	Highlights .....	8
1.3.	Reference documents .....	8
1.4.	Definition of terms .....	11
1.5.	Accuracy requirements of AC SAF products .....	12
<b>2.</b>	<b>PROCESSING CENTRE: FMI .....</b>	<b>18</b>
2.1.	Offline surface UV .....	18
2.1.1.	Availability .....	18
2.1.2.	Timeliness .....	18
2.2.	Services, main events and anomalies .....	19
<b>3.</b>	<b>PROCESSING CENTRE: DLR .....</b>	<b>22</b>
3.1.	NRT and offline total/tropospheric trace gas columns, tropical tropospheric ozone .....	22
3.1.1.	Availability .....	22
3.1.2.	Timeliness .....	24
3.2.	Services, main events and anomalies .....	26
<b>4.</b>	<b>PROCESSING CENTRE: KNMI .....</b>	<b>29</b>
4.1.	NRT and offline ozone profiles, absorbing aerosol height and index, global tropospheric ozone .....	29
4.1.1.	Availability .....	29
4.1.2.	Timeliness .....	30
4.2.	Services, main events and anomalies .....	32
<b>5.</b>	<b>PROCESSING CENTRE: DMI .....</b>	<b>35</b>
5.1.	NRT clear-sky and cloud-corrected UV index .....	35
5.1.1.	Availability .....	35
5.1.2.	Timeliness .....	35
5.2.	Services, main events and anomalies .....	36
<b>6.</b>	<b>PROCESSING CENTRE: EUMETSAT .....</b>	<b>37</b>
6.1.	NRT IASI CO, SO <sub>2</sub> , HNO <sub>3</sub> and ozone profile .....	37
6.1.1.	Availability .....	37
6.1.2.	Timeliness .....	38
6.2.	Services, main events and anomalies .....	39
<b>7.</b>	<b>VALIDATION AND QUALITY MONITORING .....</b>	<b>41</b>
7.1.	GOME-2 total ozone column products .....	41
7.1.1.	Total ozone column validation .....	41
7.1.2.	Validation website .....	47
7.1.3.	Online quality monitoring .....	48
7.2.	GOME-2 tropospheric ozone products .....	49
7.3.	GOME-2 trace gas products .....	52
7.3.1.	Online quality monitoring .....	75
7.4.	GOME-2 ozone profile products .....	80
7.4.1.	Online quality monitoring .....	82
7.5.	GOME-2 aerosol products .....	84
7.5.1.	Online quality monitoring .....	90
7.6.	GOME-2 UV products .....	91

7.6.1.	Online quality monitoring.....	91
7.7.	IASI NRT products.....	93
8.	<b>LIST OF AC SAF USERS.....</b>	<b>118</b>
8.1.	FMI archive .....	118
8.2.	DLR archive .....	130
8.3.	DMI (NUV product via FTP) .....	141
8.4.	KNMI (unofficial NRT AAI via FTP).....	141
8.5.	Known international projects that use EUMETCast or WMO/GTS.....	141
8.6.	EUMETCast .....	142
9.	<b>UPDATES DURING THE REPORTING PERIOD.....</b>	<b>143</b>
9.1.	Software updates.....	143
9.2.	Hardware updates .....	143
9.3.	Documentation updates .....	143
10.	<b>CHANGES IN APPEARANCE AND CONTENT OF THE WEB PORTAL.....</b>	<b>144</b>
<b>APPENDIX 1.....</b>		<b>145</b>
<b>APPENDIX 2.....</b>		<b>150</b>

## 1. Introduction

### 1.1. Scope

The scope of this document is to summarise the operational activities concerning the products in operation and the associated services during the reporting period to see that the general requirements applicable to these services and products of the AC SAF [RD1, RD2, RD3] are fulfilled. Intended readers of this document are the members of AC SAF project team, Review Board of the annual Operations Review, AC SAF Steering Group and EUMETSAT OPS/WG as well as the users of the AC SAF products.

Operations Reports include information about product availability/timeliness, quality assurance, website usage, and delivery statistics. Main events, major anomalies and software/hardware updates are reported also. AC SAF Operations Report is published twice a year.

### 1.2. Reporting period

This Operations Report covers the period January – June 2024.

#### 1.2.1. Highlights

##### New products

- 25 June: Demonstrational European UV product (EUV) available to users

### 1.3. Reference documents

**Table 1.1. Operations Report reference documents**

Reference	Title	Issued	Reporting period
RD1	Product Requirements Document (SAF/AC/FMI/RQ/PRD/001)	20/12/2023	N/A
RD2	Service Specification (SAF/AC/FMI/RQ/SESP/001)	15/05/2024	N/A
RD3	EUMETSAT Operational Services Specification (EUM/OPS/SPE/20/109969)	16/02/2023	N/A
RD4	O3M SAF Validation Report for NRT, offline and reprocessed total ozone columns	11/12/2015	January 2007 – December 2014
RD5	AC SAF Validation Report for NRT, offline, reprocessed and level 3 total/tropospheric NO2 columns	10/11/2017	Metop-A: January 2007 – July 2015 Metop-B: January 2013 – July 2015
RD6	O3M SAF Validation Report for Metop-A NRT and offline coarse/high-resolution ozone profiles	20/02/2012	January 2007 – May 2011

Reference	Title	Issued	Reporting period
RD7	O3M SAF Validation Report for Metop-B NRT and offline coarse/high-resolution ozone profiles	30/06/2013	December 2012 – April 2013
RD8	O3M SAF Validation Report for Metop-B NRT UV indexes	27/05/2013	May 2013
RD9	O3M SAF Validation Report for NRT, offline and reprocessed total SO <sub>2</sub> columns	09/12/2015	January 2007 – December 2014
RD10	O3M SAF Validation Report for offline and reprocessed total BrO columns	09/12/2015	January 2007 – December 2014
RD11	O3M SAF Validation Report for NRT, offline and reprocessed total HCHO columns	30/10/2015	January 2007 – July 2015
RD12	O3M SAF Validation Report for offline and reprocessed total H <sub>2</sub> O columns	30/10/2015	January 2007 – August 2015
RD13	O3M SAF Validation Report for NRT and offline aerosol products	25/06/2013	January 2007 – May 2013
RD14	O3M SAF Validation Report for Metop-B offline UV products	03/02/2015	June 2012 – May 2013
RD15	AC SAF Validation Report for GOME-2 surface LER product	27/03/2019	MSC: February 2007 – June 2018 PMD: April 2008 – June 2018
RD16	O3M SAF Validation Report for offline tropospheric ozone columns (cloud slicing)	03/07/2015	January 2007 – December 2014
RD17	O3M SAF Validation Report for NRT and offline tropospheric ozone columns (ozone profiles)	09/09/2015	January 2007 – December 2014
RD18	O3M SAF Validation Report for NRT IASI CO	17/11/2015	September 2015 – November 2015
RD19	AC SAF Validation Report for NRT IASI SO <sub>2</sub>	17/11/2017	Metop-A: January 2007 – December 2013 June 2017 – October 2017 Metop-B: June 2017 – December 2017
RD20	AC SAF Validation Report for Metop-C offline tropical tropospheric ozone columns	05/06/2020	February – December 2019

Reference	Title	Issued	Reporting period
RD21	AC SAF Validation Report for Metop-C NRT and offline global tropospheric ozone columns	05/06/2020	February – December 2019
RD22	AC SAF Validation Report for Metop-C NRT and offline high-resolution ozone profiles	05/06/2020	February – December 2019
RD23	AC SAF Validation Report for Metop-C NRT and offline total ozone columns	25/05/2020	February – July 2019
RD24	AC SAF Validation Report for Metop-C NRT and offline total/tropospheric nitrogen dioxide columns	25/11/2019	February – July 2019
RD25	AC SAF Validation Report for Metop-C NRT and offline total formaldehyde columns	19/05/2020	February – July 2019
RD26	AC SAF Validation Report for Metop-C offline total bromine monoxide columns	19/05/2020	February – July 2019
RD27	AC SAF Validation Report for Metop-C offline total water vapour columns	30/03/2020	February – July 2019
RD28	AC SAF Validation Report for NRT, offline and reprocessed absorbing aerosol height products	03/07/2020	2007-2019
RD29	AC SAF Validation Report for Metop-C NRT and offline absorbing aerosol index from PMDs products	09/10/2019	January – October 2019
RD30	AC SAF Validation Report for Metop-C NRT and offline total sulphur dioxide products	21/01/2021	February – July 2019
RD31	AC SAF Validation Report for NRT IASI total O <sub>3</sub> and O <sub>3</sub> profiles	28/02/2022	December 2019 – November 2020
RD32	AC SAF Validation Report for NRT IASI HNO <sub>3</sub>	26/04/2022	December 2019 – December 2021

Online documents:

[Service Specification](#), [Validation Reports](#)

## 1.4. Definition of terms

**Availability** is based on the definition in the EUMETSAT Operational Services Specification [RD3].

Product-specific clarifications:

- For NRT products, the monthly availability limit is 97.5 %. The availability is calculated as a “worst case scenario”:

$$\frac{\text{in time processed and disseminated L2 PDUs}}{\text{received L1b PDUs} + \text{missed L1b PDUs marked as “reception confirmed” in the EUMETCast sendlist}}$$

- For offline products, the monthly availability limit is 95.5 %. The availability is defined by the ratio of the number of in time processed, archived and quality-approved L2 products to the number of orbits for which L1b PDUs have been received per month.
- NUV and OUV are daily L3 products, and availability is defined as the fraction of days in a month with products fulfilling the timeliness requirements
- TTrOC is a monthly L3 product and availability is 100 % or 0 % depending on whether the product fulfills the timeliness requirement or not

**Timeliness** defines whether the product is near real time (NRT) product which is disseminated or ready for download in three hours from sensing at the latest or offline product which is available for download in two weeks after sensing at the latest, during system availability. System unavailability will in most cases not lead to loss of data but to delays with respect to the specified timeliness. In practice, timeliness of a product is determined by calculating the time from sensing to EUMETCast or archive upload. In the Operations Reports, the timeliness is presented as monthly average, minimum and maximum values.

**Accuracy** of a satellite product is defined as a comparison of the mean/median bias (absolute and/or relative differences) of the product against ground-based and/or satellite-based reference data. Precision around the accuracy is given as a spread around the averaged bias (either through standard deviation or other robust metrics).

## 1.5. Accuracy requirements of AC SAF products

The following table lists all operational AC SAF products and their accuracy requirements as defined in [RD2]. Also results of the semi-annual online quality assessment are reported.

**Table 1.2. Accuracy requirements and validation results of AC SAF products**

Product identifier	Product name	Threshold accuracy	Target accuracy	Optimal accuracy	Achieved accuracy according to online quality assessment (Section 7)
O3M-41.1	NRT total O3	20 %	4 % (SZA < 80°) 6 % (SZA > 80°)	1.5 %	2.5 % (SZA < 80°)
O3M-300					3.5 % (SZA < 80°)
O3M-50.1	NRT total NO2	20 % of annual mean	8 – 15 % of annual mean	4 – 8 % of annual mean	Abs. bias of $-0.25 \times 10^{15}$ molec/cm <sup>2</sup> (GOME-2B) and $-0.15 \times 10^{15}$ molec/cm <sup>2</sup> (GOME-2C) w.r.t. NDACC ZLS-DOAS
O3M-338					
O3M-52.1	NRT tropospheric NO2	50 %	30 %	20 %	Between optimal and threshold accuracy depending on the pollution levels (for the MAX-DOAS station subset tested here)
O3M-341					
O3M-55.1	NRT total SO2	100 %	50 % (SZA < 70°)	30 %	50 % (SZA < 70°)
O3M-374					
O3M-177	NRT total HCHO	100 %	50 % (polluted)	30 %	Between optimal and target accuracy depending on the pollution levels (for the MAX-DOAS station subset tested here)
O3M-344					
O3M-47.1	NRT high-resolution ozone profile	30 % in stratosphere 70 % in troposphere	15 % in stratosphere 30 % in troposphere	10 % in stratosphere 25 % in troposphere	< 11 % in stratosphere < 23 % in troposphere
O3M-311					< 14 % in stratosphere < 19 % in troposphere



Product identifier	Product name	Threshold accuracy	Target accuracy	Optimal accuracy	Achieved accuracy according to online quality assessment (Section 7)
O3M-78	NRT absorbing aerosol height	3 km (layer height < 10 km) 4 km (layer height > 10 km)	2 km (layer height < 10 km) 3 km (layer height > 10 km)	1 km (layer height < 10 km) 2 km (layer height > 10 km)	Percentage of data difference GOME-2 AAH vs. CALIOP 27.2 % (< 1 km) 48.9 % (< 2 km) 70.4 % (< 3 km)
O3M-364					Percentage of data difference GOME-2 AAH vs. CALIOP 28.3 % (< 1 km) 48.3 % (< 2 km) 66.0 % (< 3 km)
O3M-72.1	NRT absorbing aerosol index from PMDs	1.0 index points	0.5 index points	0.2 index points	0.4 index points
O3M-362					
O3M-409	NRT UV index, clear-sky	20 %	10 %	5 %	Average value of the global UV index during the reporting period deviated -2.02 % for NUV/CLEAR and +2.17 % for NUV/CLOUD
O3M-410	NRT UV index, cloud-corrected				
O3M-80	NRT IASI CO	25 % (normal conditions) 50 % (high pollution or low signal)	12 % (normal conditions) 20 % (high pollution or low signal)	5 % (normal conditions) 10 % (high pollution or low signal)	Accuracy is estimated at 7 % for the entire NDACC network. During local winter months with high solar zenith angle measurements the target accuracy can be exceeded, but remain below the threshold accuracy of 25 %. For high latitude sites the biases fall within the target accuracy of 20 %. For the high pollution site Xianghe (near Beijing), the accuracy is estimated at 12 %.
O3M-352					
O3M-57	NRT IASI SO2	200 % (below 10 km) 100 % (above 10 km)	100 % (below 10 km) 35 % (above 10 km)	50 % (below 10 km) 20 % (above 10 km)	Online quality assessment services are available in Q1/2025
O3M-377					

Product identifier	Product name	Threshold accuracy	Target accuracy	Optimal accuracy	Achieved accuracy according to online quality assessment (Section 7)
O3M-81	NRT IASI HNO <sub>3</sub>	50 %	35 %	10 %	Accuracy is estimated at 14 % for the entire NDACC network. Higher biases reaching 20 % are observed at tropical NDACC sites and in the southern hemisphere (Lauder and Wollongong). Lower relative biases below 10 % at high latitude sites.
O3M-336					Similar as for O3M-81
O3M-44	NRT IASI total O <sub>3</sub>	10 %	5 %	1 %	Online quality assessment services are available in Q1/2025
O3M-306					
O3M-49	NRT IASI ozone profile	30 % in stratosphere 50 % in troposphere	15 % in stratosphere 30 % in troposphere	5 % in stratosphere 10 % in troposphere	No IASI data available for comparison
O3M-315					
O3M-06.1	Offline total O <sub>3</sub>	20 %	4 % (SZA < 80°) 6 % (SZA > 80°)	1.5 %	
O3M-42.1					2.7 % (SZA < 80°)
O3M-301					3.2 % (SZA < 80°)
O3M-07.1	Offline total NO <sub>2</sub>	20 % of annual mean	8 – 15 % of annual mean	4 – 8 % of annual mean	
O3M-51.1					Same as for NRT total NO <sub>2</sub>
O3M-339					
O3M-37.1	Offline tropospheric NO <sub>2</sub>	50 %	30 %	20 %	
O3M-53.1					Same as for NRT tropospheric NO <sub>2</sub>
O3M-342					

Product identifier	Product name	Threshold accuracy	Target accuracy	Optimal accuracy	Achieved accuracy according to online quality assessment (Section 7)
O3M-09.1	Offline total SO <sub>2</sub>	100 %	50 % (SZA < 70°)	30 %	
O3M-56.1					50 % (SZA < 70°)
O3M-375					
O3M-08.1	Offline total BrO	50 %	30 %	15 %	Generally within the target requirements for the S5p comparisons, within optimal accuracy for comparisons to Harestua ZSL-DOAS.
O3M-82.1					
O3M-317					
O3M-10.1	Offline total HCHO	100 %	50 % (polluted cond.)	30 %	
O3M-58.1					Same as for NRT total HCHO
O3M-345					
O3M-12.1	Offline total H <sub>2</sub> O	25 %	10 %	5 %	
O3M-86.1					Good agreement against radio sounding and GPS water vapour columns, with median relative bias of about 5 %. Global long-term bias of less than 1 kg/m <sup>2</sup> against SSMIS F16/17 and EAC4-CAMS reanalysis. GOME-2B/C consistent with each other within retrieval uncertainty.
O3M-386					
O3M-35	Offline tropical tropospheric ozone	50 %	25 %	15 %	
O3M-43					Within target accuracy
O3M-302					
O3M-303	Offline L3 daily averaged total O <sub>3</sub>	20 %	4 % (SZA < 80°) 6 % (SZA > 80°)	1.5 %	Same as for the offline L2 total O <sub>3</sub>
O3M-388	Offline L3 monthly averaged total O <sub>3</sub>				

Product identifier	Product name	Threshold accuracy	Target accuracy	Optimal accuracy	Achieved accuracy according to online quality assessment (Section 7)
O3M-340	Offline L3 daily averaged total NO <sub>2</sub>	20 %	8 %	5 %	Same as for the offline L2 total NO <sub>2</sub>
O3M-389	Offline L3 monthly averaged total NO <sub>2</sub>				
O3M-343	Offline L3 daily averaged tropospheric NO <sub>2</sub>	50 %	30 %	20 %	Same as for the offline L2 tropospheric NO <sub>2</sub>
O3M-390	Offline L3 monthly averaged tropospheric NO <sub>2</sub>				
O3M-376	Offline L3 daily averaged total SO <sub>2</sub>	100 %	50 % (SZA < 70°)	30 %	Same as for the offline L2 total SO <sub>2</sub>
O3M-397	Offline L3 monthly averaged total SO <sub>2</sub>				
O3M-318	Offline L3 daily averaged total BrO	50 %	30 %	15 %	Same as for the offline L2 total BrO
O3M-391	Offline L3 monthly averaged total BrO				
O3M-387	Offline L3 daily averaged total H <sub>2</sub> O	25 %	10 %	5 %	Same as for the offline L2 total H <sub>2</sub> O
O3M-393	Offline L3 monthly averaged total H <sub>2</sub> O				
O3M-346	Offline L3 daily averaged total HCHO	100 % (polluted cond.)	50 % (polluted cond.)	30 % (polluted cond.)	Same as for the offline L2 total HCHO
O3M-394	Offline L3 monthly averaged total HCHO				
O3M-39.1	Offline high-resolution ozone profile	30 % in stratosphere 70 % in troposphere	15 % in stratosphere 30 % in troposphere	10 % in stratosphere 25 % in troposphere	
O3M-48.1					Same as for NRT high-resolution ozone profile
O3M-312					

Product identifier	Product name	Threshold accuracy	Target accuracy	Optimal accuracy	Achieved accuracy according to online quality assessment (Section 7)
O3M-172	NRT global tropospheric ozone	50 %	20 %	15 %	
O3M-174					Product complies with the target accuracy, except GOME-2C tropical region
O3M-304					
O3M-173	Offline global tropospheric ozone	50 %	20 %	15 %	
O3M-175					Product complies with the target accuracy, except GOME-2C tropical region
O3M-305					
O3M-69	Offline absorbing aerosol height	3 km (layer height < 10 km) 4 km (layer height > 10 km)	2 km (layer height < 10 km) 3 km (layer height > 10 km)	1 km (layer height < 10 km) 2 km (layer height > 10 km)	
O3M-79					Same as for NRT AAH
O3M-365					
O3M-63.1	Offline absorbing aerosol index from PMDs	1.0 index points	0.5 index points	0.2 index points	
O3M-73.1					Better than 0.4 index points
O3M-363					
O3M-450 – O3M-464	Offline surface UV	50 %	20 %	10 %	Average value of the global erythemal daily dose during the reporting period deviated -0.39 % from the long-term average. See Figure 7.27.

Latest validation reports for all pre-operational and operational AC SAF products are listed in Section 1.3.

## 2. Processing centre: FMI

### 2.1. Offline surface UV

Offline surface UV (OUV) product is a L3 multi-mission (Metop-B+C) product consisting of 15 sub-products which are listed in Table 2.1. Since they are all archived in the same file, single entries in the tables in the following sections represent them all.

**Table 2.1. OUV sub-products**

Product Identifier	Product Name	Product Acronym
O3M-450	Offline UV daily dose, erythemat (CIE) weighting	MM-O-UV_DD_CIE
O3M-451	Offline UV daily dose, plant response weighting	MM-O-UV_DD_PLANT
O3M-452	Offline UV daily dose, DNA damage weighting	MM-O-UV_DD_DNA
O3M-453	Offline UV daily dose, UVA range (315-400 nm)	MM-O-UV_DD_UVA
O3M-454	Offline UV daily dose, UVB range (280-315 nm)	MM-O-UV_DD_UVB
O3M-455	Offline UV daily maximum dose rate, erythemat (CIE) weighting	MM-O-UV_MDSR_CIE
O3M-456	Offline UV daily maximum dose rate, plant response weighting	MM-O-UV_MDSR_PLANT
O3M-457	Offline UV daily maximum dose rate, DNA damage weighting	MM-O-UV_MDSR_DNA
O3M-458	Offline UV daily maximum dose rate, UVA range (315-400 nm)	MM-O-UV_MDSR_UVA
O3M-459	Offline UV daily maximum dose rate, UVB range (280-315 nm)	MM-O-UV_MDSR_UVB
O3M-460	Offline UV solar noon UV index	MM-O-UV_NOON_UVI
O3M-461	Offline UV daily maximum ozone photolysis rate	MM-O-UV_MPHR_O3
O3M-462	Offline daily maximum nitrogen dioxide photolysis rate	M-O-UV_MPHR_NO2
O3M-463	Offline UV daily dose, vitamin D weighting	MM-O-UV_DD_VITD
O3M-464	Offline UV daily maximum dose rate, vitamin D weighting	MM-O-UV_MDSR_VITD

#### 2.1.1. Availability

Availability requirement for OUV has been defined in Section 1.4. The availability statistics of FMI products are presented in Table 2.2. If the availability requirement has been violated, those values are marked with red colour, identified by numbers and reported in Table 2.7.

**Table 2.2. Availability of OUV product during the reporting period**

1/2024	2/2024	3/2024	4/2024	5/2024	6/2024
100 %	100 %	100 %	100 %	100 %	100 %

#### 2.1.2. Timeliness

Timeliness indicates the elapsed time between sensing and product dissemination. Timeliness requirement is 15 days for offline products. If the requirement has been violated, those values are

marked with red colour. In addition, the violations are identified by numbers and reported in Table 2.7 if they have caused the availability values to drop below the allowed limits.

Note: timeliness violations are not listed as anomalies if the availability is above the limit.

The values in Table 2.3 indicate the elapsed times (days, hours and minutes in the format [ddT]hh:mm) from sensing to archive upload. In each cell, the values from top to bottom represent observed monthly average, minimum and maximum times.

**Table 2.3. Timeliness of OUV product during the reporting period**

1/2024	2/2024	3/2024	4/2024	5/2024	6/2024
avg: 04T10:36 min: 04T00:27 max: 10T10:18	avg: 04T01:18 min: 04T00:32 max: 04T01:32	avg: 04T01:14 min: 04T00:22 max: 04T01:27	avg: 04T01:13 min: 04T00:27 max: 04T01:27	avg: 04T01:18 min: 04T00:27 max: 04T01:32	avg: 04T01:16 min: 04T00:32 max: 04T01:32

## 2.2. Services, main events and anomalies

**Table 2.4. FMI service statistics related to product archiving, ordering and AC SAF Helpdesk**

Description of service / event	1/2024	2/2024	3/2024	4/2024	5/2024	6/2024
<b>Product ordering <sup>1</sup></b>						
Number of users (cumulative)	654	658	664	673	685	689
Number of orders	18	4	10	17	10	11
Number of ordered products	OHP: 1726 ARS: 2604 ARP: 4217 OUV subset: 458 OUV time-series: 1793	OHP: 28 ARP: 11209 OUV time-series: 3	OHP: 1 ARS: 2186 ARP: 2 OUV subset: 366 OUV time-series: 15	OHP: 29 ARS: 1368 ARP: 454 OUV subset: 2041	OHP: 335 ARS: 24089 ARP: 24401 OUV subset: 8070	ARS: 1537 ARP: 3851 OUV subset: 31
Ordered data volume	OHP: 433 GB ARS: 2.68 GB ARP: 30.7 GB OUV subset: 14.1 MB OUV time-series: 172 kB	OHP: 10.2 GB ARP: 70.1 GB OUV time-series: 0.76 kB	OHP: 250 MB ARS: 2.26 GB ARP: OUV subset: 14.3 MB OUV time-series: 3.74 kB	OHP: 7.29 GB ARS: 1.41 GB ARP: 3.26 GB OUV subset: 8.04 GB	OHP: 90.6 GB ARS: 24.8 GB ARP: 173 GB OUV subset: 1.36 GB	ARS: 1.59 GB ARP: 27.9 GB OUV subset: 946 kB
Number of failed orders <sup>2</sup>	0	0	0	0	0	0
<b>Archive statistics <sup>3</sup></b>						
Number of archived products (Metop-B)	OHP: 439 ARS: 439 ARP: 439	OHP: 411 ARS: 411 ARP: 411	OHP: 440 ARS: 440 ARP: 440	OHP: 425 ARS: 425 ARP: 425	OHP: 440 ARS: 441 ARP: 440	OHP: 424 ARS: 424 ARP: 424
Size of archived products (Metop-B)	OHP: 110 GB ARS: 451 MB ARP: 3.19 GB	OHP: 103 GB ARS: 422 MB ARP: 2.99 GB	OHP: 110 GB ARS: 452 MB ARP: 3.20 GB	OHP: 106 GB ARS: 440 MB ARP: 3.08 GB	OHP: 110 GB ARS: 457 MB ARP: 3.18 GB	OHP: 106 GB ARS: 439 MB ARP: 3.05 GB
Number of archived products (Metop-C)	OHP: 439 ARS: 439 ARP: 439	OHP: 408 ARS: 408 ARP: 408	OHP: 439 ARS: 439 ARP: 439	OHP: 424 ARS: 424 ARP: 424	OHP: 438 ARS: 438 ARP: 438	OHP: 424 ARS: 424 ARP: 424
Size of archived products (Metop-C)	OHP: 110 GB ARS: 454 MB ARP: 3.21 GB	OHP: 102 GB ARS: 420 MB ARP: 2.98 GB	OHP: 110 GB ARS: 453 MB ARP: 3.21 GB	OHP: 106 GB ARS: 440 MB ARP: 3.09 GB	OHP: 109 GB ARS: 456 MB ARP: 3.18 GB	OHP: 106 GB ARS: 442 MB ARP: 3.07 GB

Number of archived multi-mission products	OUV: 31	OUV: 29	OUV: 31	OUV: 30	OUV: 31	OUV: 30
Size of archived multi-mission products	OUV: 554 MB	OUV: 547 MB	OUV: 576 MB	OUV: 525 MB	OUV: 536 MB	OUV: 507 MB
<b>GOME-2 L1b PDU rolling archive statistics <sup>4</sup></b>						
PDUs archived / PDUs “reception confirmed” (Metop-B)	13638/14879 91.7 %	13129/13919 94.3 %	14815/14837 99.9 %	14396/14396 100 %	14871/14872 100 %	14298/14363 99.5 %
PDUs archived / PDUs “reception confirmed” (Metop-C)	13943/14874 93.7 %	13220/13806 95.8 %	14839/14842 100 %	14367/14367 100 %	14847/14847 100 %	14298/14362 99.6 %
<b>Helpdesk statistics</b>						
Number of emails	0	0	0	1	0	10
Number of email threads	-	-	-	1	-	3
Average response time ([ddT]hh:mm)	-	-	-	01:18	-	13:55

<sup>1</sup> More detailed information about the orders is available in Appendix 1

<sup>2</sup> Failed orders are detailed in Appendix 2

<sup>3</sup> Based on sensing start time

<sup>4</sup> For Level 1b products, the availability is defined as the number of archived L1b PDUs divided by the number of L1b PDUs with status “reception confirmed” in the EUMETCast sendlist

Data archive statistics since 2008 are illustrated in Figure 2.1.

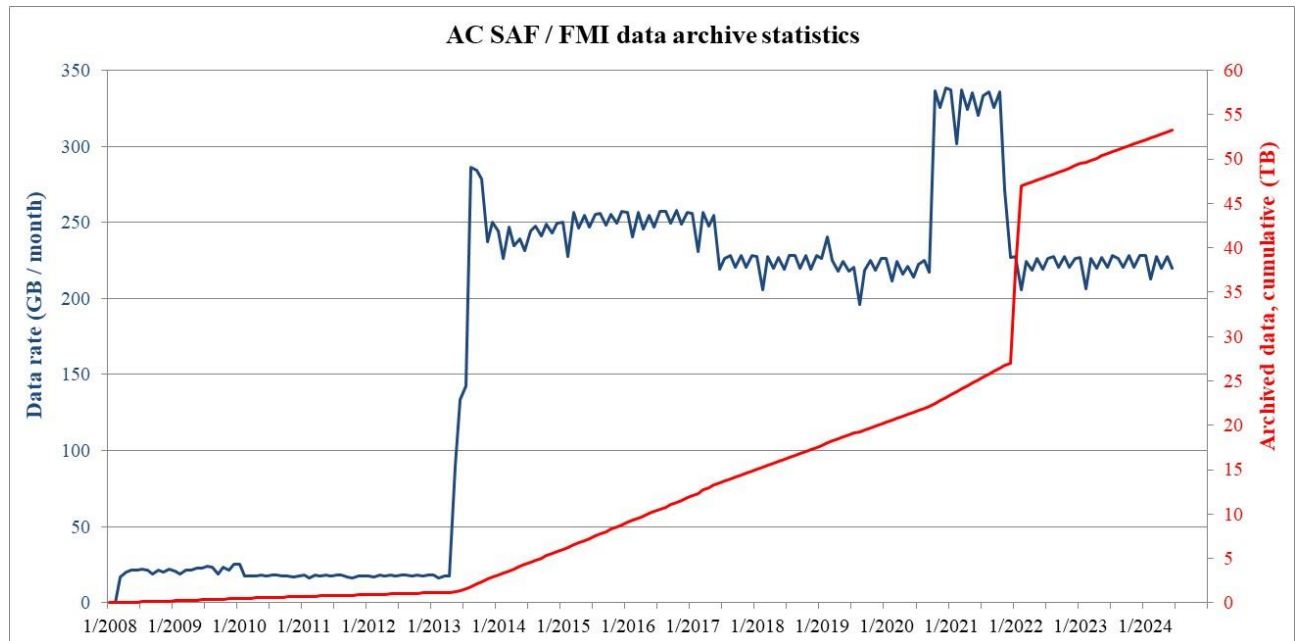


**Figure 2.1. FMI data archive statistics: data rate and cumulative amount of data**

Sudden increase in the cumulative amount of archived data in January – February 2022 is due to archiving of Metop-A/B high-resolution ozone profile data record R1.



Events affecting the data rate are presented in Table 2.5.

**Table 2.5. Events affecting the FMI archive data rate**

Date	Event	Data rate (GB/month)
03/2008	Archiving of OOP-A started	19.1 – 22.2
06/2009	Archiving of OUV-A started	19.2 – 23.8
11/2009	Archiving of ARS-A started	25.3
02/2010	Compression of OOP-A started	16.2 – 18.3
05/2013	Archiving of OHP-A started	133 – 142
08/2013	Archiving of OOP-B, OHP-B and ARS-B started	279 – 284
11/2013	Archiving of ARP-A and ARP-B started. KNMI implements shuffling algorithm in the hdf5 compression	226 – 250
03/2014	Archiving of OUV-A discontinued, archiving of OUV-B started	227 – 250
02/2015	OPERA algorithm update, tropospheric integrated profiles added	247 – 257
06/2017	Archiving of OOP-A and OOP-B discontinued	206 – 229
10/2020	Archiving of ARS-C, ARP-C and OHP-C started	302 – 338
11/2021	Archiving of OHP-A, ARS-A and ARP-A discontinued	206 – 228
01/2023	Archiving of IASI-B/C L3 CO started	206 – 228

Table 2.6 lists the main events (product/service/hardware/software updates etc.) at FMI during the reporting period.

**Table 2.6. Main events at FMI during the reporting period**

Date	Description
1 March	Operating system of the OUV processing server updated to Red Hat Enterprise Linux release 9.2

Table 2.7 lists the main local and external anomalies during the reporting period. Corrective and preventive actions should be provided also when applicable.

**Table 2.7. Main local and external anomalies affecting FMI systems and performance during the reporting period**

ID	Time period	Description
		<i>Nothing to report.</i>

### 3. Processing centre: DLR

#### 3.1. NRT and offline total/tropospheric trace gas columns, tropical tropospheric ozone

This section reports availability and timeliness of the operational NRT and offline L2 and L3 products processed for GOME-2 on Metop-B and Metop-C.

##### 3.1.1. Availability

For Level 1b products, the availability is defined as the number of L1b PDUs with status “reception confirmed”, i.e. EUMETSAT received these L1b PDUs through its EUMETCast reference receiving station, divided by the total number of L1b PDUs listed in the EUMETCast sendlist.

Availability for offline L2 and L3 products has been defined in Section 1.4. The availability statistics of DLR products are presented in Table 3.1 and Table 3.2. If the availability requirements have been violated, those values are marked with red colour, identified by numbers and reported in Table 3.7.

**Table 3.1. Availability of Metop-B total and tropospheric trace gas column products during the reporting period**

Product Identifier	Product Name	1/2024	2/2024	3/2024	4/2024	5/2024	6/2024
L1b	PDUs received / PDUs “reception confirmed”	14258/14879 95.8 % (1)	13913/13919 99.9 %	14794/14813 99.9 %	14031/14341 97.8 %	14046/14872 94.4 % (3)	14362/14242 100.8 %
O3M-41.1	NRT total O3	95.5 % (1)	99.9 %	99.9 %	97.8 %	93.3 % (3)	100.8 %
O3M-50.1	NRT total NO2						
O3M-52.1	NRT tropospheric NO2						
O3M-55.1	NRT total SO2						
O3M-177.0	NRT total HCHO						
O3M-42.1	Offline total O3	99.8 %	99.8 %	99.6 %	99.3 %	99.8 %	96.0 %
O3M-51.1	Offline total NO2						
O3M-53.1	Offline tropospheric NO2						
O3M-56.1	Offline total SO2						
O3M-58.1	Offline total HCHO						
O3M-82.1	Offline total BrO						
O3M-86.1	Offline total H2O						
O3M-43	Offline tropical tropospheric ozone	100 %	100 %	100 %	100 %	100 %	100 %

**Table 3.2. Availability of Metop-C total and tropospheric trace gas column products during the reporting period**

Product Identifier	Product Name	1/2024	2/2024	3/2024	4/2024	5/2024	6/2024
L1b	PDU received / PDUs “reception confirmed”	14189/14874 95.4 %	13799/14806 99.9 %	14834/14842 99.9 %	14114/14297 98.7 %	14825/14847 99.9 %	14318/14233 100.6 %
O3M-300	NRT total O3	94.9 % (1)	99.9 %	99.9 %	98.7 %	99.9 %	100.6 %
O3M-338	NRT total NO2						
O3M-341	NRT tropospheric NO2						
O3M-374	NRT total SO2						
O3M-344	NRT total HCHO						
O3M-301	Offline total O3	99.8 %	98.5 %	99.8 %	98.8 %	99.3 %	96.0 %
O3M-339	Offline total NO2						
O3M-342	Offline tropospheric NO2						
O3M-375	Offline total SO2						
O3M-345	Offline total HCHO						
O3M-317	Offline total BrO						
O3M-386	Offline total H2O						
O3M-302	Offline tropical tropospheric ozone	100 %	100 %	100 %	100 %	100 %	100 %

### 3.1.2. Timeliness

Timeliness indicates the elapsed time between sensing and product dissemination. Timeliness requirements are 3 hours for NRT products, 14 days for the offline tropical tropospheric ozone product and 15 days for the other offline products. If the requirements have been violated, those values are marked with red colour. In addition, the violations are identified by numbers and reported in Table 3.7 if they have caused the availability values to drop below the allowed limits.

Note: timeliness violations are not listed as anomalies if the availability is above the limit.

The values in Table 3.3 and Table 3.4 indicate the elapsed times (days, hours and minutes in the format [ddT]hh:mm) from sensing to EUMETCast (NRT) or AC SAF FTP site (offline) upload. For the offline tropical tropospheric ozone product, however, the values indicate the elapsed time from the end of the preceding month to product upload to the AC SAF FTP site.

In each cell, the values from top to bottom represent observed monthly average, minimum and maximum times.

**Table 3.3. Timeliness of Metop-B total and tropospheric trace gas column products during the reporting period**

Product Identifier	Product Name	1/2024	2/2024	3/2024	4/2024	5/2024	6/2024
O3M-41.1	NRT total O3	avg: 01:00 min: 00:48 max: 03:00 (1)	avg: 00:58 min: 00:30 max: 01:45	avg: 01:08 min: 00:30 max: 02:00	avg: 01:00 min: 00:29 max: 01:51	avg: 01:04 min: 00:31 max: 02:51	avg: 00:58 min: 00:31 max: 04:21
O3M-50.1	NRT total NO2						
O3M-52.1	NRT tropospheric NO2						
O3M-55.1	NRT total SO2						
O3M-177.0	NRT total HCHO						
O3M-42.1	Offline total O3	avg: 01T02:03 min: 01T00:55 max: 01T13:34	avg: 01T01:30 min: 01T01:01 max: 01T09:32	avg: 01T01:52 min: 01T00:47 max: 01T13:07	avg: 01T02:27 min: 01T00:45 max: 01T15:21	avg: 01T02:52 min: 01T01:02 max: 02T15:32	avg: 01T01:47 min: 01T01:01 max: 01T10:27
O3M-51.1	Offline total NO2						
O3M-53.1	Offline tropospheric NO2						
O3M-56.1	Offline total SO2						
O3M-58.1	Offline total HCHO						
O3M-82.1	Offline total BrO						
O3M-86.1	Offline total H2O						
O3M-43	Offline tropical tropospheric ozone	33T14:52 (2)	04T14:52	45T12:55 (2)	15T10:06 (2)	19T15:33 (2)	16T10:34 (2)

**Table 3.4. Timeliness of Metop-C total and tropospheric trace gas column products during the reporting period**

Product Identifier	Product Name	1/2024	2/2024	3/2024	4/2024	5/2024	6/2024
O3M-300	NRT total O3	avg: 01:36 min: 01:10 max: 02:58	avg: 01:36 min: 00:41 max: 02:07	avg: 01:36 min: 00:34 max: 02:09	avg: 01:37 min: 00:34 max: 02:08	avg: 01:38 min: 00:35 max: 02:18	avg: 01:38 min: 00:36 max: 02:09
O3M-338	NRT total NO2						
O3M-341	NRT tropospheric NO2						
O3M-374	NRT total SO2						
O3M-344	NRT total HCHO						
O3M-301	Offline total O3	avg: 01T01:58 min: 01T00:47 max: 01T12:39	avg: 01T09:41 min: 01T00:50 max: 04T14:11	avg: 01T06:08 min: 22:34 max: 03T22:00	avg: 01T02:33 min: 01T00:45 max: 01T14:28	avg: 01T02:10 min: 01T01:02 max: 01T15:04	avg: 01T01:44 min: 01T00:47 max: 01T10:06
O3M-339	Offline total NO2						
O3M-342	Offline tropospheric NO2						
O3M-375	Offline total SO2						
O3M-345	Offline total HCHO						
O3M-317	Offline total BrO						
O3M-386	Offline total H2O						
O3M-302	Offline tropical tropospheric ozone	33T14:52 (2)	04T14:52	45T10:06 (2)	15T10:06 (2)	19T15:34 (2)	16T10:34 (2)

### 3.2. Services, main events and anomalies

**Table 3.5. DLR service statistics related to product archiving and ordering**

Description of service / event	1/2024	2/2024	3/2024	4/2024	5/2024	6/2024
<b>Archive statistics <sup>2</sup></b>						
Number of archived products (cumulative) – according to product insertion time	546672	547493	548371	549219	550088	550938
Size of archived products (TB, cumulative)	17.29	17.33	17.38	17.42	17.46	17.51
Number of missing orbit products – according to sensing time	0	0	0	0	10	0
Number of archived products with good/poor/error <sup>3</sup> quality assessed per month – according to product insertion time	858/3/8	816/2/4	865/5/8	819/4/24	863/1/5	837/4/9
<b>Online Access <sup>1</sup></b>						
Number of FTP (ATMOS/VELA) subscribers	598	603	603	613	621	623
Number of FTP (ATMOS/VELA) downloads	73140	125444	172843	149874	147987	138009
Downloaded data volume (GB)	332.9	631.9	637.6	926.3	911.1	703.8

<sup>1</sup> NTO product and OTO product is stored at the DLR for external search and download

<sup>2</sup> O3MOTO product (collection GOME.TC, Metop missions) is archived and available to non-NRT users

<sup>3</sup> good: max. 2 PDUs missing, poor/error: more than 2 PDUs missing

Table 3.6 lists the main events (product/service/hardware/software updates etc.) at DLR during the reporting period.

**Table 3.6. Main events at DLR during the reporting period**

Date	Event
1 – 2 January	<p>The ingestion of Metop-B and Metop-C PDUs into the NRT processing system failed repeatedly due to issues related to the ingestion processor. This issue appeared after switching from Oracle Java to OpenJDK and was soon reverted back to using Oracle Java on the processing systems.</p> <p>Currently, development and testing work is in progress regarding the upgrade of the processing control system (PSM) to version 2.13, of which one part is the processing-system-wide utilization of OpenJDK. The processing control system upgrade for the different processing services will also be documented in the System Release Note (SRN). According to the current planning the service upgrades in the production environment will be performed in Q1/Q2 2025.</p>

Table 3.7 lists the main and external local anomalies at DLR during the reporting period. Corrective and preventive actions should be provided also when applicable.

**Table 3.7. Main local and external anomalies affecting DLR systems and performance during the reporting period**

ID	Time period	Description
1	1 – 2 January (continued from 2023)	<p>The ingestion of Metop-B and Metop-C PDUs into the NRT processing system failed repeatedly due to issues related to the ingestion processor. This issue appeared after switching from Oracle Java to OpenJDK. The switch to OpenJDK has been properly and extensively tested in the test environment. However, the issue was not directly related to the switch, but more likely related the combination of switching to OpenJDK and the size of the database of the processing system. Testing revealed that a reset of the database avoided the issues in the ingestion processor.</p> <p>Corrective action: The immediate action was to revert back to using Oracle Java on the processing systems and a close monitoring. The issue did not reoccur since.</p> <p>Preventive action: Since the switch to OpenJDK on the systems is obligatory the preventive action is to adhere to the result from the test environment and perform the switch to OpenJDK with prior database reset (including database backup creation) on the operational systems.</p> <p>Corrective action: Reverted back NRT processing systems to Oracle Java, which proofed reliable in the past.</p> <p>Preventive action: Activities started in the direction of upgrading the processing system to a higher version (2.13) in order to (besides others) solve the above described issue.</p>
2	January, March-June	<p>The timeliness of <math>\leq 2</math> weeks as specified in the currently applicable version (2.1) of the Product Requirements Document has been violated consistently (except for 02/2024 for both missions Metop-B and Metop-C) in the reporting period. The generation of the tropospheric ozone products is triggered manually after a certain (and not fully fixed) time period after all L2 data covering the respective month plus its nominal 14 days timeliness have passed.</p> <p>Corrective action: None</p> <p>Preventive action: Discussion and potential adaption of the timeliness criterion for the tropospheric O3 product (O3M-43) planned for Operations Review 16 at the end of 2024.</p>

ID	Time period	Description
3	30 April – 3 May	<p>The Metop-B NRT processing system stalled with a “NoTransactionInProgress” exception, which prevented any further handling of incoming PDUs. The exception occurred in the evening before a succeeding public holiday and the service could be resumed on 3 May. This specific exception has never been observed before and the actual root cause of the issue couldn’t be identified. Since the issue didn’t reoccur since the first occurrence and after an extensive observation period, the issue was closed. In case of re-occurrence deeper analysis will be conducted in order to find the root cause.</p> <p>Corrective action: Creation of backup of database of the processing system and restart of the processing system.</p> <p>Preventive action: Not applicable here, since handled internally as a one-time issue.</p>



## 4. Processing centre: KNMI

### 4.1. NRT and offline ozone profiles, absorbing aerosol height and index, global tropospheric ozone

#### 4.1.1. Availability

For Level 1b products, the availability is defined as the number of unique L1b PDUs received either via EUMETCast Satellite or EUMETCast Terrestrial (demonstrational dissemination service), divided by the number of L1b PDUs not marked as “not sent” in the EUMETCast Satellite sendlist. This approximation presumes that all PDUs marked as “sent not confirmed” are still available via EUMETCast Terrestrial.

Availability for offline L2 products has been defined in Section 1.4. The availability statistics of KNMI products are presented in Table 4.1 and Table 4.2. If the availability requirements have been violated, those values are marked with red colour, identified by numbers and reported in Table 4.9.

Tropospheric ozone products are included in the ozone profile products and have the same statistics. The same applies to scattering aerosol index products which are included in the absorbing aerosol index products.

**Table 4.1. Availability of Metop-B L1b PDUs, ozone profile products and aerosol products during the reporting period**

Product Identifier	Product Name	1/2024	2/2024	3/2024	4/2024	5/2024	6/2024
<b>EUMETCast</b>							
L1b	PDUs received / sent	14878/14879 100 %	13918/13919 100 %	14837/14837 100 %	14396/14396 100 %	14872/14872 100 %	14377/14242 101 %
O3M-47.1	NRT high-resolution ozone profile	100 %	100 %	99.8 %	100 %	99.6 %	100 %
O3M-78	NRT absorbing aerosol height	100 %	100 %	99.8 %	100 %	99.6 %	100 %
O3M-72.1	NRT absorbing aerosol index from PMDs	100 %	100 %	99.8 %	100 %	99.6 %	100 %
<b>WMO/GTS</b>							
O3M-47.1	NRT high-resolution ozone profile	100 %	100 %	99.8 %	100 %	99.6 %	100 %
<b>FMI archive</b>							
O3M-48.1	Offline high-resolution ozone profile	100 %	100 %	100 %	100 %	100 %	100 %
O3M-79	Offline absorbing aerosol height	100 %	100 %	100 %	100 %	100 %	100 %
O3M-73.1	Offline absorbing aerosol index from PMDs	100 %	100 %	100 %	100 %	100 %	100 %

**Table 4.2. Availability of Metop-C L1b PDUs, ozone profile products and aerosol products during the reporting period**

Product Identifier	Product Name	1/2024	2/2024	3/2024	4/2024	5/2024	6/2024
<b>EUMETCast</b>							
L1b	PDUs received / sent	14875/14876 100 %	13806/13806 100 %	14842/14842 100 %	14367/14367 100 %	14846/14847 100 %	14361/14233 101 %
O3M-311	NRT high-resolution ozone profile	100 %	100 %	100 %	100 %	99.6 %	100 %
O3M-364	NRT absorbing aerosol height	100 %	100 %	100 %	100 %	99.6 %	100 %
O3M-362	NRT absorbing aerosol index from PMDs	100 %	100 %	100 %	100 %	99.6 %	100 %
<b>WMO/GTS</b>							
O3M-311	NRT high-resolution ozone profile	100 %	100 %	100 %	100 %	99.6 %	100 %
<b>FMI archive</b>							
O3M-312	Offline high-resolution ozone profile	100 %	100 %	100 %	100 %	100 %	100 %
O3M-365	Offline absorbing aerosol height	100 %	100 %	100 %	100 %	100 %	100 %
O3M-363	Offline absorbing aerosol index from PMDs	100 %	100 %	100 %	100 %	100 %	100 %

**4.1.2. Timeliness**

Timeliness indicates the elapsed time between sensing and product dissemination. Timeliness requirements are 3 hours for NRT products and 15 days for offline products. If the requirements have been violated, those values are marked with red colour. In addition, the violations are identified by numbers and reported in Table 4.9 if they have caused the availability values to drop below the allowed limits.

Note: timeliness violations are not listed as anomalies if the availability is above the limit.

The values in Table 4.3 and Table 4.4 indicate elapsed times (days, hours and minutes in the format [ddT]hh:mm) from sensing to EUMETCast and WMO/GTS (NRT) or archive upload (offline). In each cell, the values from top to bottom represent observed monthly average, minimum and maximum times.

Tropospheric ozone products are included in the ozone profile products and have the same statistics.

**Table 4.3. Timeliness of Metop-B ozone profile and aerosol products during the reporting period**

Product Identifier	Product Name	1/2024	2/2024	3/2024	4/2024	5/2024	6/2024
<b>EUMETCast</b>							
O3M-47.1	NRT high-resolution ozone profile	avg: 01:11 min: 00:30 max: 01:58	avg: 01:09 min: 00:29 max: 02:02	avg: 01:18 min: 00:30 max: 03:48	avg: 01:11 min: 00:31 max: 02:13	avg: 01:15 min: 00:32 max: 05:59	avg: 01:08 min: 00:33 max: 02:22
O3M-78	NRT absorbing aerosol height	avg: 00:58 min: 00:29 max: 01:46	avg: 00:57 min: 00:29 max: 01:45	avg: 01:05 min: 00:30 max: 03:31	avg: 00:58 min: 00:29 max: 01:50	avg: 01:04 min: 00:30 max: 05:59	avg: 00:56 min: 00:30 max: 02:09
O3M-72.1	NRT absorbing aerosol index from PMDs	avg: 00:58 min: 00:29 max: 01:46	avg: 00:57 min: 00:29 max: 01:45	avg: 01:05 min: 00:30 max: 03:31	avg: 00:58 min: 00:29 max: 01:50	avg: 01:04 min: 00:30 max: 05:59	avg: 00:56 min: 00:30 max: 02:09
<b>WMO/GTS</b>							
O3M-47.1	NRT high-resolution ozone profile	avg: 01:12 min: 00:31 max: 01:59	avg: 01:10 min: 00:31 max: 02:02	avg: 01:19 min: 00:31 max: 03:49	avg: 01:12 min: 00:32 max: 02:14	avg: 01:16 min: 00:34 max: 06:00	avg: 01:09 min: 00:35 max: 02:24
<b>FMI archive</b>							
O3M-48.1	Offline high-resolution ozone profile	avg: 07:55 min: 06:48 max: 02T02:15	avg: 07:38 min: 06:54 max: 02T02:02	avg: 07:39 min: 06:51 max: 09:50	avg: 09:50 min: 06:42 max: 02T03:06	avg: 13:42 min: 06:48 max: 02T18:49	avg: 13:52 min: 06:39 max: 02T03:14
O3M-79	Offline absorbing aerosol height	avg: 07:53 min: 06:52 max: 02T02:10	avg: 07:36 min: 06:55 max: 02T02:52	avg: 07:37 min: 06:46 max: 09:40	avg: 09:50 min: 06:40 max: 02T03:01	avg: 13:41 min: 06:49 max: 02T18:29	avg: 13:50 min: 06:34 max: 02T03:07
O3M-73.1	Offline absorbing aerosol index from PMDs	avg: 07:54 min: 06:49 max: 02T02:40	avg: 07:33 min: 06:49 max: 02T02:22	avg: 07:34 min: 06:52 max: 10:10	avg: 09:48 min: 06:43 max: 02T03:01	avg: 13:37 min: 06:46 max: 02T18:34	avg: 13:50 min: 06:46 max: 02T03:16

**Table 4.4. Timeliness of Metop-C ozone profile and aerosol products during the reporting period**

Product Identifier	Product Name	1/2024	2/2024	3/2024	4/2024	5/2024	6/2024
<b>EUMETCast</b>							
O3M-311	NRT high-resolution ozone profile	avg: 01:48 min: 00:40 max: 02:11	avg: 01:46 min: 00:34 max: 02:11	avg: 01:45 min: 00:34 max: 02:24	avg: 01:45 min: 00:34 max: 02:26	avg: 01:49 min: 00:36 max: 05:53	avg: 01:46 min: 00:38 max: 02:22
O3M-364	NRT absorbing aerosol height	avg: 01:35 min: 00:40 max: 01:55	avg: 01:34 min: 00:33 max: 02:07	avg: 01:32 min: 00:34 max: 02:10	avg: 01:33 min: 00:34 max: 02:07	avg: 01:37 min: 00:34 max: 05:59	avg: 01:34 min: 00:34 max: 02:08
O3M-362	NRT absorbing aerosol index from PMDs	avg: 01:35 min: 00:40 max: 01:55	avg: 01:34 min: 00:33 max: 02:08	avg: 01:32 min: 00:34 max: 02:14	avg: 01:33 min: 00:34 max: 02:07	avg: 01:37 min: 00:34 max: 05:59	avg: 01:34 min: 00:34 max: 02:08

Product Identifier	Product Name	1/2024	2/2024	3/2024	4/2024	5/2024	6/2024
<b>WMO/GTS</b>							
O3M-311	NRT high-resolution ozone profile	avg: 01:49 min: 00:40 max: 02:12	avg: 01:47 min: 00:35 max: 02:17	avg: 01:46 min: 00:34 max: 02:24	avg: 01:46 min: 00:35 max: 02:28	avg: 01:50 min: 00:37 max: 05:50	avg: 01:47 min: 00:39 max: 02:24
<b>FMI archive</b>							
O3M-312	Offline high-resolution ozone profile	avg: 08:18 min: 07:21 max: 01T05:46	avg: 07:56 min: 07:18 max: 08:32	avg: 08:15 min: 07:12 max: 02T03:09	avg: 12:00 min: 07:12 max: 02T03:41	avg: 16:27 min: 07:27 max: 03T02:22	avg: 16:16 min: 07:21 max: 02T03:50
O3M-365	Offline absorbing aerosol height	avg: 08:15 min: 07:19 max: 01T05:36	avg: 07:54 min: 07:19 max: 08:28	avg: 08:13 min: 07:16 max: 02T03:04	avg: 11:59 min: 07:19 max: 02T03:34	avg: 16:26 min: 07:25 max: 03T02:17	avg: 16:15 min: 07:19 max: 02T03:43
O3M-363	Offline absorbing aerosol index from PMDs	avg: 08:12 min: 07:13 max: 01T05:26	avg: 07:53 min: 06:55 max: 08:31	avg: 08:12 min: 07:13 max: 02T03:22	avg: 11:58 min: 07:16 max: 02T03:34	avg: 16:24 min: 07:19 max: 03T02:12	avg: 16:16 min: 07:19 max: 02T03:43

## 4.2. Services, main events and anomalies

Tropospheric ozone products are included in the ozone profile products and have the same statistics.

**Table 4.5. Number of products sent to FMI archive<sup>1</sup>**

Product Identifier	Product Name	Metop satellite	1/2024	2/2024	3/2024	4/2024	5/2024	6/2024
O3M-48.1	Offline high-resolution ozone profile	B	439	411	440	425	440	424
O3M-312		C	439	408	439	424	438	424
O3M-79	Offline absorbing aerosol height	B	439	411	440	425	441	424
O3M-365		C	439	408	439	424	438	424
O3M-73.1	Offline absorbing aerosol index from PMDs	B	439	411	440	425	440	424
O3M-363		C	439	408	439	424	438	424

**Table 4.6. Number of products stored locally at KNMI<sup>2</sup>**

Product Identifier	Product Name	Metop satellite	1/2024	2/2024	3/2024	4/2024	5/2024	6/2024
O3M-47.1	NRT high-resolution ozone profile	B	8803	8262	8782	8426	8570	8299
O3M-311		C	8809	8161	8752	8340	8509	8259
O3M-78	NRT absorbing aerosol height	B	8803	8262	8782	8426	8564	8299
O3M-364		C	8809	8161	8752	8340	8519	8259

Product Identifier	Product Name	Metop satellite	1/2024	2/2024	3/2024	4/2024	5/2024	6/2024
O3M-72.1	NRT absorbing aerosol index from PMDs	B	8803	8262	8782	8426	8564	8299
O3M-362		C	8809	8161	8752	8340	8519	8259
O3M-48.1	Offline high-resolution ozone profile	B	439	411	440	425	440	424
O3M-312		C	439	408	439	424	438	424
O3M-79	Offline absorbing aerosol height	B	439	411	440	425	441	424
O3M-365		C	439	408	439	424	438	424
O3M-73.1	Offline absorbing aerosol index from PMDs	B	439	411	440	425	440	424
O3M-363		C	439	408	439	424	438	424

**Table 4.7. EUMETCast and WMO/GTS uploads<sup>3</sup>**

Product Identifier	Product Name	Metop satellite	1/2024	2/2024	3/2024	4/2024	5/2024	6/2024
O3M-47.1	NRT high-resolution ozone profile	B	8803/8803	8262/8262	87658765/	8426/8426	8537/8528	8299/8286
O3M-311		C	8809/8809	8161/8161	8752/8752	8340/8340	8480/8462	8259/8259
O3M-78	NRT absorbing aerosol height	B	8803	8262	8765	8426	8532	8299
O3M-364		C	8809	8161	8752	8340	8487	8259
O3M-72.1	NRT absorbing aerosol index from PMDs	B	8803	8262	8765	8426	8534	8299
O3M-362		C	8809	8161	8752	8340	8487	8259

<sup>1</sup> Products are archived in HDF5 format.

<sup>2</sup> Products are stored for 3 years (in HDF5 and BUFR formats).

<sup>3</sup> NRT high-resolution ozone profile is disseminated via EUMETCast and WMO/GTS in BUFR format. NRT absorbing aerosol index and NRT absorbing aerosol index from PMDs are disseminated only via EUMETCast (in HDF5 and BUFR formats).

Table 4.8 lists the main events (product/service/hardware/software updates etc.) at KNMI during the reporting period.

**Table 4.8. Main events at KNMI during the reporting period**

Date	Description
14 May	Operating system and PGE upgrade of the operational processors for the ozone profile, aerosol and SIF products, and derived L3 grids.

Table 4.9 lists the main local and external anomalies at KNMI during the reporting period. Corrective and preventive actions should be provided also when applicable.

**Table 4.9. Main local and external anomalies affecting KNMI systems and performance during the reporting period**

ID	Time period	Description
		<i>Nothing to report.</i>

## 5. Processing centre: DMI

### 5.1. NRT clear-sky and cloud-corrected UV index

#### 5.1.1. Availability

NUV product is required to be produced every day, either on the basis of new GOME ATO input or in the case of ATO delivery failure based on back-up total ozone data (ECMWF or climatology).

Availability requirement for NUV has been defined in Section 1.4. The availability statistics of DMI products are presented in Table 5.1. If the requirement is violated, those values are marked with red colour, identified by numbers and reported in Table 5.5.

**Table 5.1. Availability of NRT UV products during the reporting period**

Product Identifier	Product Name	1/2024	2/2024	3/2024	4/2024	5/2024	6/2024
O3M-409	NRT UV index, clear-sky	100 %	100 %	100 %	100 %	100 %	100 %
O3M-410	NRT UV index, cloud-corrected						

#### 5.1.2. Timeliness

Timeliness requirement for NUV says that the final NUV product is to be delivered to users no later than 04:00 UTC. The timeliness reported in Table 5.2 is calculated as the time difference (hours and minutes in format hh:mm) between 04:00 UTC and the time when the NUV products are available to users. Thus **positive** values refer to situations where the timeliness requirement is violated, and marked in red colour. In addition, the violations are identified by numbers and reported in Table 5.5 if they have caused the availability values to drop below the allowed limits.

Days where no products are produced or could be delivered to users (as indicated in Table 5.1) are not included in Table 5.2.

From top to bottom, the values in Table 5.2 represent observed monthly average, minimum and maximum time differences.

**Table 5.2. Timeliness of NRT UV products during the reporting period**

Product Identifier	Product Name	1/2024	2/2024	3/2024	4/2024	5/2024	6/2024
O3M-409	NRT UV index, clear-sky	avg: -00:52 min: -00:54 max: -00:45	avg: -00:54 min: -00:54 max: -00:53	avg: -00:53 min: -00:54 max: -00:53	avg: -00:54 min: -00:54 max: -00:53	avg: -00:54 min: -00:54 max: -00:53	avg: -00:54 min: -00:54 max: -00:53
O3M-410	NRT UV index, cloud-corrected						

## 5.2. Services, main events and anomalies

**Table 5.3. Number of products stored locally at DMI<sup>1</sup>**

Description of service / event	1/2024	2/2024	3/2024	4/2024	5/2024	6/2024
Storage statistics						
Number of stored products (NRT UV index, clear-sky)	31	29	31	30	31	30
Number of stored products (NRT UV index, cloud-corrected)	31	29	31	30	31	30
Total size of stored products (MB)	248	232	248	240	248	240

<sup>1</sup> NUV products are stored at the DMI at least until the end of the Metop programs.

Table 5.4 lists the main events (product/service/hardware/software updates etc.) at DMI during the reporting period.

**Table 5.4. Main events at DMI during the reporting period**

Date	Event
	<i>Nothing to report.</i>

Table 5.5 lists the main local and external anomalies at DMI during the reporting period. Corrective and preventive actions should be provided also when applicable.

**Table 5.5. Main local and external anomalies affecting DMI systems and performance during the reporting period**

ID	Time period	Description
		<i>Nothing to report.</i>



## 6. Processing centre: EUMETSAT

### 6.1. NRT IASI CO, SO<sub>2</sub>, HNO<sub>3</sub> and ozone profile

#### 6.1.1. Availability

For Level 1c products, the availability is defined as the number of available PDUs divided by the number of maximum expected PDUs.

For NRT products, the availability requirement is 97.5 % and it is defined by the ratio of the number of in time processed and disseminated products to the number of maximum expected input products (L1c PDUs) per month.

The availability statistics of EUMETSAT products are presented in Table 6.1 and Table 6.2. If the availability requirements have been violated, those values are marked with **red** colour, identified by numbers and reported in Table 6.7 and/or Table 6.8.

Note that in the frame of this product processing centre being the EUMETSAT HQ in Darmstadt, the L1c data is directly available to the L2+ algorithm, i.e., its availability is not dependable of EUMETCast dissemination, which can sometimes be translated into higher L2+ availability than the applicable L1c, depending on the data which has been successfully disseminated. Furthermore, since there is no relay of information from *Satellite* processing centres, the L2 product availability in the following tables concern the end-to-end availability as they were recorded in the EUMETSAT Reference Receiving Stations.

**Table 6.1. Availability of Metop-B L1c PDUs and IASI NRT products during the reporting period**

Product Identifier	Product Name	1/2024	2/2024	3/2024	4/2024	5/2024	6/2024
L1c	PDUs available / PDUs expected	14823/14880	13841/13920	14793/14880	14267/14400	14876/14880	14196/14400
L1c	Availability	99.6 %	99.4 %	99.4 %	99.1 %	100 %	98.6 %
O3M-80	NRT IASI CO	99.6 %	99.4 %	99.4 %	99.1 %	100 %	99.2 %
O3M-57	NRT IASI SO <sub>2</sub>	99.6 %	99.4 %	99.4 %	99.1 %	100 %	99.2 %
O3M-81	NRT IASI HNO <sub>3</sub>	99.6 %	99.4 %	99.4 %	99.1 %	100 %	99.2 %
O3M-49	NRT IASI ozone profile	99.6 %	99.4 %	99.4 %	99.1 %	100 %	99.2 %

**Table 6.2. Availability of Metop-C L1c PDUs and IASI NRT products during the reporting period**

Product Identifier	Product Name	1/2024	2/2024	3/2024	4/2024	5/2024	6/2024
L1c	PDUs available / PDUs expected	14865/14880	13699/13920	14702/14880	14171/14400	14689/14880	14353/14400
L1c	Availability	99.9 %	98.4 %	98.8 %	98.4 %	98.7 %	99.7 %
O3M-352	NRT IASI CO	100 %	98.6 %	99.1 %	98.6 %	99.3 %	99.7 %
O3M-377	NRT IASI SO <sub>2</sub>	100 %	98.6 %	99.1 %	98.6 %	99.3 %	99.7 %
O3M-336	NRT IASI HNO <sub>3</sub>	100 %	98.6 %	99.1 %	98.6 %	99.3 %	99.7 %
O3M-315	NRT IASI ozone profile	100 %	98.6 %	99.1 %	98.6 %	99.3 %	99.7 %

**6.1.2. Timeliness**

Timeliness indicates the elapsed time between sensing and product dissemination. Timeliness requirement is 3 hours for NRT products. If the requirements have been violated, those values are marked with red colour. In addition, the violations are identified by numbers and reported in Table 6.8 if they have caused the availability values to drop below the allowed limits.

Note: timeliness violations are not listed as anomalies if the availability is above the limit.

The values in Table 6.3 and Table 6.4 indicate elapsed times (hours and minutes in the format hh:mm) from sensing to EUMETCast Reference Receiving Station, i.e., end-to-end timeliness. In each cell, the values from top to bottom represent observed monthly average, minimum and maximum times.

**Table 6.3. Timeliness of Metop-B IASI NRT products during the reporting period**

Product Identifier	Product Name	1/2024	2/2024	3/2024	4/2024	5/2024	6/2024
O3M-80	NRT IASI CO	avg: 01:11 min: 00:58 max: 02:07	avg: 01:10 min: 00:47 max: 02:08	avg: 01:23 min: 00:59 max: 03:11	avg: 01:17 min: 00:58 max: 02:11	avg: 01:23 min: 00:53 max: 02:47	avg: 01:10 min: 00:34 max: 02:11
O3M-57	NRT IASI SO <sub>2</sub>	avg: 01:11 min: 00:58 max: 02:07	avg: 01:10 min: 00:47 max: 02:08	avg: 01:23 min: 00:59 max: 03:11	avg: 01:17 min: 00:59 max: 02:11	avg: 01:23 min: 00:53 max: 02:47	avg: 01:10 min: 00:34 max: 02:11
O3M-81	NRT IASI HNO <sub>3</sub>	avg: 01:11 min: 00:58 max: 02:07	avg: 01:10 min: 00:47 max: 02:08	avg: 01:23 min: 00:59 max: 03:11	avg: 01:17 min: 00:59 max: 02:11	avg: 01:23 min: 00:53 max: 02:47	avg: 01:10 min: 00:34 max: 02:11
O3M-49	NRT IASI ozone profile	avg: 01:11 min: 00:58 max: 02:07	avg: 01:10 min: 00:47 max: 02:08	avg: 01:23 min: 00:59 max: 03:11	avg: 01:17 min: 00:59 max: 02:11	avg: 01:23 min: 00:53 max: 02:47	avg: 01:10 min: 00:34 max: 02:11

**Table 6.4. Timeliness of Metop-C IASI NRT products during the reporting period**

Product Identifier	Product Name	1/2024	2/2024	3/2024	4/2024	5/2024	6/2024
O3M-352	NRT IASI CO	avg: 01:53 min: 01:32 max: 02:32	avg: 01:51 min: 01:03 max: 02:38	avg: 01:52 min: 01:05 max: 03:57	avg: 01:51 min: 01:08 max: 02:39	avg: 01:54 min: 01:02 max: 02:47	avg: 01:46 min: 01:00 max: 02:23
O3M-377	NRT IASI SO <sub>2</sub>	avg: 01:53 min: 01:32 max: 02:32	avg: 01:51 min: 01:03 max: 02:39	avg: 01:52 min: 01:05 max: 03:57	avg: 01:51 min: 01:08 max: 02:39	avg: 01:54 min: 01:02 max: 02:50	avg: 01:47 min: 01:00 max: 02:23
O3M-336	NRT IASI HNO <sub>3</sub>	avg: 01:53 min: 01:32 max: 02:32	avg: 01:51 min: 01:03 max: 02:39	avg: 01:52 min: 01:05 max: 03:57	avg: 01:51 min: 01:08 max: 02:39	avg: 01:54 min: 01:02 max: 02:50	avg: 01:47 min: 01:00 max: 02:23
O3M-315	NRT IASI ozone profile	avg: 01:53 min: 01:32 max: 02:32	avg: 01:51 min: 01:03 max: 02:39	avg: 01:52 min: 01:05 max: 03:57	avg: 01:51 min: 01:08 max: 02:39	avg: 01:54 min: 01:02 max: 02:50	avg: 01:47 min: 01:00 max: 02:23

## 6.2. Services, main events and anomalies

**Table 6.5. Number of products stored locally at EUMETSAT<sup>1</sup>**

Product Identifier	Product Name	Metop satellite	1/2024	2/2024	3/2024	4/2024	5/2024	6/2024
O3M-80	NRT IASI CO	B	14824	13841	14807	14321	14826	14284
O3M-352		C	14872	13731	14766	14251	14717	14355
O3M-57	NRT IASI SO <sub>2</sub>	B	14824	13841	14807	14319	14825	14284
O3M-377		C	14872	13731	14766	14250	14716	14354
O3M-81	NRT IASI HNO <sub>3</sub>	B	14824	13841	14807	14319	14825	14284
O3M-336		C	14872	13731	14766	14250	14716	14354
O3M-49	NRT IASI ozone profile	B	14824	13841	14807	14319	14825	14284
O3M-315		C	14872	13731	14766	14250	14716	14354

<sup>1</sup> PDUs are concatenated back to orbit-based products before being stored

Table 6.6. EUMETCast uploads<sup>1</sup>

Product Identifier	Product Name	Metop satellite	1/2024	2/2024	3/2024	4/2024	5/2024	6/2024
O3M-80	NRT IASI CO	B	14824	13841	14807	14321	14826	14284
O3M-352		C	14872	13731	14766	14251	14717	14355
O3M-57	NRT IASI SO2	B	14824	13841	14807	14319	14825	14284
O3M-377		C	14872	13731	14766	14250	14716	14354
O3M-81	NRT IASI HNO3	B	14824	13841	14807	14319	14825	14284
O3M-336		C	14872	13731	14766	14250	14716	14354
O3M-49	NRT IASI ozone profile	B	14824	13841	14807	14319	14825	14284
O3M-315		C	14872	13731	14766	14250	14716	14354

<sup>1</sup> NRT IASI products are disseminated via EUMETCast (in BUFR format)

Table 6.7 lists the main events (product/service/hardware/software updates etc.) at EUMETSAT during the reporting period.

Table 6.7. Main planned activities at EUMETSAT during the reporting period

ID	Date	Description
1		<i>Nothing to report.</i>

Table 6.8 lists the main local and external anomalies at EUMETSAT during the reporting period. Corrective and preventive actions should be provided also when applicable.

Table 6.8. Main local and external anomalies affecting EUMETSAT systems and performance during the reporting period

ID	Time period	Description
		<i>Nothing to report.</i>

## 7. Validation and quality monitoring

This section describes the validation status and validation/quality monitoring activities of NRT and offline data products during the reporting period. Validation reports for data records are found from <https://acsaf.org/valreps.html>

Reference documents are listed in Section 1.3 and accuracy requirements in Section 1.5.

### 7.1. GOME-2 total ozone column products

**Table 7.1. Validation status of total ozone column products**

Product Identifier	Product Name	Accuracy	Reference	Validating Institute	Correlative data sources
O3M-41.1	NRT total O3	Fulfil threshold accuracy requirement	RD4	AUTH	<a href="#">World Ozone Mapping Centre</a>
O3M-300			RD23		
O3M-06.1	Offline total O3	Fulfil threshold accuracy requirement	RD4	AUTH	World Ozone and Ultraviolet Radiation Data Center ( <a href="#">WOUDC</a> ), of the World Meteorological Organization, ( <a href="#">WMO</a> ), Global Atmosphere Watch, ( <a href="#">GAW</a> )
O3M-42.1					
O3M-301			RD23		

Validation results can be found in more detail on the AC SAF validation & quality assessment website at [http://acsaf.physics.auth.gr/eumetsat/validation/near\\_real](http://acsaf.physics.auth.gr/eumetsat/validation/near_real) and <http://acsaf.physics.auth.gr/eumetsat/validation/offline>

#### 7.1.1. Total ozone column validation

This summary presents the validation activities for total ozone column products (TOCs), reported by the GOME-2/Metop-B and GOME-2/Metop-C instruments (hereafter GOME-2B and GOME-2C, respectively). Members of the Laboratory of Atmospheric Physics of the Aristotle University of Thessaloniki ([LAP/AUTH](#)), Thessaloniki, Greece, involved in the validation activities include Professor, Dr. Dimitris Balis, Special Teaching Fellow & Researcher, Dr. Katerina Garane and Research Associate, Dr. MariLiza Koukouli.

During the reporting period, the operational validation of offline total ozone and NRT total ozone products continued as per previous periods.

##### 7.1.1.1 Update of database for reference ground-based data

For the nominal validation, the ground-based TOCs from Brewer, Dobson and M-124 instruments reported to the World Ozone and Ultraviolet Radiation Data Centre ([WOUDC](#)), are employed. WOUDC is one of the World Data Centres which are part of the Global Atmosphere Watch ([GAW](#)) programme of the World Meteorological Organization ([WMO](#)). For the quality of the reference ground-based data used for the validation of the total ozone products, updated information were extracted from recent inter-comparisons and calibration records. This continuously updated selection of ground-based measurements has already been used numerous times in the validation and analysis of global total ozone records such as the inter-comparison between the OMI/Aura TOMS and OMI/Aura DOAS algorithms [Balis *et al.*, 2007a], the validation of ten years of GOME/ERS-2 ozone record [Balis *et al.*, 2007b], the validation of the updated version of the OMI/Aura TOMS algorithm [Antón *et al.*, 2009], the GOME-2/Metop-A validation [Loyola *et al.*,

2011; Koukouli *et al.*, 2012], the GOME-2B validation [Hao *et al.*, 2014] and the evaluation of the European Space Agency's Ozone Climate Change Initiative project [O<sub>3</sub>-CCI] TOCs [Koukouli *et al.*, 2015, Garane *et al.*, 2018], as well as in TROPOMI/S5P TOCs validation [Garane *et al.*, 2019]. In all the aforementioned works, LAP/AUTH assumes the leading role in the validation efforts. The number of Woudc ground-based stations used in the full operational periods of the two instruments, alongside the mean difference between ground- and space-based TOC estimates is given in Table 7.2.

The comparisons and validation results with respect to the M-124 instruments are available via the [validation website](#), but not shown herein for reasons of brevity.

#### **7.1.1.2 Validation results for the offline total ozone products**

GOME-2B and GOME-2C OTO data for the period December 2012 (or January 2019 for GOME-2C) to June 2024 have been downloaded, quality-assured and pre-processed in order to perform the validation strategies. The GDP-4.8 algorithm is the latest version of the GDP-4.x suite of algorithms that have been used for the operational processing of GOME-2B total ozone columns. GOME-2C is processed with GDP-4.9. The main differences between GDP-4.8 and GDP-4.9 concern the SO<sub>2</sub> vertical column retrieval. For ozone only minor updates have been performed, such as the optimization of the slit function, the introduction of a pseudo absorber for possible orbital variations of the resolution etc. Therefore, the ozone columns from GOME-2C can be assumed to be similar to the respective data from GOME-2B, analyzed with the previous version of the algorithm.

This period's satellite-to-ground-based measurements comparisons were performed and added to the existing time series. The majority of the quality-assured ground-based Brewer and Dobson TOCs are reported to the Woudc repository between 3 and 6 months after measurement, which accounts for the last couple of months missing from the comparative plots shown below. This is a common reporting feature, quite unavoidable.

In Figure 7.1, left column of figures, the status of GOME-2B and GOME-2C TOCs since the beginning of each individual mission is shown in the form of a monthly mean time-series of the percentage differences between each sensor and ground-based observations. Panel a shows the co-locations with Brewer Northern Hemisphere (NH) stations, panel c with Dobson NH stations and panel e with Dobson Southern Hemisphere (SH) stations. The plots shown in the right column of Figure 7.1 (panels (b), (d) and (f), show the common time period of operation of the GOME-2B and GOME-2C sensors, hence since the beginning of 2019 onwards.

The monthly mean percentage differences of the two sensors with respect to the ground network range between:

#### **GOME-2B**

- 1a) -1 to +3 % before 2022, and
- 1b) -3 to +2.5 % afterwards (especially decreasing below -2 % in 2024)

#### **GOME-2C**

- 2a) 0 to +2.5 % for the first year of the GOME-2C operation,
  - 2b) which is shifted to +1.5 to +4 % after March 2020,
- depending on the season and the ground-based reference.

This seasonality in the differences between satellite and ground-based is more pronounced in the Dobson co-locations (panels c – f) and is a well-known feature which appears in most operational

and scientific satellite TOC comparisons, see for e.g. the validation of the OMI/Aura products [Balis *et al.*, 2007a], the GOME/ERS-2 product [Balis *et al.*, 2007b] and even the recent GOME/ERS-2, SCIAMACHY/Envisat and GOME-2A ESA products [Koukouli *et al.*, 2015, Garane *et al.*, 2018]. The reasons have to do with the treatment of the variability of the stratospheric temperature and how that affects the ozone absorption coefficients used in the different algorithms [Fragkos *et al.*, 2013; Serdyuchenko *et al.*, 2014]. Hence, when the stratospheric temperature deviates strongly from what is assumed by the algorithms, which is usually the case during the winter months, the differences between ground and satellite increase. See the work of Koukouli *et al.*, 2016, and discussion therein, on this topic.

The well-known reason for the Dobson total ozone seasonality could be treated following a methodology (see Komhyr *et al.*, 1993 and Koukouli *et al.*, 2016) that is utilized by the LAP/AUTH validation chain to post-correct the Dobson ground-based measurements for their effective temperature dependence, but the correction is always dependent on the temperature dataset that is used for its implementation. Additionally, the official repositories such as WOUDC do not provide temperature corrected data and to keep our validation analysis compatible with other studies and validation reports on various other sensors, it was chosen to use the Dobson ground-based dataset as originally provided by WOUDC.

Using the ground-based measurements as a common reference, Figure 7.1 leads to the noticeable difference in the agreement levels between the two sensors in the NH, which is different before and after spring of 2020:

- Before that point, the deviation of the two sensors was  $\sim 0 - 1$  %, with GOME-2C reporting higher TOCs during summer months by up to  $\sim 0.8$  % with respect to GOME-2B.
- Since March 2020, their deviation gradually increases up to  $\sim 3$  % (June 2022 and 2023), with GOME-2B reporting continuously lower TOCs than GOME-2C. The increased difference between the two sensors also has a seasonal dependence, being lower during winter months ( $\sim 0.5$  % for January 2020,  $\sim 1$  % for January 2021,  $\sim 1.2$  % for January 2022,  $\sim 1.5$  % for January 2023) and higher during summer months ( $\sim 1.6$  % for June 2020,  $\sim 2.3$  % for June 2021,  $\sim 3.0$  % for June 2022 and June 2023).

In the SH (panels c and f) an increased difference, especially pronounced during the spring-summer months, is also seen since March or April 2020, going up to 3 % in January 2024, with GOME-2B reporting continuously lower O<sub>3</sub> values than GOME-2C.

The explanation of GOME-2B continuously decreasing total ozone observations since early 2020 is also confirmed by direct satellite-to-satellite comparisons (not shown here) and is under investigation by the algorithm team.

The observed drift between the two GOME-2 instruments is likely caused by the degradation of the L1 data. For the O<sub>3</sub> slant column density (SCD) fit, we added two pseudo absorbers in the non-operational DOAS retrieval. This improved the observed drift in the SCDs between the two instruments.

A large-scale test in the official testing environment is in preparation. This test will also include the AMF part. Once a reasonable amount of data has been processed, they will be provided to AUTH for comparison to ground based observations. We expect the changes to be in the order of the allowed uncertainty range. Based on a successful validation phase, the updated dataset will be released as operational product.



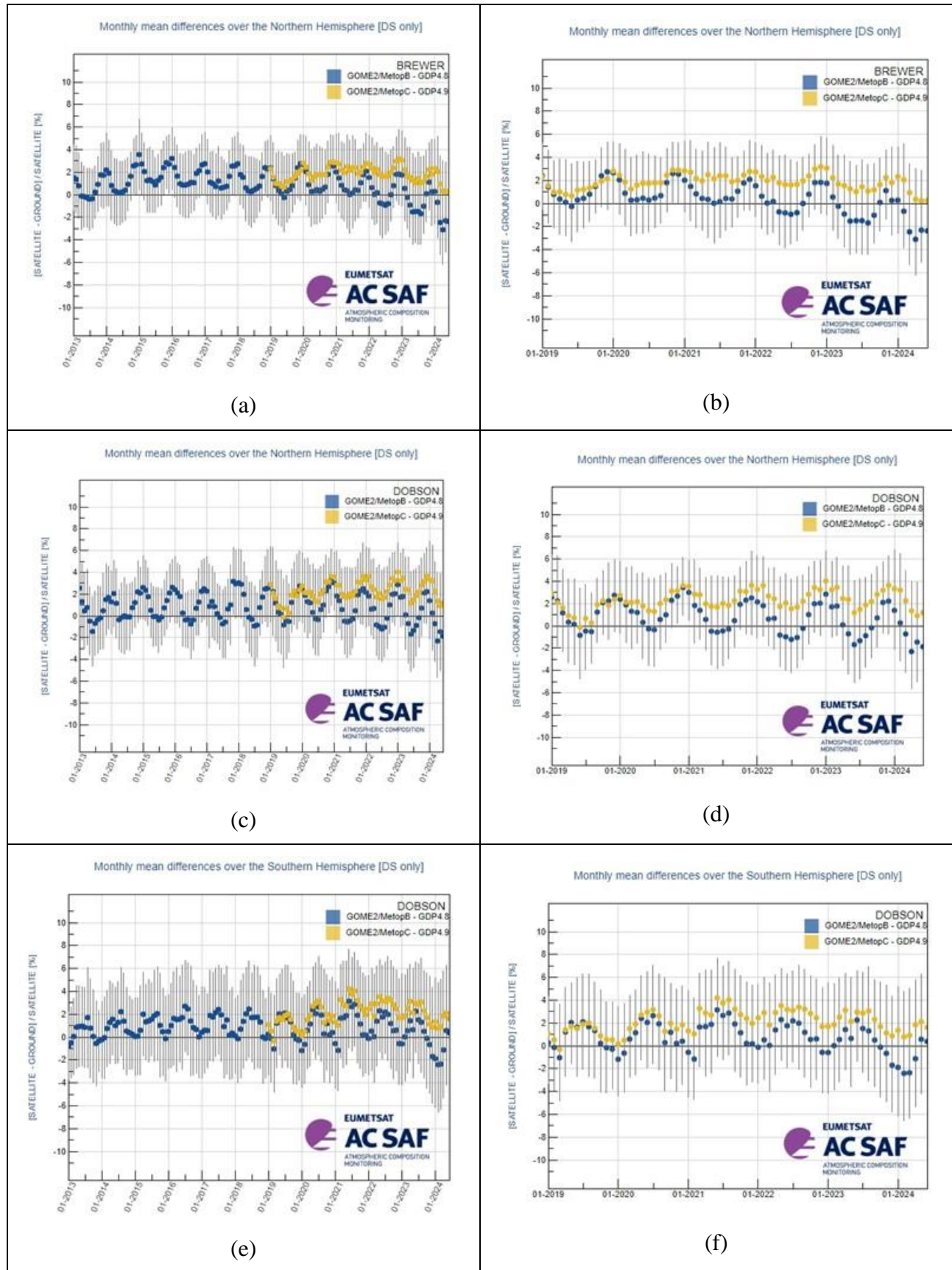


**Figure 7.1. Hemispherical time-series of the monthly mean percentage differences between GOME-2B GDP-4.8 (blue symbols) and GOME-2C GDP-4.9 (orange symbols) total ozone products against**



ground-based observations. Panels a – d: Northern Hemisphere, panels e and f: Southern Hemisphere. Brewer co-locations are shown in panels a and b (Northern Hemisphere only). Dobson co-locations are shown in panels c – f. The difference between the left and the right column of figures is the time period covered.

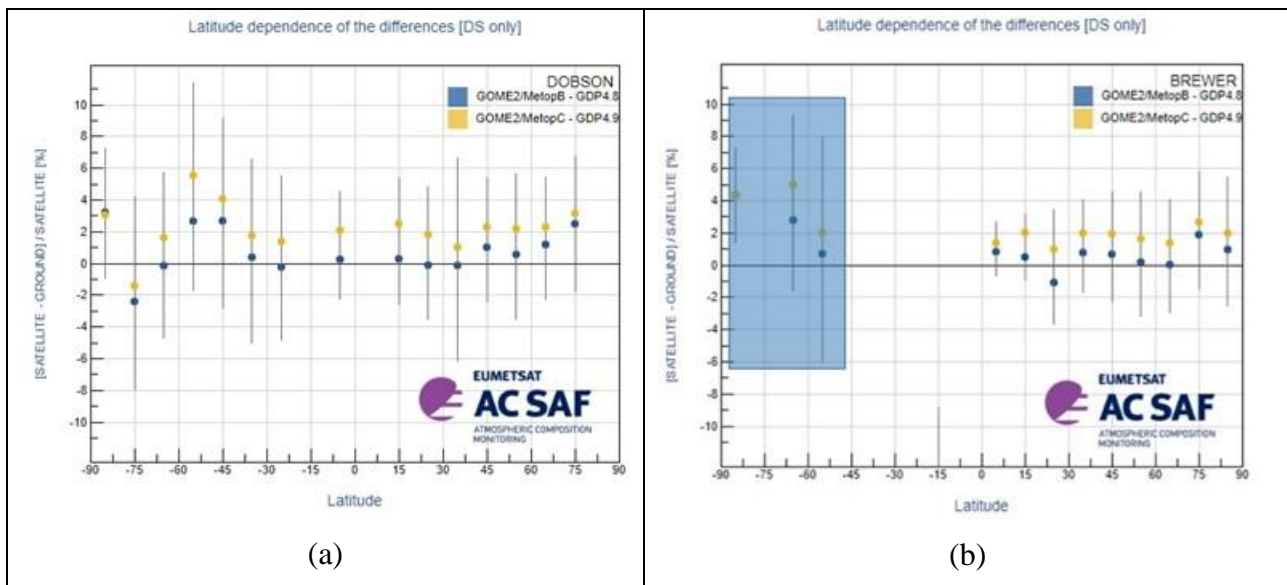


**Figure 7.2. The latitudinal dependency of the differences for the Dobson (panel a) and the Brewer network (panel b). The Brewer SH mean biases are greyed-out because the limited number of stations in this part of the earth cannot provide reliable validation results.**

In the latitudinal plot (Figure 7.2), it is shown that the overall agreement of both sensors to the ground-based measurements is within 0 – 2 % in the tropics and the mid-latitudes. Additionally, it is noticeable that the comparisons of GOME-2C with respect to ground-based measurements have almost no dependency on latitude, having a very stable relative mean bias of ~2 % for the NH stations and for co-locations northwards 70°S. The TOC underestimation of GOME-2B with respect to GOME-2C is also shown to be global, but it appears to be more evident for the mid-latitudes and the tropics, where GOME-2B reports lower TOCs by about 1 – 2 % with respect to GOME-2C.

It should be noted that the co-locations used in Figure 7.2 cover the time-period of the two sensors operating in tandem, since January 2019. The respective latitudinal plot made with co-locations covering only 2022 (not shown here), when the divergence between the two sensors is stronger, indicates that these recently increased differences between the GOME-2B and GOME-2C total ozone observations result almost equally from all latitude belts.

### 7.1.1.3 Tables of statistics

In Table 7.2, the summary statistics for the GOME-2B and GOME-2C comparisons against co-located total ozone observations from the Dobson and Brewer stations presented in the previous section, are enumerated. The number of individual daily common observations for the Dobsons apply to the entire globe, whereas the Brewer comparisons depict only the NH. As can be noted, the relative differences between GOME-2B and Brewer and Dobson stations is quite stable, with an average mean difference of about  $+0.6 \pm 4.5$  %. GOME-2C has a higher mean relative bias with respect to ground-based measurements, of  $+1.4$  to  $+2.2 \pm 4.0$  %. Nevertheless, **both total ozone products are within the product accuracy requirements (4 % for SZA < 80° and 8 % for SZA > 80°).**

**Table 7.2. Summary statistics for the respective time period of operation of each sensor, based on GOME-2B and GOME-2C OTO data compared to WOUDC Brewer & Dobson observations**

		Brewer	Dobson
<b>GOME-2B</b> <b>01/2013 – 06/2024</b>	# stations:	68	64
	# obs:	184 877	126 176
	Mean Rel. Bias (%):	<b><math>0.55 \pm 4.30</math></b>	<b><math>0.72 \pm 4.81</math></b>
<b>GOME-2C</b> <b>01/2019 – 06/2024</b>	# stations:	57	52
	# obs:	78 350	50 993
	Mean Rel. Bias (%):	<b><math>1.39 \pm 3.96</math></b>	<b><math>2.19 \pm 4.91</math></b>

**7.1.1.4 Validation results for the NRT total ozone products**

The GOME-2B and GOME-2C NRT total ozone products are continuously validated against Brewer and Dobson TOCs routinely deposited in the World Meteorological Organisation (WMO) [Ozone Mapping Centre](#), also hosted by the Laboratory of Atmospheric Physics, AUTH. The comparative datasets that cover the last two-three years of observations, are updated weekly and they are operationally available by the [online quality monitoring tool operated by AUTH](#). Some indicative plots are shown in Figure 7.3.

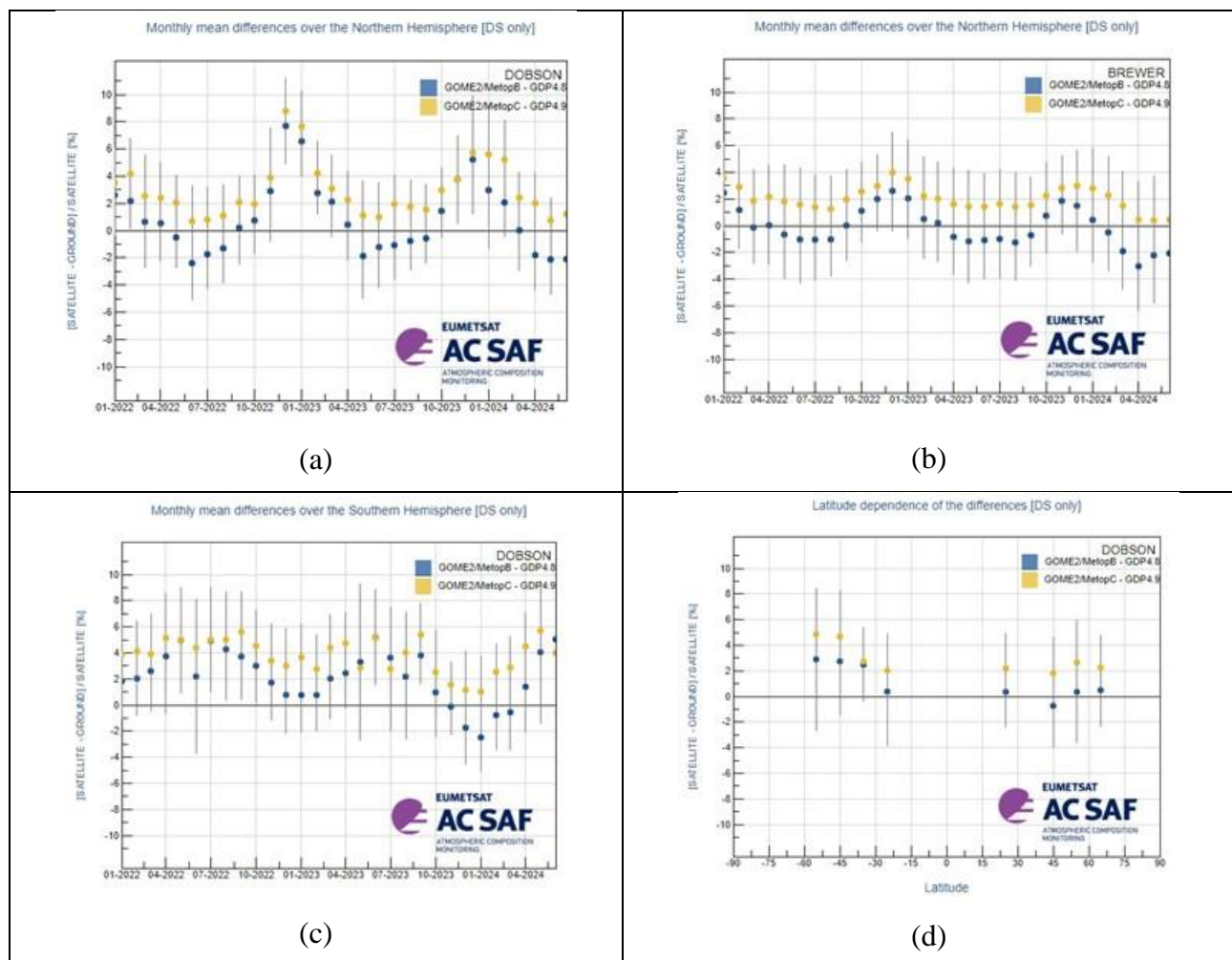


**Figure 7.3. The percentage differences of the GOME-2B (blue) and GOME-2C (orange) NRT total ozone observations against the Dobson (panels a, c, and d) and Brewer (panel b) ground-based co-located measurements. Panels (a) and (c) show the Dobson NH (panel a) and SH (panel c) monthly mean timeseries. Panel (b) shows the Brewer NH monthly mean timeseries. The Dobson latitudinal dependency plot is shown in panel (d), made with co-locations since January 2022.**

### 7.1.2. Validation website

The [AC SAF Ozone Validation & Quality Assessment](#) was launched on the initiation of the project's CDOP 2 phase in 2013. The validation webpages host the validation results of GOME-2A GDP-4.8, GOME-2B GDP4.8 and GOME-2C GDP4.9 near real-time and offline total ozone data. Currently, the validation results are available until August 2024.

The website and the processing algorithms that run behind it are routinely inspected and quality controlled. All the necessary actions, needed to keep it at its current good state, are taken by the LAP/AUTH team.

### References:

- Antón, M., Loyola, D., López, M., Vilaplana, J. M., Bañón, M., Zimmer, W., and Serrano, A.: Comparison of GOME-2/MetOpA total ozone data with Brewer spectroradiometer data over the Iberian Peninsula, *Annales Geophysicae*, 27, 1377–1386, 2009.  
<https://doi.org/10.5194/angeo-27-1377-2009>
- Balis, D., Kroon M., Koukouli, M.E., Brinksma, E. J., Labow, G., Veefkind, J. P., and McPeters, R. D.: Validation of Ozone Monitoring Instrument total ozone column measurements using Brewer and Dobson spectrophotometer ground-based observations, *J. Geophys. Res.*, 112, D24S46, 2007a.  
<https://doi.org/10.1029/2007JD008796>
- Balis, D., Lambert, J-C., Van Roozendael, M., Spurr, R., Loyola, D., Livschitz, Y., Valks, P., Amiridis, V., Gerard, P., Granville, J., and Zehner, C.: Ten years of GOME/ERS-2 total ozone data – The new GOME data processor (GDP) version 4: 2. Ground-based validation and comparisons with TOMS V7/V8, *J. Geophys. Res.*, vol. 112, D07307, 2007b.  
<https://doi.org/10.1029/2005JD006376>
- Fragkos, K., Bais, A. F., Balis, D., Meleti, C., and Koukouli, M. E.: The effect of three different absorption cross-sections and their temperature dependence on total ozone measured by a mid-latitude Brewer spectrophotometer, *Atmos. Ocean*, 53, 2015.  
<https://doi.org/10.1080/07055900.2013.847816>
- Hao, N., Koukouli, M. E., Inness, A., Valks, P., Loyola, D. G., Zimmer, W., Balis, D. S., Zyrichidou, I., Van Roozendael, M., Lerot, C., and Spurr, R. J. D.: GOME-2 total ozone columns from MetOp-A/MetOp-B and assimilation in the MACC system, *Atmos. Meas. Tech.*, 7, 2937–2951, 2014.  
<https://doi.org/10.5194/amt-7-2937-2014>
- Koukouli, M. E., Balis, D. S., Loyola, D., Valks, P., Zimmer, W., Hao, N., Lambert, J.-C., Van Roozendael, M., Lerot, C., and Spurr, R. J. D.: Geophysical validation and long-term consistency between GOME-2/MetOp-A total ozone column and measurements from the sensors GOME/ERS-2, SCIAMACHY/ENVISAT and OMI/Aura, *Atmos. Meas. Tech.*, 5, 2169–2181, 2012.  
<https://doi.org/10.5194/amt-5-2169-2012>
- Koukouli, M. E., Lerot, C., Granville, J., Goutail, F., Lambert, J.-C., Pommereau, J.-P., Balis, D., Zyrichidou, I., Van Roozendael, M., Coldewey-Egbers, M., Loyola, D., Labow, G., Frith, S., Spurr, S., and Zehner, C.: Evaluating a new homogeneous total ozone climate data record from

GOME/ERS-2, SCIAMACHY/Envisat and GOME-2/MetOp-A, *J. Geophys. Res. Atmos.*, 120, 12296-12312, 2015.

<https://doi.org/10.1002/2015JD023699>

Koukouli, M. E., Zara, M., Lerot, C., Fragkos, K., Balis, D., van Roozendael, M., Allart, M. A. F., and van der A, R. J.: The impact of the ozone effective temperature on satellite validation using the Dobson spectrophotometer network, *Atmos. Meas. Tech.*, 9, 2055-2065, 2016.

<https://doi.org/10.5194/amt-9-2055-2016>

Loyola, D. G., Koukouli, M. E., Valks, P., Balis, D. S., Hao, N., Van Roozendael, M., Spurr, R. J. D., Zimmer, W., Kiemle, S., Lerot, C., and Lambert, J.-C.: The GOME-2 total column ozone product: Retrieval algorithm and ground-based validation, *J. Geophys. Res.*, 116, 2011.

<https://doi.org/10.1029/2010JD014675>

Serdyuchenko, A., Gorshelev, V., Weber, M., Chehade, W., and Burrows, J. P.: High spectral resolution ozone absorption cross-sections – Part 2: Temperature dependence, *Atmos. Meas. Tech.*, 7, 625–636, 2014.

<https://doi.org/10.5194/amt-7-625-2014>

Garane, K., Lerot, C., Coldewey-Egbers, M., Verhoelst, T., Koukouli, M. E., Zyrichidou, I., Balis, D. S., Danckaert, T., Goutail, F., Granville, J., Hubert, D., Keppens, A., Lambert, J.-C., Loyola, D., Pommereau, J.-P., Van Roozendael, M., and Zehner, C.: Quality assessment of the Ozone\_cci Climate Research Data Package (release 2017) – Part 1: Ground-based validation of total ozone column data products, *Atmos. Meas. Tech.*, 11, 1385-1402, 2018.

<https://doi.org/10.5194/amt-11-1385-2018>

Garane, K., Koukouli, M.-E., Verhoelst, T., Lerot, C., Heue, K.-P., Fioletov, V., Balis, D., Bais, A., Bazureau, A., Dehn, A., Goutail, F., Granville, J., Griffin, D., Hubert, D., Keppens, A., Lambert, J.-C., Loyola, D., McLinden, C., Pazmino, A., Pommereau, J.-P., Redondas, A., Romahn, F., Valks, P., Van Roozendael, M., Xu, J., Zehner, C., Zerefos, C., and Zimmer, W.: TROPOMI/S5P total ozone column data: global ground-based validation and consistency with other satellite missions, *Atmos. Meas. Tech.*, 12, 5263–5287, 2019.

<https://doi.org/10.5194/amt-12-5263-2019>

### 7.1.3. Online quality monitoring

The online quality monitoring tool is operational and consists of the continuous generation of plots showing the slant column density (SCD) distribution, the vertical column density (VCD) distribution as well as the root mean square (RMS) as histograms per sensing day as well as time series per sensing month. These plots are generated for three different geographic regions, the Pacific ocean (25-15S, 210-250E), the Sahara desert (20-30N, 0-30E) and global, in order to represent typical extremes of ground reflectivity and atmospheric conditions as well as the global mean. The plots are generated per sensing instrument (GOME-2B, GOME-2C) and per product (O<sub>3</sub>, NO<sub>2</sub>, BrO, HCHO, SO<sub>2</sub>, H<sub>2</sub>O).

The online quality monitoring plots are published in PDF format on the DLR AC SAF FTP server ([acsaf.eoc.dlr.de](https://acsaf.eoc.dlr.de)) using the following directory schemes:

/oq/GOME-2[BC]/[O<sub>3</sub> NO<sub>2</sub> BrO HCHO SO<sub>2</sub> H<sub>2</sub>O]/daily/YYYY/MM/DD/[global sahara pacific]/\*.[vcd scd rms]\_hist.pdf

/oq/GOME-2[BC]/[O<sub>3</sub> NO<sub>2</sub> BrO HCHO SO<sub>2</sub> H<sub>2</sub>O]/monthly/YYYY/MM/[global sahara pacific]/\*.[vcd scd rms]\_series.pdf

More information about quality monitoring of the operational GOME-2 total ozone columns by other AC SAF and external partners is available at the following websites:

<https://acsaf.org> → Validation & QA → QM websites

[http://acsaf.physics.auth.gr/eumetsat/validation/near\\_real](http://acsaf.physics.auth.gr/eumetsat/validation/near_real)

<http://acsaf.physics.auth.gr/eumetsat/validation/offline>

<https://www.temis.nl/acsaf/vod.php>

## 7.2. GOME-2 tropospheric ozone products

**Table 7.3. Validation status of tropospheric ozone products**

Product Identifier	Product Name	Accuracy	Reference	Validating Institute	Correlative data sources	
O3M-35	Offline tropical tropospheric ozone	Fulfils target accuracy requirement	RD16	KMI	Ozonesonde data from <a href="#">SHADOZ</a> , <a href="#">NDACC</a> , <a href="#">NILU</a> and <a href="#">WOUDC</a>	
O3M-43			RD20			
O3M-302						
O3M-174	NRT global tropospheric ozone	Fulfils target accuracy requirement	RD17	KMI	Ozonesonde data from <a href="#">SHADOZ</a> , <a href="#">NDACC</a> , <a href="#">NILU</a> and <a href="#">WOUDC</a>	
O3M-304			RD21			
O3M-173	Offline global tropospheric ozone	Fulfils target accuracy requirement	RD17	KMI	Ozonesonde data from <a href="#">SHADOZ</a> , <a href="#">NDACC</a> , <a href="#">NILU</a> and <a href="#">WOUDC</a>	
O3M-175			RD21			
O3M-305						

### Validation activities summary for global tropospheric ozone:

This summary contains validation results of the GOME-2B and GOME-2C high resolution (HR) global tropospheric ozone column (TrOC) products, retrieved by the Ozone Profile Retrieval Algorithm (OPERA) at KNMI. It covers the time period July 2023 – June 2024. Validation results are shown from two TrOC products, i.e. the tropopause related product and a fixed altitude TrOC product. The TrOC products are derived from the daily operational ozone profile product.

Since these TrOC products are derived from the OPERA ozone profile product, OPERA averaging kernel smoothing has been applied to the ground-based reference profiles before calculating comparison statistics. This AVK smoothing is expected to reduce the vertical smoothing difference error between satellite and ground-based measurements. The outcome is summarized at the end of this section.

The global tropospheric ozone column (TrOC) product has the following user requirements:

- Threshold accuracy: within 50 %
- Target accuracy: within 20 %
- Optimal accuracy: within 15 %

This summary was made available by Dr. Andy Delcloo from KMI. More information on how these values are extracted is available in the [validation report](#). The collocation data used are the same as for the ozone profiles (Figure 7.21).



The statistics on the accuracy of the GOME-2B and GOME-2C HR tropospheric ozone column products (tropopause related) for different latitude belts, validated against  $X_{\text{AVK-sonde}}$ , are shown in Table 7.4 and Table 7.5.

**Table 7.4. Relative differences (RD) and standard deviation (STDEV) are shown (in percent) together with the absolute difference (DU) on the accuracy of the GOME-2B HR tropospheric ozone column products (tropopause related) for five different latitude belts, validated against  $X_{\text{AVK-sonde}}$**

July 2023 – June 2024		GOME-2B HR		
	RD (%)	STDEV (%)	AD (DU)	STDEV (DU)
Northern Polar Region	-7.74	28.6	-1.54	8.17
Northern Mid-Latitudes	-3.03	25.7	-0.64	7.36
Tropical region	12.1	33.5	2.55	7.33
Southern Mid-Latitudes	2.76	31.7	0.78	6.34
Southern Polar Region	-21.5	19.8	-3.58	3.76

**Table 7.5. Relative differences (RD) and standard deviation (STDEV) are shown (in percent) together with the absolute difference (DU) on the accuracy of the GOME-2C HR tropospheric ozone column products (tropopause related) for five different latitude belts, validated against  $X_{\text{AVK-sonde}}$**

July 2023 – June 2024		GOME-2C HR		
	RD (%)	STDEV (%)	AD (DU)	STDEV (DU)
Northern Polar Region	-2.16	12.9	-0.68	3.64
Northern Mid-Latitudes	6.46	19.0	1.76	5.60
Tropical region	42.6	40.7	9.29	7.78
Southern Mid-Latitudes	1.31	24.1	0.32	4.56
Southern Polar Region	-18.9	23.6	-2.54	3.59

The statistics on the accuracy of the GOME-2B and GOME-2C HR tropospheric ozone column products (fixed altitude) for different latitude belts, validated against  $X_{\text{AVK-sonde}}$ , are shown in Table 7.6 and Table 7.7.

**Table 7.6. Relative differences (RD) and standard deviation (STDEV) are shown (in percent) together with the absolute difference (DU) on the accuracy of the GOME-2B HR tropospheric ozone column products (fixed altitude) for five different latitude belts, validated against  $X_{\text{AVK-sonde}}$**

July 2023 – June 2024		GOME-2B HR		
	RD (%)	STDEV (%)	AD (DU)	STDEV (DU)
Northern Polar Region	-2.18	12.8	-0.36	2.32
Northern Mid-Latitudes	-2.64	12.6	-0.34	2.31
Tropical region	5.43	32.0	0.66	3.93
Southern Mid-Latitudes	0.73	14.6	0.09	1.55
Southern Polar Region	-15.8	12.0	-1.45	1.18

**Table 7.7. Relative differences (RD) and standard deviation (STDEV) are shown (in percent) together with the absolute difference (DU) on the accuracy of the GOME-2C HR tropospheric ozone column products (fixed altitude) for five different latitude belts, validated against X<sub>AVK-sonde</sub>**

July 2023 – June 2024	GOME-2C HR			
	RD (%)	STDEV (%)	AD (DU)	STDEV (DU)
Northern Polar Region	-1.03	5.09	-0.21	0.95
Northern Mid-Latitudes	2.44	10.5	0.37	1.78
Tropical region	31.2	33.1	3.80	3.51
Southern Mid-Latitudes	0.54	10.3	0.02	1.10
Southern Polar Region	-8.99	10.2	-0.73	1.00

For the GOME-2B and GOME-2C TrOC products, most of these products comply with the target accuracy requirement. Only for the tropical region (GOME-2C), this is obviously not the case. Between all sensors, there is a clear offset visible in the results. Also here, a degradation correction will be necessary to correct for this offset.

### Validation activities summary for tropical tropospheric ozone:

This summary contains validation results of the GOME-2B and GOME-2C tropical tropospheric ozone column (TTrOC) products, using the cloud slicing method. The tropospheric ozone retrieval is based on the GOME-2 ozone columns as derived by the GOME Data Processor (GDP, version 4.8) and covers the tropical latitude belt (20S – 20N). This product is available on a monthly basis and has a resolution of 1.25° latitude x 2.5° longitude.

The tropical tropospheric ozone column product has the following user requirements:

- Threshold accuracy: within 50 %
- Target accuracy: within 25 %
- Optimal accuracy: within 15 %

This summary was made available by Dr. Andy Delcloo from KMI. More information on how these values are extracted is available in the [validation report](#). The collocation data used are the same as for the ozone profiles (Figure 7.21).

The time period covered is January 2022 – December 2023 for the GOME-2B and GOME-2C offline TTrOC products.

In Table 7.8 and Table 7.9, the statistics on the accuracy of the GOME-2B/C tropical tropospheric ozone column products for different stations under consideration are shown, showing some general statistics for both datasets.

It is shown that for GOME-2C, most of the stations are within the optimal accuracy (15 %). The correlation varies between 0.3 and 0.7 with a rmse between 2.9 and 7.8 DU. These TTrOC products still fulfill the user requirements.

**Table 7.8. Relative Differences (RD), standard deviation (STDEV), correlation, bias and RMSE are shown on the accuracy of the GOME-2B TTrOC product for the time period January 2022 – December 2023**

Station	RD (%)	STDEV (%)	Correlation	Bias (DU)	RMSE (DU)
Paramaribu	3.61	28.2	0.43	0.59	5.32
Samoa	20.1	28.8	0.56	2.82	5.18
Ascension Island	4.04	13.0	0.83	1.10	3.44
Kuala Lumpur	-6.62	12.1	0.73	-1.47	2.98
Nairobi	15.9	12.1	0.67	2.66	3.09
Natal	6.44	21.5	0.80	1.93	5.47

**Table 7.9. Relative Differences (RD), standard deviation (STDEV), correlation, bias and RMSE are shown on the accuracy of the GOME-2C TTrOC product for the time period January 2022 – December 2023**

Station	RD (%)	STDEV (%)	Correlation	Bias (DU)	RMSE (DU)
Paramaribu	11.1	21.5	0.66	1.96	4.21
Samoa	14.4	23.1	0.66	1.83	3.49
Ascension Island	3.16	27.0	0.50	0.80	7.80
Kuala Lumpur	9.85	18.7	0.35	1.32	2.94
Nairobi	17.4	10.6	0.70	3.01	3.37
Natal	8.66	27.9	0.65	1.75	5.58

### 7.3. GOME-2 trace gas products

**Table 7.10. Validation status of trace gas products**

Product Identifier	Product Name	Accuracy	Reference	Validating Institute	Correlative data sources
O3M-50.1	NRT total NO2	Fulfil threshold accuracy requirement	RD5	BIRA-IASB	NDACC zenithSky measurements
O3M-338			RD24		
O3M-52.1	NRT tropospheric NO2	Fulfil threshold accuracy requirement	RD5	BIRA-IASB	BIRA-IASB and other MAXDOAS stations
O3M-341			RD24		
O3M-55.1	NRT total SO2	Fulfil threshold accuracy requirement	RD9	AUTH	
O3M-374			RD30		
O3M-177	NRT total HCHO	Fulfil threshold accuracy requirement	RD11	BIRA-IASB	BIRA-IASB and other MAXDOAS stations
O3M-344			RD25		



Product Identifier	Product Name	Accuracy	Reference	Validating Institute	Correlative data sources
O3M-51.1	Offline total NO2	Fulfil threshold accuracy requirement	RD5	BIRA-IASB	NDACC zenithSky measurements
O3M-339			RD24		
O3M-37.1	Offline tropospheric NO2	Fulfil threshold accuracy requirement	RD5	BIRA-IASB	BIRA-IASB and other MAXDOAS stations
O3M-53.1			RD24		
O3M-342					
O3M-09.1	Offline total SO2	Fulfil threshold accuracy requirement	RD9	AUTH	
O3M-56.1			RD30		
O3M-375					
O3M-08.1	Offline total BrO	Fulfil threshold accuracy requirement	RD10	BIRA-IASB	BIRA-IASB Harestua zenithSky station and satellite comparisons
O3M-82.1			RD26		
O3M-317					
O3M-10.1	Offline total HCHO	Fulfil target accuracy requirement	RD11	BIRA-IASB	BIRA-IASB and other MAXDOAS stations
O3M-58.1			RD25		
O3M-345					
O3M-12.1	Offline total H2O	Fulfil threshold accuracy requirement	RD12	FMI, DLR	<a href="#">IGRA</a> , <a href="#">COSMIC-SuomiNet</a> , <a href="#">SSM/I</a>
O3M-86.1			RD27		Comparison against GOME-2B water vapour data
O3M-386					

### Validation activities summary:

This summary presents validation activities for offline total and tropospheric NO<sub>2</sub>, total HCHO, and total BrO data products of GOME-2B/C as performed at BIRA-IASB and SO<sub>2</sub> data as performed at AUTH.

The authors of this summary are Gaia Pinardi (for tropospheric NO<sub>2</sub> and HCHO validation), Jean-Christopher Lambert, José Granville and Tijn Verhoelst (for total/stratospheric NO<sub>2</sub> validation), François Hendrick and Jeroen van Gent (for BrO validation) and Jeroen van Gent and MariLiza Koukouli (for quality assessment).

Validation exercises are performed following the protocols described in the original Metop-A, Metop-B and Metop-C [validation reports](#) and updated in Pinardi *et al.* (AMT 2020) and Verhoelst *et al.* (AMT 2021), and the results presented in this report are based on updates of the correlative datasets with the last available – and sometimes improved – versions. While illustrations at a few stations are included in this report, all the updated figures are reported on the [BIRA-IASB trace gases validation server](#).

### Update of database for reference data

For this report, the validation database was updated with ground-based NDACC UVVIS ZenithSky NO<sub>2</sub> data (as usual) and MAXDOAS NO<sub>2</sub> and HCHO data from KNMI and IUPB (as collected for the NIDFORVAL S5p validation project and already used in Pinardi *et al.* (AMT 2020), Verhoelst

*et al.* (AMT 2021) and De Smedt *et al.* (ACP 2021), in order to cover as much as possible the period until mid-2024. BIRA-IASB ZenithSky BrO data at Harestua could not be updated for this report, due to BIRA-IASB responsible personnel absence and are replaced by some comparisons of GOME-2 to TROPOMI BrO VCD.

ZenithSky NO<sub>2</sub> total columns are collected from the NDACC Data Host Facility (to where the data have to be uploaded by instrument PIs within 1 year after data acquisition) and from the SAOZ rapid delivery operational facility operated by LATMOS. The SAOZ at Bauru (Brazil) is unfortunately no longer operational. The ground-based data are then quality assessed and post-processed at BIRA-IASB in preparation for the data comparisons. This preparation includes calculation of the effective ground-based airmasses with which GOME-2 data co-locations will be sought.

The BIRA-IASB MAXDOAS ground-based dataset are automatically retrieved with an improved version of the bePRO profiling algorithm (Cl  mer *et al.*, 2010; Hendrick *et al.*, 2014, Vlemmix *et al.*, 2015) developed within the EU FP7 NORS and QA4ECV projects (aiming at rapid delivery of improved NO<sub>2</sub> and HCHO profiles), and is progressively shifting to the FRM4DOAS analysis chain. The FRM4DOAS (Fiducial Reference Measurements for Ground-Based DOAS Air-Quality Observations) is an ESA activity aiming at the development of the first centralised NRT processing system for MAX-DOAS instruments operated within the international Network for the Detection of Atmospheric Composition Change (NDACC). It includes the launch of the NDACC MAX-DOAS Processing Service in a demonstration mode, focusing on tropospheric and stratospheric NO<sub>2</sub> vertical profiles, total O<sub>3</sub> columns, and tropospheric HCHO profiles as target MAX-DOAS products for the first phase of the project (July 2016 – August 2021), see <https://frm4doas.aeronomie.be/>. The lower tropospheric profiles and vertical columns processing chain rely on parallel runs of optimal-estimation based MMF (Friedrich *et al.*, 2019) and parametrized approach MAPA (Beirle *et al.*, 2019) algorithms and testings of their results coherence. The service is running in a best-effort mode at the time of writing for a limited number of stations belonging to the project partners, and only tropospheric NO<sub>2</sub> and total O<sub>3</sub> are to the NDACC RD database. More details can be found in Van Roozendaal *et al.* 2024.

IUPB and KNMI sites are retrieved respectively with the QA4ECV database approach ([https://uv-vis.aeronomie.be/groundbased/QA4ECV\\_MAXDOAS/index.php](https://uv-vis.aeronomie.be/groundbased/QA4ECV_MAXDOAS/index.php)), as discussed and used in Pinardi *et al.* (AMT 2020) and Verhoelst *et al.* (AMT 2021) for NO<sub>2</sub> and De Smedt *et al.* (ACP 2021) for HCHO. This approach only provides VCD columns, and profiles are not retrieved. These datasets are also used for the online validation of S5p (<https://mpc-vdaf-server.tropomi.eu/no2/no2-offl-maxdoas> and <https://mpc-vdaf-server.tropomi.eu/hcho/hcho-offl-maxdoas>).

The NO<sub>2</sub> and HCHO datasets include the following ground-based stations:

- OHP (from June 2007 to July 2014 with the geometrical approximation, and since August 2014 to March 2017 with the bePRO profiling tool)
- Uccle (from April 2011 to March 2016 with a miniMAXDOAS instrument (Uccle-miniDOAS) and from end of January 2017 to February 2020 with a scientific grade MAXDOAS: Uccle-SG)
- Bujumbura (from November 2013 to July 2017; since then the instrument had a power failure and only limited operations and data transfer was possible)
- LePort, on Reunion Island (from April 2016 to 10 January 2018). The instrument has been reinstalled in June 2018 on the Maïdo site, and data analysis from the FRM4DOAS analysis chain was tested, but it is not adapted for tropospheric (NO<sub>2</sub>, HCHO) gases validation at this mountaneous site and is not used for this report.

- Xianghe (from March 2010 to July 2018 and from October 2019 to August 2022). Since November 2021 the retrievals in the UV are of bad quality and the UV channel broke down early 2022. SO<sub>2</sub> MAXDOAS profiles were also analysed for the whole time-series (2010 to Oct. 2021), although the SO<sub>2</sub> levels are very low now in China nowadays.
- Kinshasa (from Dec 2019 to March 2024). The instrument and the FRM4DOAS processing is described in Yombo Phaka *et al.*, 2023.
- IUPB Bremen and Athens and KNMI Cabauw and De Bilt data used here covers the periods from April/May 2018 to end of June 2024 for NO<sub>2</sub> and the KNMI also for HCHO.

### **Status of GOME-2B and GOME-2C tropospheric NO<sub>2</sub>**

Comparisons with ground-based MAXDOAS instruments is performed similarly as in previous [validation report](#). In Pinardi *et al.* (2020) it is shown that best results are achieved by filtering out the largest pixels and selecting only pixels covering the stations. For GOME-2, the selection includes keeping only pixels with a size of less than 100 km, while selecting pixels over the station, only slightly changes the results, as generally pixels with their center within 50 km, are covering the station. This improvement of the biases comes at the expenses of a strongly reduced number of pixels (see AC SAF Operations Report 1/2020).

Only BIRA MAXDOAS station from Kinshasa can be used over the first period of 2024, and we also used some available MAXDOAS data from KNMI and IUPB, as presented above.

Figure 7.4 shows example of results for GOME-2B and GOME-2C for the newly included site of Kinshasa. Monthly mean differences are calculated for every year and for the whole time-series in order to see the evolution in time of the bias. Table 7.11 reports the median differences and the spread (half the percentile 68) at the stations, with and without the smoothing, and the figures for all the stations can be found on the [BIRA-IASB validation web server](#).

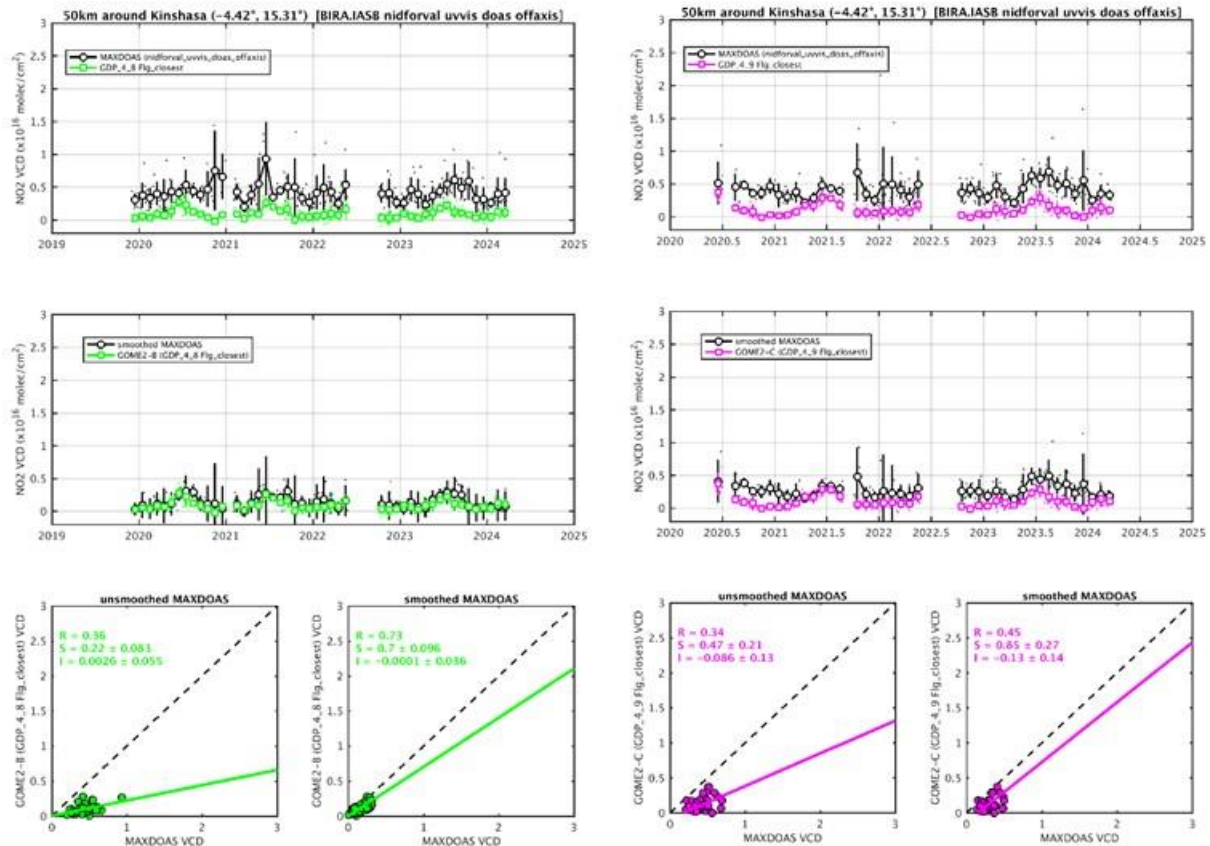


Figure 7.4. Illustration for the Kinshasa MAXDOAS versus GOME-2B GDP-4.8 (left) and GOME-2C GDP-4.9 (right) tropospheric NO<sub>2</sub> comparisons.

Table 7.11. Median Absolute Differences (AD=SAT-GB, in  $10^{15}$  molec/cm<sup>2</sup>), Relative Differences (RD, in %) and spread ( $0.5 \cdot \text{IP68}$ ) on the accuracy of GOME-2B and GOME-2C tropospheric NO<sub>2</sub> products when comparing to MAXDOAS data (NOT cloud filtered). Values for the last 12 months are given, and the values for the whole time-series are reported in brackets for comparison. Results for both the original comparisons (pixels over the station, for pixels smaller than 100 km side) and for the smoothed comparisons are reported. Only the first rows are stations with recent data (in bold below), the others are given as examples of past results.

	GOME-2B			GOME-2C		
	AD ( $\times 10^{15}$ )	RD (%)	SPREAD (%)	AD ( $\times 10^{15}$ )	RD (%)	SPREAD (%)
<b>Bremen (IUPB)</b> <b>Last 12 months:</b> <b>7/2023 – 6/2024</b> <b>[whole period: since 04/2018]</b>	-2.2 [-2.2]	-33 [-38]	46 [58]	-1.4 [-2.2]	-45 [-46]	73 [47]
Athens (IUPB) Last 12 months: 7/2023 – 6/2024 [whole period: since 05/2018]	-2.2 [-1.6]	-39 [-38]	53 [38]	-2.2 [-1.8]	-47 [-39]	19 [38]

	GOME-2B			GOME-2C		
<b>Cabauw (KNMI)</b> <b>Last 12 months:</b> <b>7/2023 – 6/2024</b> <b>[whole period: since 04/2018]</b>	-1.4 [0.22]	-36 [3]	67 [36]	-0.8 [-0.3]	-15 [-4.2]	32 [29]
<b>De Bilt (KNMI)</b> <b>Last 12 months:</b> <b>7/2023 – 6/2024</b> <b>[whole period: since 04/2018]</b>	-0.2 [-0.1]	-5.4 [-1.2]	48 [36]	-0.1 [-0.1]	-12 [-1.2]	75 [41]
<b>Kinshasa *</b> <b>last 12 months:</b> <b>4/2023 – 03/2024</b> <b>[whole period:</b> <b>12/2019 – 03/2024]</b>	-2.8 [-3.1]	-76 [-80]	26.2 [25.3]	-3.3 [-3.1]	-76 [-78]	32 [28]
<b>Kinshasa smoothed *</b>	-0.2 [-0.2]	-23 [-24]	82.5 [53]	-2 [-1.6]	-64 [-66]	35 [38]
Uccle SG last 12 months: 03/2019 – 02/2020 [whole period: 02/2017 – 02/2020]	-1.2 [-1.4]	-16 [-20]	33 [36]	-	-	-
Uccle SG smoothed	-2.5 [-2.7]	-26 [-29]	38 [36]	-	-	-
Reunion Maito (last 12 months: 12/2018 – 11/2019) [whole period: 06/2018 – 11/2019]	-0.02 [-0.02]	-4.2 [-4.3]	76 [93]	-	-	-
Reunion Maito smoothed	-0.03 [-0.01]	-1.4 [-9]	85 [115]	-	-	-
Xianghe (last 12 months: 12/2020 – 07/2022) [whole period: 03/2010 – 07/2022]	0.9 [-0.8]	-4.9 [-4.4]	26 [25]	-0.3 [-0.8]	-1.2 [-9]	23 [21]
Xianghe smoothed	-2.2 [-3.8]	-17 [-18]	28 [36]	-2.1 [-2.4]	-13 [-21]	29 [36]
Bujumbura (last 12 months: 07/2016 – 07/2017) [whole period: 11/2013 – 07/2017]	-3.4 [-3.2]	-83 [-81]	42 [28]	-	-	-
Bujumbura smoothed	-2 [-1.8]	-70 [-74]	21 [35]	-	-	-
OHP (last 12months:	-0.7 [-0.6]	-37 [-28]	34 [36]	-	-	-

	GOME-2B			GOME-2C		
03/2016 – 03/2017) [whole period: 08/2014 – 03/2017]						
OHP smoothed	-0.5 [-0.4]	-36 [-24]	41 [39]	-	-	-
Reunion LePort Last 12 months: 12/2016 – 12/2017) [whole period: 04/2016 – 12/2017]	-1.4 [-1.4]	-83 [-84]	25 [25]	-	-	-
Reunion LePort smoothed	-0.41 [-0.42]	-59 [-60]	22 [25]	-	-	-
Uccle minDOAS (last 12 months: 03/2015 – 03/2016) [whole period: 04/2011 – 03/2016]	-2.6 [-3]	-26 [-31]	25 [24]	-	-	-
Uccle minDOAS smoothed	-3.6 [-3.3]	-29 [-33]	20 [30]	-	-	-

\* The Kinshasa site had to be processed with a different satellite pixels selection (closest valid flagged pixel instead of valid poxel over the site) to have enough daily coincidences and allow meaningful comparisons.

From Figure 7.4 it can be seen, that GOME-2C scatter plot is similar to what obtained with GOME-2B (confirming past results from Xianghe), although the statistics are slightly different, probably due to the presence in GOME-2B period of a few larger NO<sub>2</sub> columns (between  $1 - 2 \times 10^{15}$  molec/cm<sup>2</sup>) that strongly influence the regression analysis (Pinardi *et al.*, 2020). There are some differences in the absolute and relative differences for GOME-2B and GOME-2C and for the last 12 months compared to the whole period. These depend from one station to the other (ie. -15 % bias for GOME-2C compared to -36 % for GOME-2B in Cabauw, -45 % compared to -33 % for Bremen and -12 % compared to -5 % for De Bilt).

The biases results are usually within or close to the requirements (target accuracy requirement of 30 % in polluted conditions and optimal accuracy of 20 %), as it was the case for the other sensors for Xianghe and Uccle in the past. Kinshasa, Cabauw and De Bilt sites are remote sites, with low levels of NO<sub>2</sub> pollution and low biases, while Bremen and Athens are more urban polluted sites, with biases around the -40 % levels, with a spatial comparison mismatch (horizontal dilution component) as highlighted in Pinardi *et al.* (2020) and also seen for other BIRA-IASB sites in the past. Beijing and OHP report about 50 % biases, while larger values are found for Bujumbura and Reunion, as previously (Pinardi *et al.*, 2014; NO<sub>2</sub> Validation Report 2015; Pinardi *et al.*, 2020). As before, smoothing the MAXDOAS profiles with the satellite averaging kernels is not always reducing the mean comparison differences, with an impact of ~10 – 20 % depending on the station (AC SAF Operations Report 1/2018, PT meeting of May 2018). The comparison improvement for Kinshasa is clear in Figure 7.4.

In terms of stability most of the stations report differences over time up to 15 % for both GOME-2B and GOME-2C, which is also about the level of difference between GOME-2B and GOME-2C (10 to 15 %, except Cabauw in this case), and the levels we had in the past between GOME-2A and

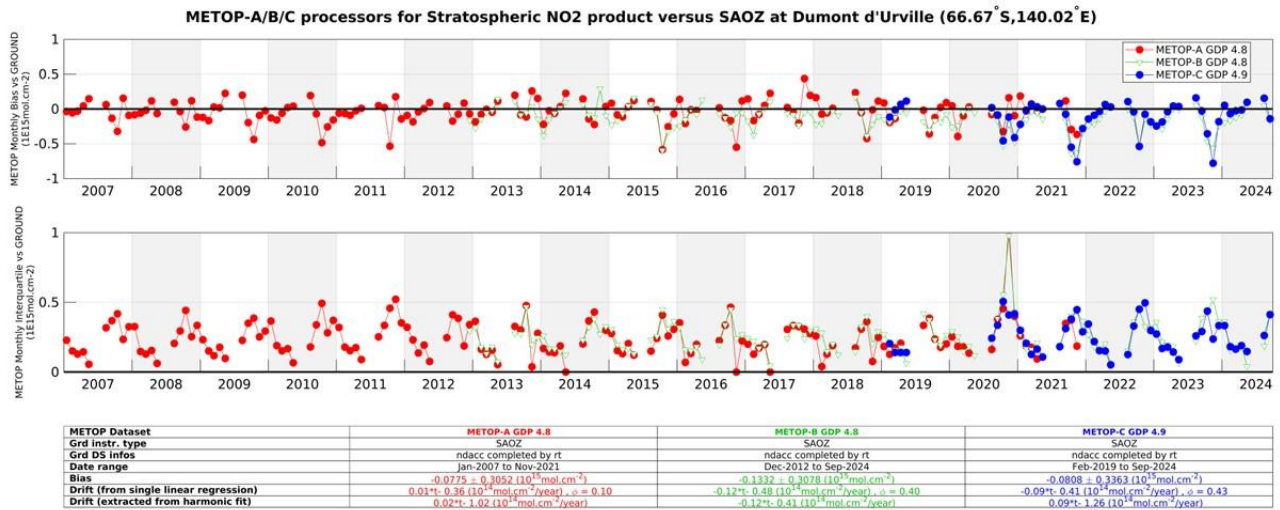


GOME-2B. These biases could be partly reduced in the future with the improved GDP-4.9 GOME-2 algorithm (Liu *et al.*, 2019).

### Status of GOME-2B and GOME-2C total (stratospheric) NO<sub>2</sub>

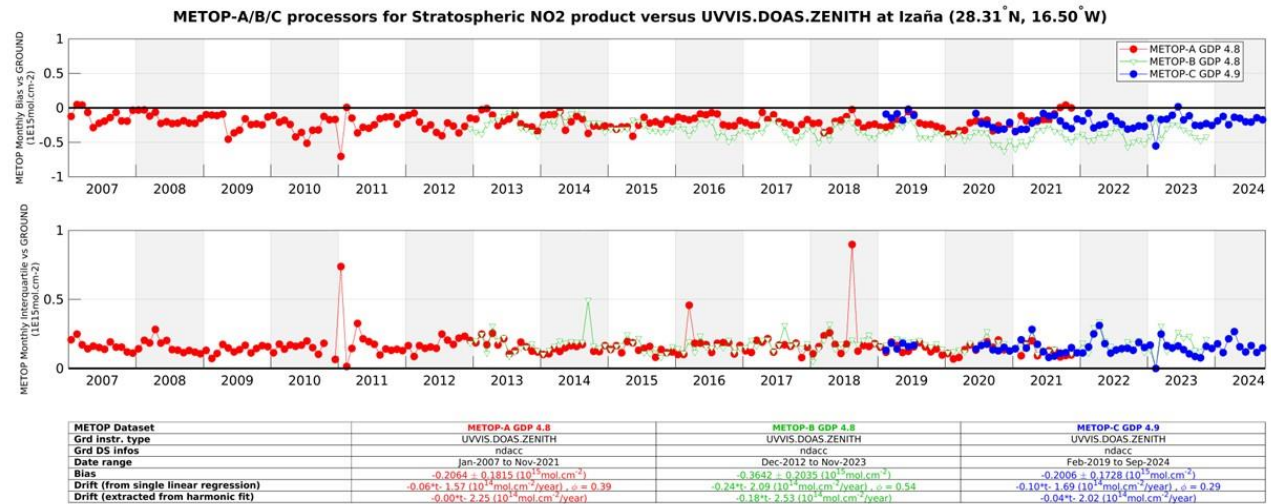
Quality monitoring of the GOME-2 NO<sub>2</sub> total (stratospheric) column data is regularly carried out using correlative ground-based measurements collected from about 20 Zenith-Scattered-Light DOAS UV-visible (ZSL-DOAS) instruments affiliated with the Network for the Detection of Atmospheric Composition Change (NDACC). The NO<sub>2</sub> column validation protocol has already been described in previous AC SAF validation reports with its latest updates published in Verhoelst *et al.* (AMT 2021). This protocol includes the selection of GOME-2/NDACC co-located data pairs based on the air-mass matching technique, a model-based photochemical correction compensating for significant solar local time differences between GOME-2 mid-morning and NDACC twilight observations in polar summer, and a cloud-based filtering of NO<sub>2</sub> data over polluted stations aiming at the removal of pollution-affected pixels. At some stations, real-time processing of the ground-based observations still uses NO<sub>2</sub> absorption cross-sections at room temperature instead of stratospheric temperature. As a result, the retrieved total NO<sub>2</sub> column is affected by a negative systematic bias of 15 – 20 % with a seasonal component. Such data are removed. Thanks to this strict protocol, data comparisons can be carried out within a residual uncertainty of about  $2 - 3 \times 10^{14}$  molec/cm<sup>2</sup> combining both the ground-based data uncertainty and comparison errors. This uncertainty is indicated by the shaded area on the pole-to-pole graphs. Drift estimates are performed using both a strict linear regression (but reporting on the autocorrelation  $\phi$  in the residuals) and a regression including annual and semi-annual terms. The latter can for instance absorb the seasonally varying bias due to the fixed assumed effective temperature in the ZSL-DOAS retrievals.

Figure 7.5 shows the comparison of NO<sub>2</sub> column data at the NDACC Antarctic station of Dumont d'Urville, a station located on the polar circle, in a pristine environment without any known source of tropospheric NO<sub>2</sub>. Comparison results at this station are representative of the validation of purely stratospheric data series, at moderate and large solar zenith angle, and over the full range of NO<sub>2</sub> stratospheric column values from winter lows of about  $1 \times 10^{14}$  molec/cm<sup>2</sup> (wintertime denoxification episodes) up to summer highs of  $7 \times 10^{15}$  molec/cm<sup>2</sup> (complete depletion of N<sub>2</sub>O<sub>5</sub> into NO<sub>2</sub> due to polar midnight Sun). On a monthly median basis, and over the 16 years covered by the three satellites, the target bias of  $3 - 5 \times 10^{14}$  molec/cm<sup>2</sup> hasn't often been exceeded, except occasionally in October when the station is overpassed frequently by the border of the polar vortex, thus when atmospheric variability contributes significant co-location mismatch noise and bias to the difference in stratospheric NO<sub>2</sub>. The ground dataset shown in this figure is a composite dataset consisting of the NDACC reprocessed dataset extended through the last year by the near-real-time dataset (latmos\_rt).



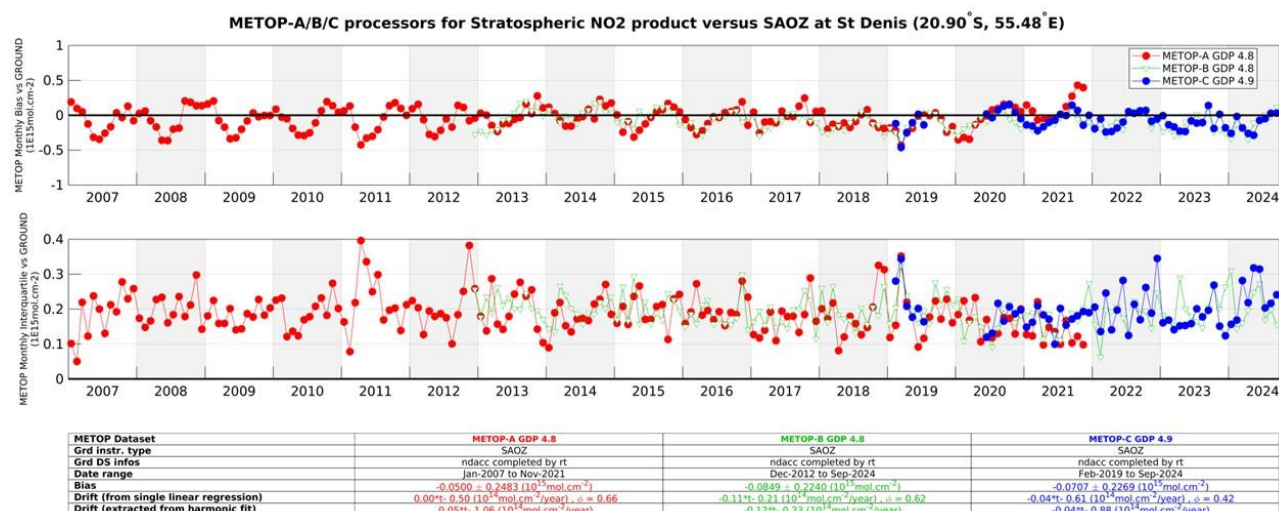
**Figure 7.5.** Comparison of NO<sub>2</sub> column data measured at the NDACC Antarctic station of Dumont d'Urville by the GOME-2 instruments) and by the CNRS/LATMOS ZSL-DOAS spectrometer. Top: time-series of the median NO<sub>2</sub> column difference per month; centre: time-series of the dispersion of the NO<sub>2</sub> column difference per month; bottom (table): summary statistics.

Figure 7.6 and Figure 7.7 display similar results obtained at the NDACC station of Izaña on Tenerife (Canary Islands) and the NDACC Southern Tropic station of Saint-Denis de la Réunion, thus in occasional presence of pollution and over a wider range of solar zenith angle. Again, the target bias of  $3 - 5 \times 10^{14}$  molec/cm<sup>2</sup> has rarely been exceeded, except in very few cases.



**Figure 7.6.** Same as Figure 7.5 but at the NDACC station of Izaña on Tenerife (Canary Islands).





**Figure 7.7. Same as Figure 7.5, but at the NDACC Southern Tropical station of Saint-Denis de la Reunion.**

Figure 7.8 reports from pole to pole the median value and the dispersion of the differences between GOME-2 and NDACC ZSL-DOAS data, while Figure 7.9 displays, again from pole to pole, the linear drift between GOME-2A/B/C and NDACC data. Those graphs show the good long-term stability of the satellite NO<sub>2</sub> column data with respect to NDACC ZSL-DOAS data at all stations.

They also show that the target bias of  $3 - 5 \times 10^{14}$  molec/cm<sup>2</sup> in unpolluted conditions is achieved at virtually all sites for all three satellites. Figure 7.7 also confirms the slight difference already noticed in previous validation reports between the biases observed respectively in the Southern and Northern hemispheres. Averaging median differences separately over the Northern and Southern Hemispheres concludes to an inter-hemispheric bias of about  $2 - 3 \times 10^{14}$  molec/cm<sup>2</sup>. GOME-2C NO<sub>2</sub> column data present a slightly more positive bias across all latitudes. Drift estimates show a bit more scatter for GOME-2C, in particular at high Northern latitudes, but the mission lifetime of GOME-2C is still relatively short for stable drift determination.

Note that for these global statistics visualized in Figure 7.8 and Figure 7.9, only ground instruments yielding co-locations with all 3 satellite instruments (on Metop-A/B/C) were used so as to limit selection biases between sounders.

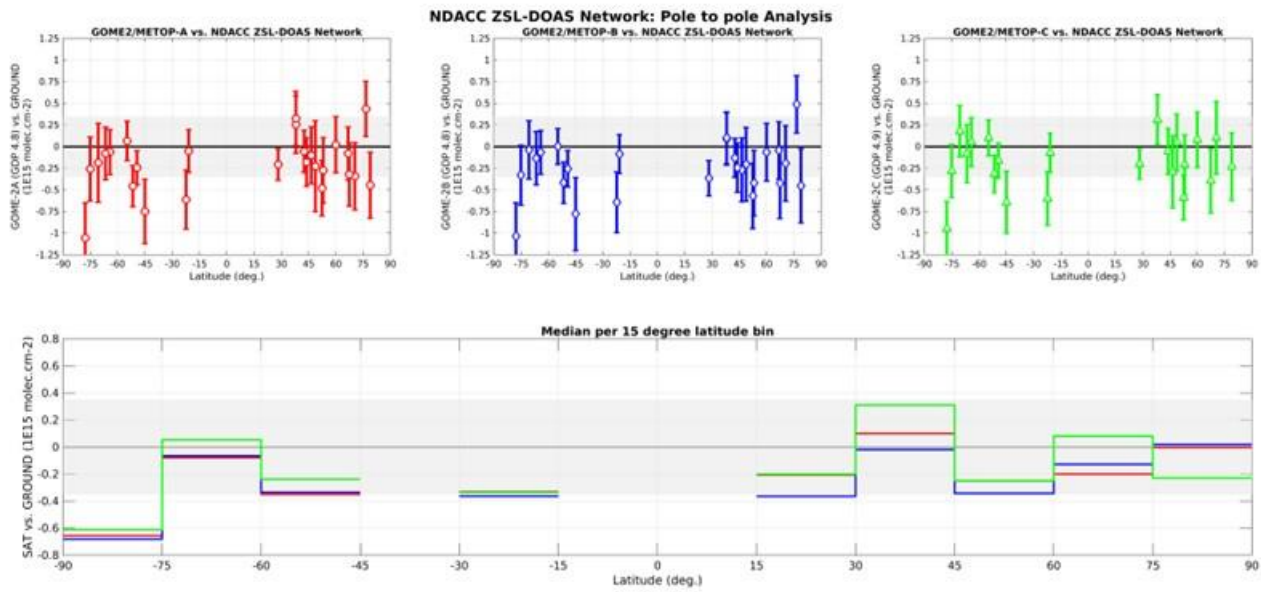


**Figure 7.8.** From pole to pole, median difference between the NO<sub>2</sub> column data reported by GOME-2A/B/C (red/blue/green) GDP-4.8 (GDP 4.9 for GOME-2C) and by ground-based ZSL-DOAS spectrometers at about 20 NDACC stations, calculated over 2007 – November 2021 for GOME-2A, 2012 – March 2024 for GOME-2B and 2019 – March 2024 for GOME-2C. Top: median difference at individual stations. Bottom: median difference averaged over 15° latitude bins.

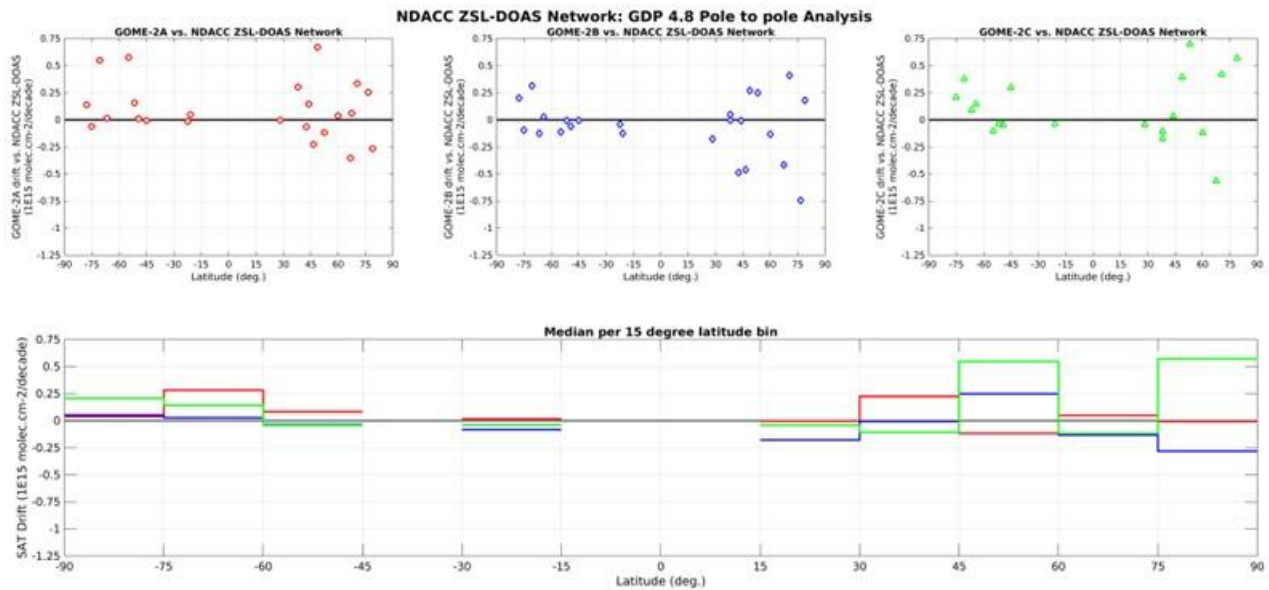


**Figure 7.9.** From pole to pole, linear drift (in percent by decade, from a regression model including annual and semi-annual harmonic terms) of the difference between the NO<sub>2</sub> column data reported by GOME 2A/B/C (red/ blue/ green) GDP 4.8 (GDP 4.9 for GOME-2C) and by ground-based ZSL-DOAS spectrometers at about 20 NDACC stations, calculated over 2007 – November 2021 for GOME-2A, 2012 – March 2024 for GOME-2B and 2019 – March 2024 for GOME-2C. Top: linear drift estimates at individual stations. Bottom: same linear drift estimates but averaged over 15° latitude bins.

### Status of GOME-2B and GOME-2C total HCHO

This validation exercise is an extension of what is presented in the [HCHO GDP-4.8 validation report](#), relying on correlative observations from MAX-DOAS instruments operated by BIRA-IASB at Xianghe, Bujumbura, Uccle (miniDOAS and SG), OHP and Reunion (Le Port and Maito). As discussed above, the only update possible from BIRA-IASB stations is the newly introduced Kinshasa site, so the KNMI Cabauw and De Bilt sites are also included in this report. An illustration of the comparisons for Cabauw are presented in Figure 7.10, past figures can be found on the [BIRA validation web server](#) and a summary is presented in Table 7.12.

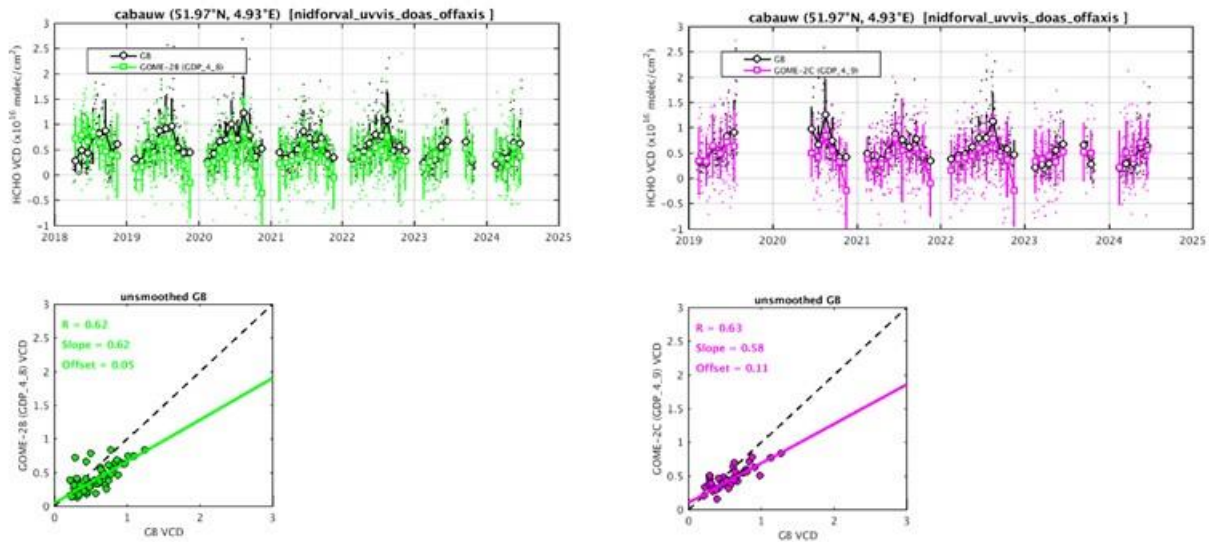


**Figure 7.10.** Illustration for the Cabauw MAXDOAS versus GOME-2B GDP-4.8 (left) and GOME-2C GDP-4.9 (right) HCHO comparisons.

**Table 7.12. Summary of the mean biases (SAT-GB, in  $10^{15}$  molec/cm<sup>2</sup>) between GOME-2B/C and MAX-DOAS HCHO VCDs. The values in parentheses correspond to the mean relative biases (in %) and R is the correlation coefficients and S the slope of the linear regression of the monthly mean points. Only the first two rows are stations with recent data (Cabauw, De Bilt and Kinshasa), the others are given as examples of past results.**

	GOME-2B	GOME-2C
<b>CABAUW</b> (51.97°N, 4.93°E) (whole period: 04/2018 – 05/2023)	$-1.7 \pm 2$ (-29 ± 45) R = 0.62, S = 0.62	$-1.3 \pm 2$ (-23 ± 46) R = 0.63, S = 0.58
<b>DE BILT</b> (52.10°N, 5.18°E) (whole period: 05/2018 – 05/2023)	$-2.3 \pm 2.4$ (-37 ± 57) R = 0.67, S = 0.64	$-1.7 \pm 2.5$ (-29 ± 74) R = 0.64, S = 0.54
<b>KINSHASA</b> (4.42°S, 15.31°E) (whole period: 12/2019 – 10/2023)	$0.4 \pm 2.8$ (-0.3 ± 21) R = 0.8, S = 0.94	$0.1 \pm 3$ (0.5 ± 24) R = 0.78, S = 0.74
<b>UCCLE-SG</b> (50.8°N, 4.3°E) (whole period: 02/2017 – 12/2019)	$0.3 \pm 1.6$ (7 ± 52) R = 0.75, S = 0.96	-
<b>With smoothing</b>	$1.6 \pm 1.7$ (49 ± 75) R = 0.76, S = 1.34	-
<b>REUNION MAIDO</b> (20.9°S, 55.3°E) (whole period: 06/2018 – 11/2019)	$2.1 \pm 0.8$ (94 ± 54) R = 0.84, S = 1.17	-
<b>With smoothing</b>	$1.7 \pm 0.8$ (68 ± 43) R = 0.69, S = 1.29	-
<b>XIANGHE</b> (39.7°N, 117.0°E) (whole period: 03/2010 – 12/2021)	$-6.4 \pm 2.7$ (-48 ± 16) R = 0.88, S = 0.67	$-8.9 \pm 2.6$ (-60 ± 21) R = 0.82, S = 0.76
<b>With smoothing</b>	$0.59 \pm 2.2$ (-8 ± 31) R = 0.88, S = 1.19	$-2.4 \pm 2.7$ (-29 ± 37) R = 0.79, S = 1.40
<b>BUJUMBURA</b> (3.0°S, 29.0°E) (whole period: 11/2013 – 07/2017)	$-4.4 \pm 2.2$ (-32 ± 10) R = 0.88, S = 0.52	-
<b>With smoothing</b>	$0.3 \pm 2.0$ (3.2 ± 25) R = 0.72, S = 0.65	-
<b>OHP</b> (whole period: 08/2014 – 03/2017)	$0.3 \pm 1.1$ (4.2 ± 21) R = 0.90, S = 0.75	-
<b>With smoothing</b>	$103.51 \pm 1.0$ (17 ± 22) R = 0.86, S = 1.01	-
<b>REUNION LEPORT</b> (20.9°S, 55.3°E) (whole period: 04/2016 – 12/2017)	$103.51 \pm 0.8$ (39 ± 26) R = 0.80, S = 1.56	-

<b>With smoothing</b>	2.6 ± 0.1 (180 ± 56) R = 0.78, S = 2.83	-
<b>UCCLE-miniDOAS</b> (50.8°N, 4.3°E) (whole period: 04/2011 – 05/2015)	-0.6 ± 1.6 (-9.4 ± 29) R = 0.76, S = 0.89	-
<b>With smoothing</b>	-0.4 ± 1.7 (7.1 ± 34) R = 0.73, S = 0.88	-

Results obtained at Cabauw, De Bilt and Kinshasa confirm that both satellite instruments capture well the HCHO VCD seasonality. Results for GOME-2B and GOME-2C are similar (as shown also in the past for Xianghe), to within 10 %. Results for the whole period (shown here) and for the last 12 months generally show differences up to 15 % (not shown here, see the different figures for each stations on the BIRA validation web server). In Reunion the signal is very small (less than  $\sim 0.5 \times 10^{16}$  molec/cm<sup>2</sup>) and is more difficult to have firm conclusions.

A significant bias exists between GOME-2B/C and MAX-DOAS observations at the some of the stations (up to 50 %), but as already shown in the GDP-4.8 validation report, for some stations this bias can be significantly reduced when smoothing the MAX-DOAS profiles with the satellite column averaging kernels (see also values with smoothing in Table 7.12).

### Status of GOME-2B and GOME-2C total BrO

GOME-2B/C total columns of BrO from GDP-4.8 (4.9 in the case of GOME-2C) operational product are usually compared to ground-based UV-visible zenith-sky measurements at Harestua, Norway (60°N, 11°E), as done in previous [validation report](#). The ground-based columns are derived from the vertical profiles retrieved by applying an OEM (Optimal Estimation Method) –based profiling technique to zenith-sky measurements at sunrise (Hendrick *et al.*, 2007). The instrument was temporarily off due to problems at the Harestua observatory since 09/12/2022 and is now back in operations since the end of April 2023 with a change of management at the Harestua Solar Observatory. Moreover, due to long-period sickness of key personnel, the ground-based BrO data could not yet be analyzed and this comparison with the GOME-2 instruments could not be updated for this report. We leave the results and discussion of the Operations Report 1/2022 further down in this section.

As a replacement, first introduced in the 2/2023 report, a comparison of total BrO columns from GOME-2B (GDP 4.8 product) and GOME-2C (GDP 4.9 product) on one hand and S5P/TROPOMI on the other hand is made below. The TROPOMI data derives from the total BrO retrieval algorithm TCBRO, developed at BIRA-IASB, that is currently running in the so-called pre-operational environment of the ESA S5P-PAL system (<https://data-portal.s5p-pal.com/>). For this edition, we directly used the high resolution (0.022°) TROPOMI BrO L3 monthly-averaged data from S5P-PAL.

For the satellite-satellite comparison, monthly average BrO VCD values over 2023 have been derived over a 150 km area around 12 well known ground stations, ranging in latitude from the northern to the southern polar region. The geographic locations of these stations are shown in Figure 7.11.



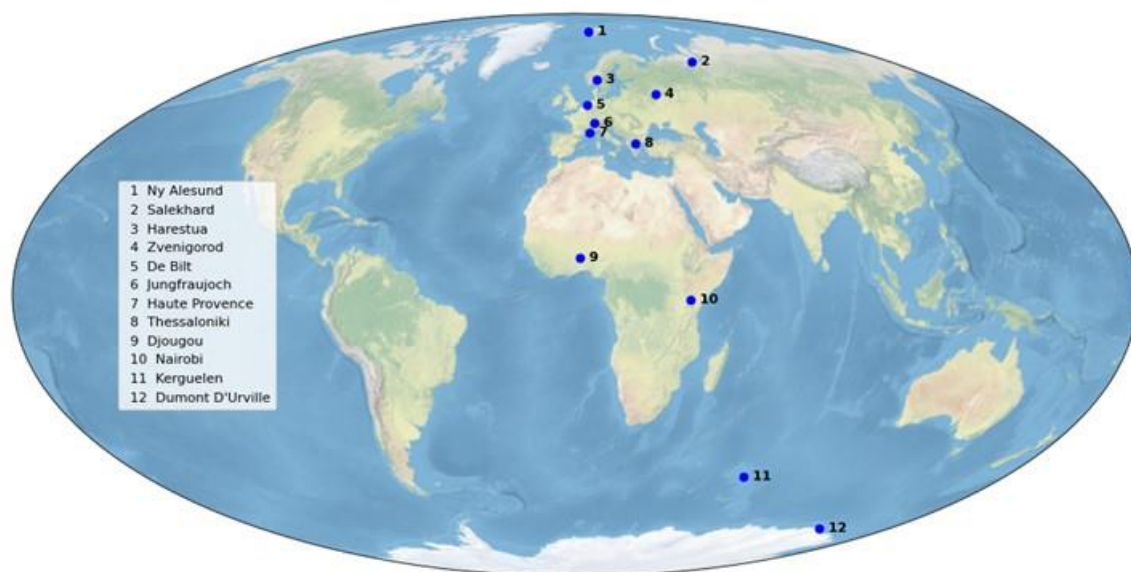


**Figure 7.11. Location of the 12 stations for which overpass BrO VCD values were determined for the three sensors GOME-2A and GOME-2B and TROPOMI. VCD values were determined as average values over an area with a radius of 150 km from the station.**

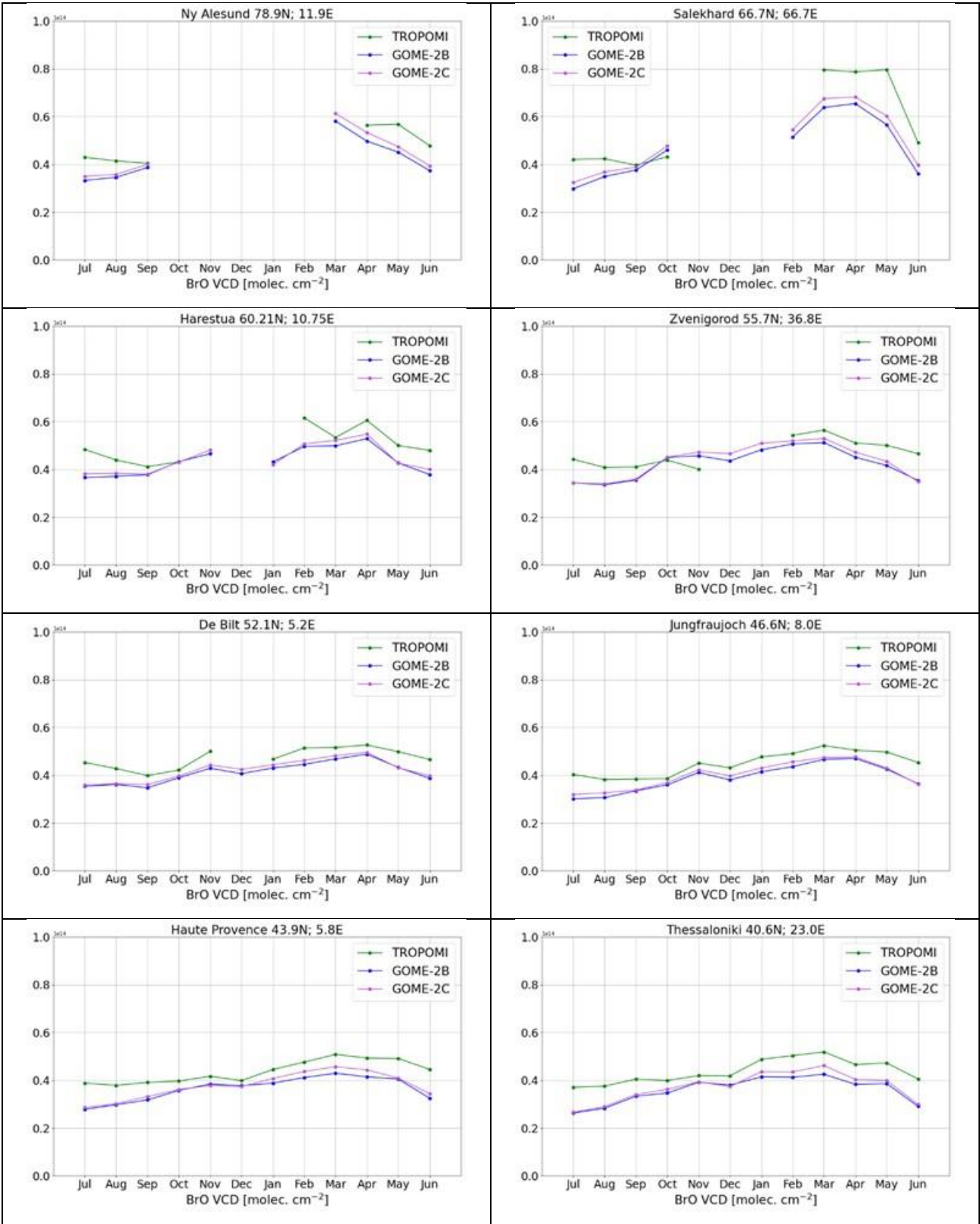
The actual comparison of the BrO VCD values for the three instruments is depicted in Figure 7.12.

Overall, the two GOME-2 instruments closely agree with each other. Although not always, the TROPOMI VCD values tend to be higher than the GOME-2 results. The results from the three instruments agree well, however, when it comes to the variation over the year.

The origin of the negative offset of the GOME-2 values with respect to TROPOMI is not clear. Comparisons of TROPOMI values with Harestua ground measurements for 2019 show a very good agreement (Van Gent and Hendrick, 2022). This agrees with the observed lower values for the GOME-2 instruments with respect to Harestua measurements, as shown in earlier editions of this report (see the results for 2022 below).

Unfortunately, the TROPOMI monthly-averaged data obtained from S5P-PAL seems to show more missing data points than when calculating those values manually. This is quite likely due to the fact that the S5P-PAL data is filtered for qa value > 0.5, which, for example, eliminates pixels with large cloud cover. In future editions of this report we may reconsider the use of S5p-Pal L3 data.

Overall, the deviation of the GOME-2 VCD's with respect to TROPOMI remains within the requirements of 30 %, although somewhat larger deviations are occasionally observed for GOME-2B.



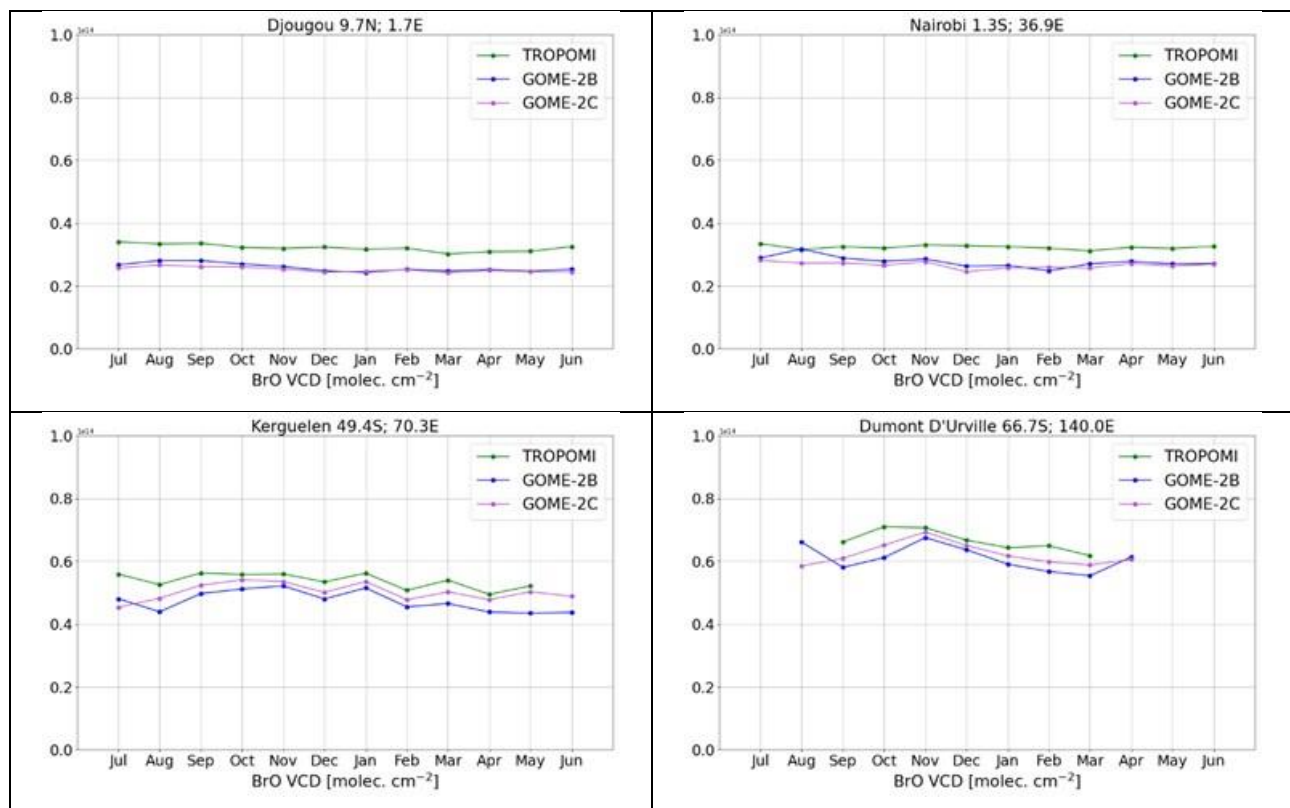


**Figure 7.12. Comparison of monthly average total BrO VCD over 12 ground stations for the sensors GOME-2 B+C and TROPOMI, from July 2023 to end June 2024.**

Below we repeat the results of the comparison of the GOME-2 VCDs with those from Harestua ground measurements of the Operations Report 1/2022.

The sensitivity of these measurements to the troposphere is increased by using a fixed reference spectrum corresponding to clear-sky noon summer conditions for the spectral analysis. In order to ensure the photochemical matching between satellite and ground-based observations, sunrise ground-based columns have been photochemically converted to the satellite overpass SZAs using a stacked box photochemical model (Hendrick *et al.*, 2007 and 2008).

Comparison results (150 km overpasses) for GOME-2B and GOME-2C are shown in Figure 7.13 and Figure 7.14, respectively.

Mean biases values between GOME-2B/C and ground-based data are of  $-15 \pm 11$  % and  $-9 \pm 10$  %. GOME-2B/C BrO columns are thus all within the target accuracy of 30 % and also within the optimal accuracy of 15 %, except GOME-2B which is slightly above the required optimal accuracy threshold.



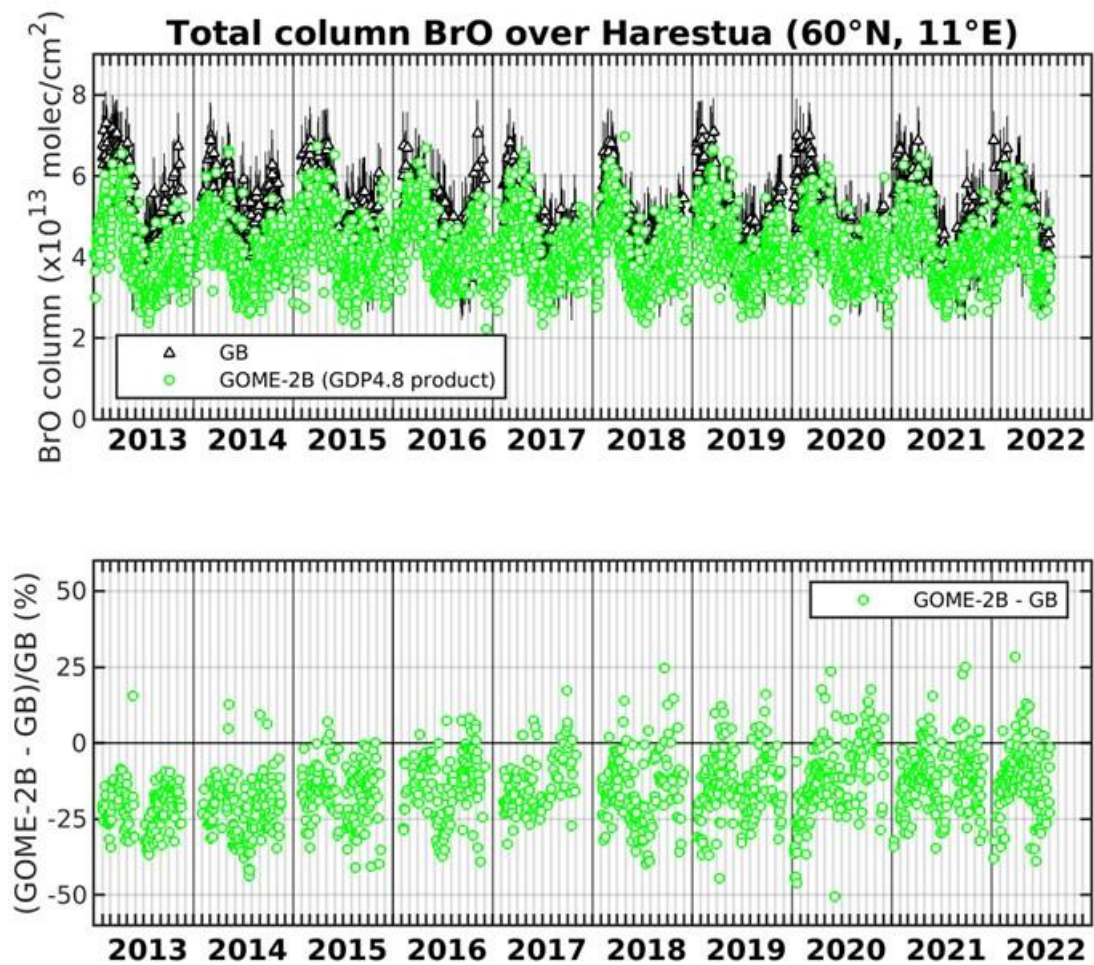
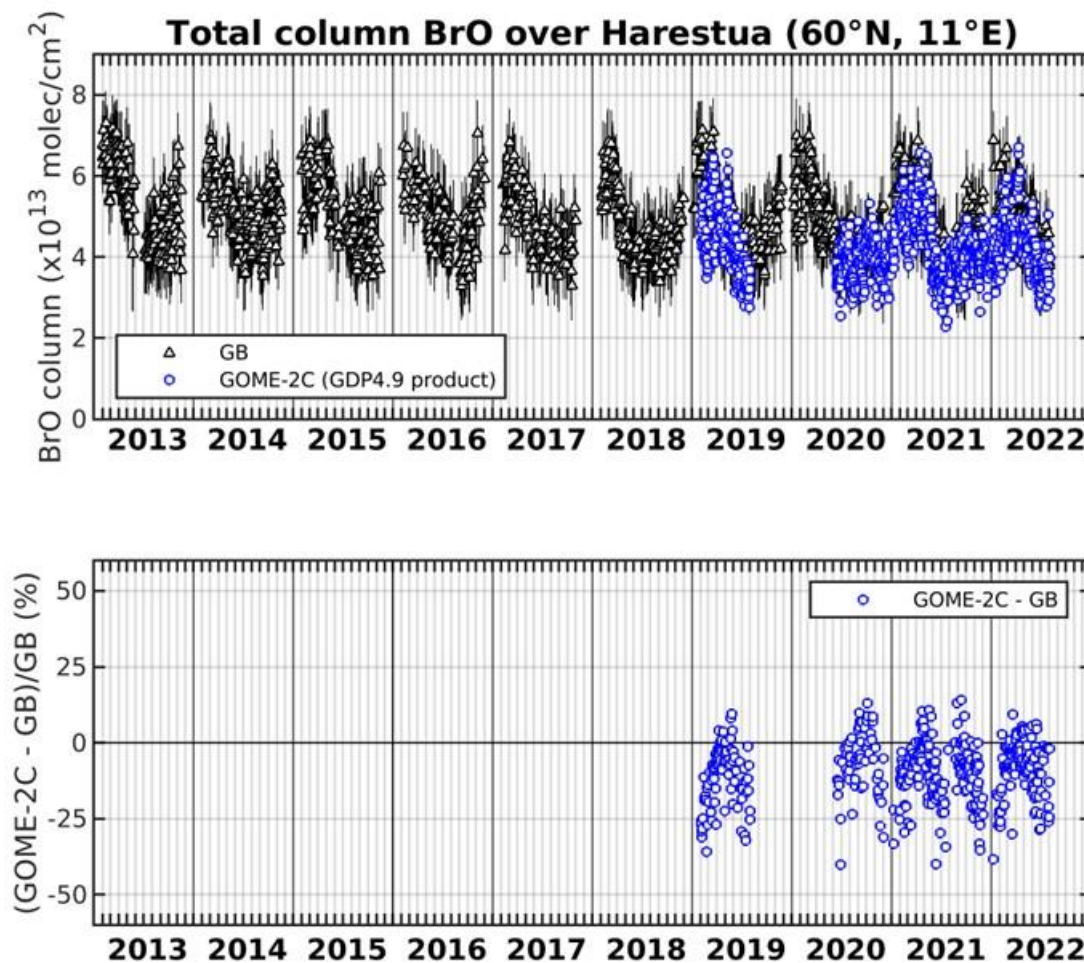


Figure 7.13. Comparison between GOME-2B GDP-4.8 and ground-based total BrO columns at Harestua (60°N, 11°E). The relative differences appear in the lower plot.



**Figure 7.14.** Comparison between GOME-2C GDP-4.9 and ground-based total BrO columns at Harestua (60°N, 11°E). The relative differences appear in the lower plot.

### Status of GOME-2B and GOME-2C SO<sub>2</sub>

GOME-2 SO<sub>2</sub> GDP-4.8 continues to be used for the near-real-time observation of volcanic activity within the SACS service. The Support to Aviation Control Service (SACS) hosted by the Royal Belgian Institute for Space Aeronomy (BIRA-IASB) aims at supporting the Volcanic Ash Advisory Centers, like Toulouse VAAC and London VAAC. This is achieved by delivering near real-time data of SO<sub>2</sub> and aerosols derived from satellite measurements regarding volcanic emissions by UV-VIS (OMI, GOME-2A and GOME-2B composite until 31 March 2021 and GOME-2B and GOME-2C composite since then, OMPS, TROPOMI) and infrared (AIRS, IASI-A, IASI-B) instruments. In case of volcanic eruptions, notifications are sent out by email to interested parties. The SACS notification archive service gathers all the notifications; the results can be found [here](#).

In the first half of 2024, SACS reported a moderate level of volcanic activity throughout, with only two major events of more than 20 DU in SO<sub>2</sub> load as shown in Figure 7.15. GOME-2B issued 114 alerts, with SO<sub>2</sub> loads ranging between 2 and 85.9 DU, with a mean global level of  $5.5 \pm 10.2$  DU and median 3.0 DU. GOME-2C issued 102 alerts, with SO<sub>2</sub> loads ranging between 2 – 83 DU, with a mean global level of  $4.8 \pm 8.4$  DU and median of 2.9 DU.

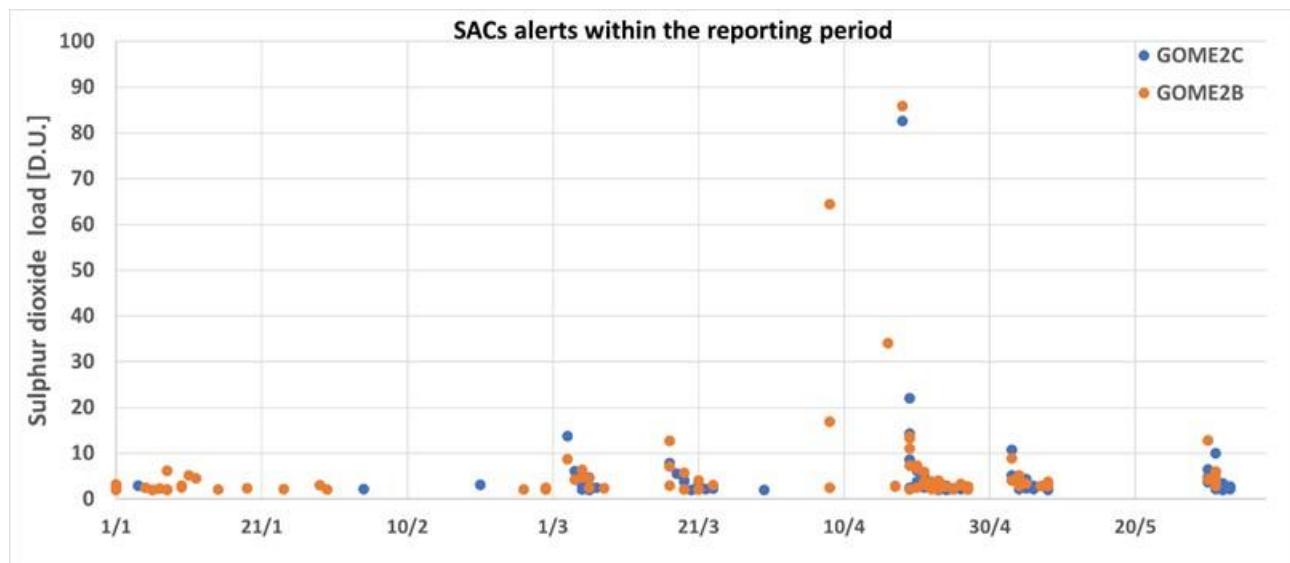


**Figure 7.15. GOME-2B [orange] and GOME-2C [blue] SACS alerts during the reporting period as a function of the SO<sub>2</sub> load observed.**

Dukono, a remote volcano on Indonesia's Halmahera Island, has been erupting continuously since 1933, with frequent ash explosions and sulphur dioxide plumes. The highest reported plume of the period reached 9.4 km above the summit on 14 November 2022. T<sub>h</sub>E Pusat Vulkanologi dan Mitigasi Bencana Geologi (PVMBG; also known as Indonesian Center for Volcanology and Geological Hazard Mitigation, CVGHM) reported that the eruption at Dukono was ongoing during the week of 17 to 23 April 2024. Gray-and-white ash plumes rose 100 – 1200 m above the summit and drifted E, N, and W almost daily. The Alert Level remained at Level 2 (on a scale of 1 – 4), and the public was warned to remain outside of the 3-km exclusion zone. In Figure 7.16 the Mt. Dukono eruptive days of April 18<sup>th</sup> and April 19<sup>th</sup>, 2024, are presented. The GOME2-B/C combined product appears to capture the event very well, both in terms of sulphur dioxide load and location of the volcanic SO<sub>2</sub> plume.



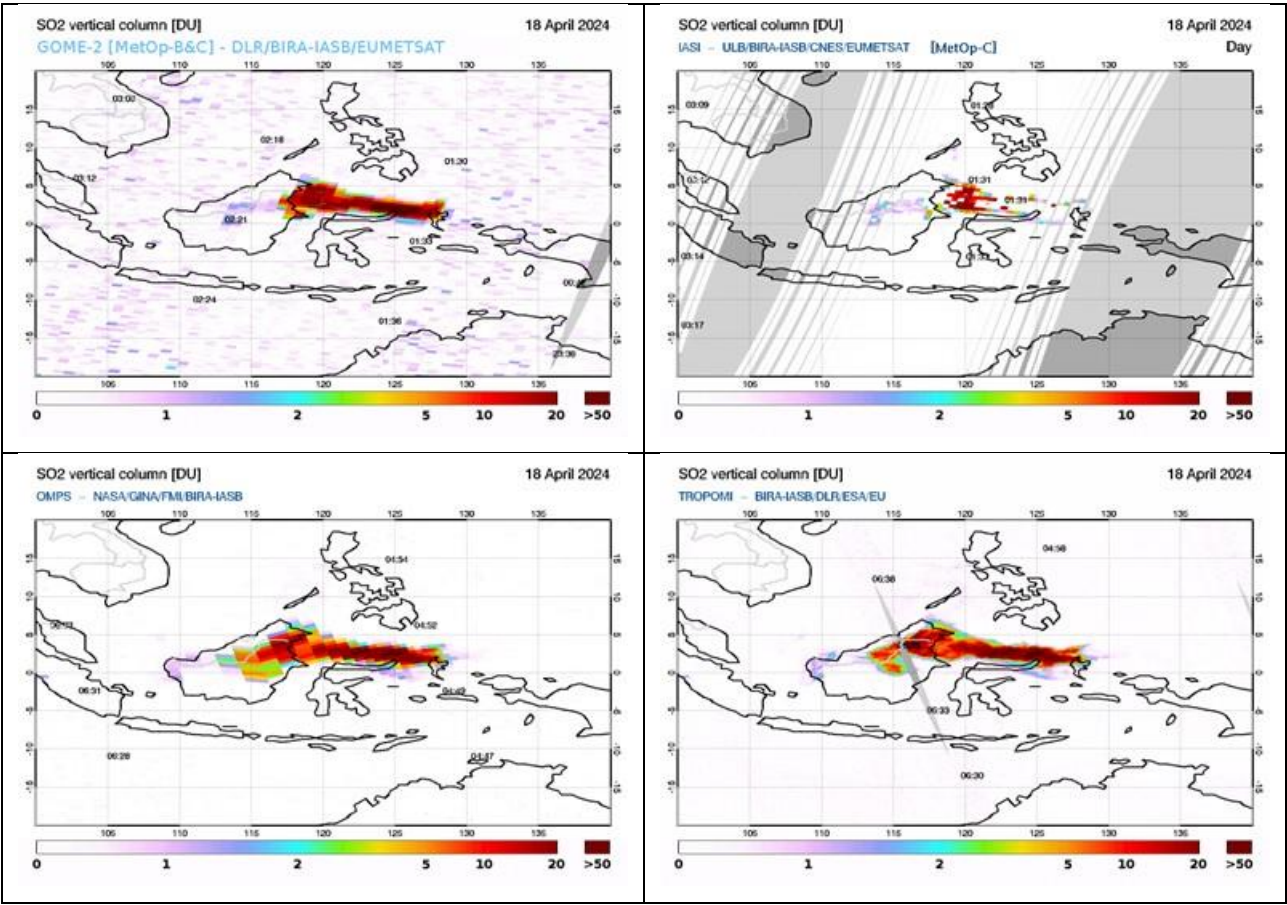
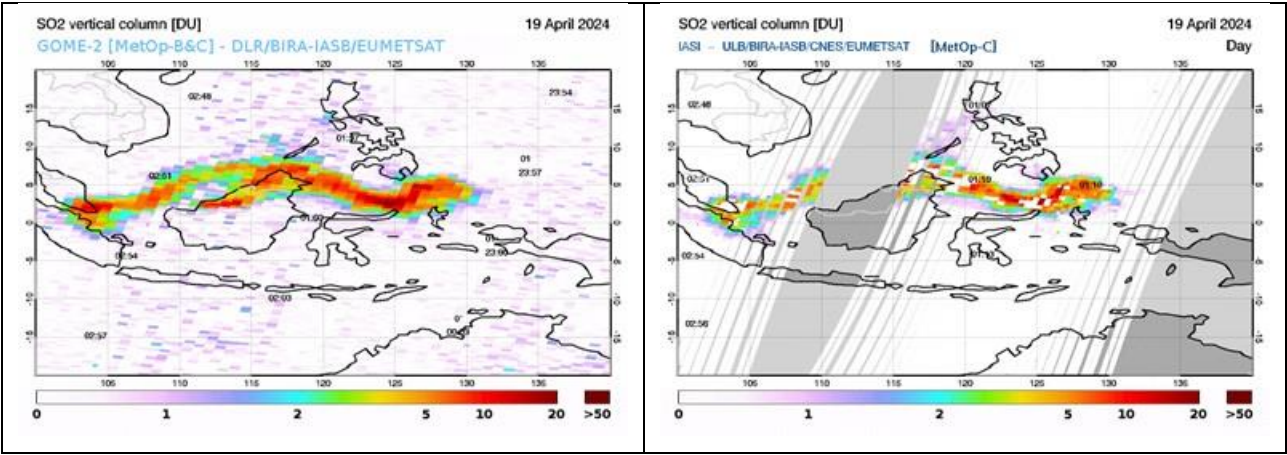
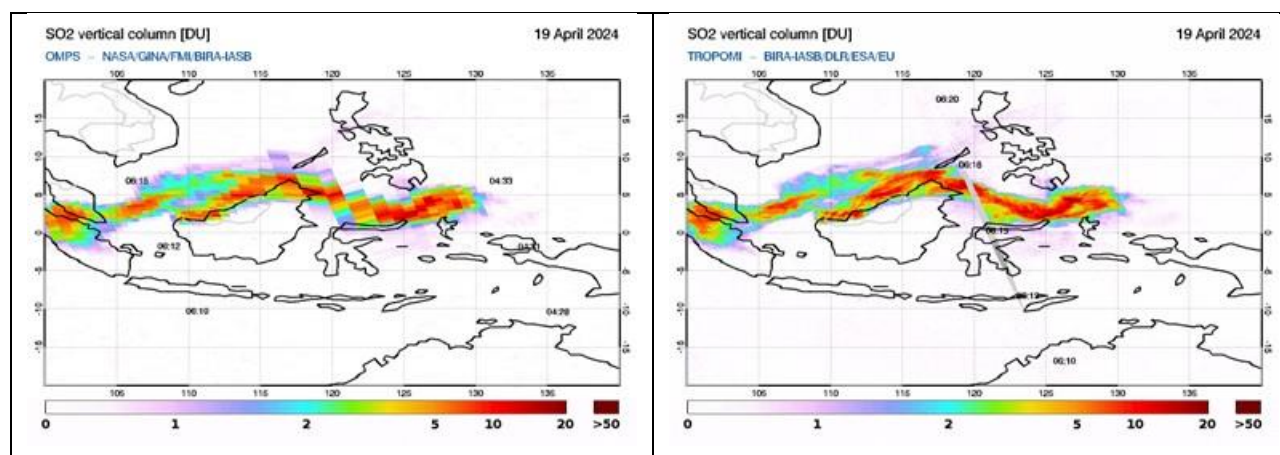


Figure 7.16. Mt Dukono eruption on the 18<sup>th</sup> of April 2024, sensed by GOME2-B/C [upper left], IASI/Metop-C [upper right], OMPS/NPP [bottom left] and S5P/TROPOMI [bottom right] from the [SACS](#) monitoring pages.





**Figure 7.17.** As Figure 7.16, but for 19 April 2024.

The coherence of the GOME-2B/C measurements with the other morning instruments (Figure 7.16) is clear, as is the temporal evolution with the afternoon platform instruments (Figure 7.17).

### References:

Clémer, K., Van Roozendaal, M., Fayt, C., Hendrick, F., Hermans, C., Pinardi, G., Spurr, R., Wang, P., and De Mazière, M.: Multiple wavelength retrieval of tropospheric aerosol optical properties from MAXDOAS measurements in Beijing, *Atmos. Meas. Tech.*, 3, 863-878, 2010.  
<https://doi.org/10.5194/amt-3-863-2010>

De Smedt, I., Stavrou, T., Hendrick, F., Danckaert, T., Vlemmix, T., Pinardi, G., Theys, N., Lerot, C., Gielen, C., Vigouroux, C., Hermans, C., Fayt, C., Veeckind, P., Müller, J.-F., and Van Roozendaal, M.: Diurnal, seasonal and long-term variations of global formaldehyde columns inferred from combined OMI and GOME-2 observations, *Atmos. Chem. Phys.*, 15, 12519-12545, 2015.  
<https://doi.org/10.5194/acp-15-12519-2015>

De Smedt, I., Pinardi, G., Vigouroux, C., Compernelle, S., Bais, A., Benavent, N., Boersma, F., Chan, K.-L., Donner, S., Eichmann, K.-U., Hedelt, P., Hendrick, F., Irie, H., Kumar, V., Lambert, J.-C., Langerock, B., Lerot, C., Liu, C., Loyola, D., PETERS, A., Richter, A., Rivera Cárdenas, C., Romahn, F., Ryan, R. G., Sinha, V., Theys, N., Vlietinck, J., Wagner, T., Wang, T., Yu, H., and Van Roozendaal, M.: Comparative assessment of TROPOMI and OMI formaldehyde observations and validation against MAX-DOAS network column measurements, *Atmos. Chem. Phys.*, 21, 12561–12593, 2021.  
<https://doi.org/10.5194/acp-21-12561-2021>

Gielen, C., Van Roozendaal, M., Hendrick, F., Pinardi, G., Vlemmix, T., De Bock, V., De Backer, H., Fayt, C., Hermans, C., Gillotay, D., and Wang, P.: A simple and versatile cloud-screening method for MAX-DOAS retrievals, *Atmos. Meas. Tech.*, 7, 3509–3527, 2014.  
<https://doi.org/10.5194/amt-7-3509-2014>

Hendrick, F.M., Van Roozendaal, M., Chipperfield, M.P., Dorf, M., Goutail, F., Yang, X., Fayt, C., Hermans, C., Pfeilsticker, K., Pommereau, J.-P., Pyle, J.A., Theys, N., and De Mazière, M.: Retrieval of stratospheric and tropospheric BrO profiles and columns using ground-based zenith-sky DOAS observations at Harestua, 60° N., *Atmos. Chem. Phys.*, 7, 4869-4885, 2007.  
<https://doi.org/10.5194/acp-7-4869-2007>

Hendrick, F., Johnston, P.V., De Mazière, M., Fayt, C., Hermans, C., Kreher, K., Theys, N., Thomas, A., and Van Roozendael, M.: One-decade trend analysis of stratospheric BrO over Harestua (60°N) and Lauder (45°S) reveals a decline, *Geophys. Res. Letters*, 35, L14801, 2008.  
<https://doi.org/10.1029/2008gl034154>

Hendrick, F., Müller, J.-F., Clémer, K., Wang, P., De Mazière, M., Fayt, C., Gielen, C., Hermans, C., Ma, J.Z., Pinardi, G., Stavrakou, T., Vlemmix, T., and Van Roozendael, M.: Four years of ground-based MAX-DOAS observations of HONO and NO<sub>2</sub> in the Beijing area, *Atmos. Chem. Phys.*, 14, 765–781, 2014.  
<https://doi.org/10.5194/acp-14-765-2014>

Pinardi, G., Van Roozendael, M., Lambert, J.-C., Granville, J., Hendrick, F., Tack, F., Yu, H., Cede, A., Kanaya, Y., Irie, I., Goutail, F., Pommereau, J.-P., Pazmino, A., Wittrock, F., Richter, A., Wagner, T., Gu, M., Remmers, J., Friess, U., Vlemmix, T., PETERS, A., Hao, N., Tiefengraber, M., Herman, J., Abuhassan, N., Bais, A., Kouremeti, N., Hovila, J., Holla, R., Chong, J., Postlyakov, O., Ma, J.: GOME-2 total and tropospheric NO<sub>2</sub> validation based on zenith-sky, direct-sun and multi-axis DOAS network observations, *Proceeding of the EUMETSAT conference*, 22-26 September 2014, Geneva, Switzerland.

Pinardi, G., Van Roozendael, M., Hendrick, F., Theys, N., Abuhassan, N., Bais, A., Boersma, F., Cede, A., Chong, J., Donner, S., Drosoglou, T., Frieß, U., Granville, J., Herman, J. R., Eskes, H., Holla, R., Hovila, J., Irie, H., Kanaya, Y., Karagkiozidis, D., Kouremeti, N., Lambert, J.-C., Ma, J., Peters, E., PETERS, A., Postlyakov, O., Richter, A., Remmers, J., Takashima, H., Tiefengraber, M., Valks, P., Vlemmix, T., Wagner, T., and Wittrock, F.: Validation of tropospheric NO<sub>2</sub> column measurements of GOME-2A and OMI using MAX-DOAS and direct sun network observations, *Atmos. Meas. Tech.*, 13, 6141-6174, 2020.  
<https://doi.org/10.5194/amt-13-6141-2020>

Richter, A., Behrens, L., Hilboll, A., Munassar, S., Burrows, J.P., Pinardi, G., and Van Roozendael, M.: Cloud effects on satellite retrievals of tropospheric NO<sub>2</sub> over China, oral presentation at the DOAS workshop, September 2017, Yokohama, Japan.

Theys, N., De Smedt, I., Yu, H., Danckaert, T., van Gent, J., Hörmann, C., Wagner, T., Hedelt, P., Bauer, H., Romahn, F., Pedernana, M., Loyola, D., and Van Roozendael, M.: Sulfur dioxide retrievals from TROPOMI onboard Sentinel-5 Precursor: algorithm theoretical basis, *Atmos. Meas. Tech.*, 10, 119-153, 2017.  
<https://doi.org/10.5194/amt-10-119-2017>

Van Gent, J. and Hendrick, F.: S5P/TROPOMI total BrO algorithm TCBRO: Validation report, issue: 1.0.0, date: 09/01/2022, [https://data-portal.s5p-pal.com/product-docs/bro/S5P-L2-BIRA-VR\\_TCBRO\\_1.0.0\\_20220110.pdf](https://data-portal.s5p-pal.com/product-docs/bro/S5P-L2-BIRA-VR_TCBRO_1.0.0_20220110.pdf)

Verhoelst, T., Compernelle, S., Pinardi, G., Lambert, J.-C., Eskes, H. J., Eichmann, K.-U., Fjæraa, A. M., Granville, J., Niemeijer, S., Cede, A., Tiefengraber, M., Hendrick, F., Pazmiño, A., Bais, A., Bazureau, A., Boersma, K. F., Bogner, K., Dehn, A., Donner, S., Elovkov, A., Gebetsberger, M., Goutail, F., Grutter de la Mora, M., Gruzdev, A., Gratsea, M., Hansen, G. H., Irie, H., Jepsen, N., Kanaya, Y., Karagkiozidis, D., Kivi, R., Kreher, K., Levelt, P. F., Liu, C., Müller, M., Navarro Comas, M., PETERS, A. J. M., Pommereau, J.-P., Portafaix, T., Prados-Roman, C., Puentedura, O., Querel, R., Remmers, J., Richter, A., Rimmer, J., Rivera Cárdenas, C., Saavedra de Miguel, L., Sinyakov, V. P., Stremme, W., Strong, K., Van Roozendael, M., Veefkind, J. P., Wagner, T., Wittrock, F., Yela González, M., and Zehner, C.: Ground-based validation of the Copernicus Sentinel-5P TROPOMI NO<sub>2</sub> measurements with the NDACC ZSL-DOAS, MAX-DOAS and Pandonia global networks, *Atmos. Meas. Tech.*, 14, 481–510, 2021.

<https://doi.org/10.5194/amt-14-481-2021>

Vlemmix, T., Hendrick, F., Pinardi, G., Smedt, I., Fayt, C., Hermans, C., Piter, A., Wang, P., Levelt, P., and Van Roozendaal, M.: MAX-DOAS observations of aerosols, formaldehyde and nitrogen dioxide in the Beijing area: comparison of two profile retrieval approaches, *Atmos. Meas. Tech.*, 2, 941–963, 2015.

<https://doi.org/10.5194/amt-8-941-2015>

Wang, T., Hendrick, F., Wang, P., Tang, G., Cl  mer, K., Yu, H., Fayt, C., Hermans, C., Gielen, C., M  ller, J.-F., Pinardi, G., Theys, N., Brenot, H., and Van Roozendaal, M.: Evaluation of tropospheric SO<sub>2</sub> retrieved from MAX-DOAS measurements in Xianghe, China, *Atmos. Chem. Phys.*, 14(20), 11149–11164, 2014.

<https://doi.org/10.5194/acp-14-11149-2014>

### 7.3.1. Online quality monitoring

Online quality monitoring plots are continuously generated at DLR and published for O<sub>3</sub>, NO<sub>2</sub>, BrO, HCHO, SO<sub>2</sub>, H<sub>2</sub>O products as described in Section 7.1.3.

BIRA-IASB provides quality assessment (QA) pages for vertical column amounts of NO<sub>2</sub>, HCHO, BrO and SO<sub>2</sub> derived from GOME-2B and GOME-2C. The goal is to provide an easy tool to quickly spot anomalies and trends in the L2 data, by selecting and examining geographical regions of interest. These pages are available under <https://cdop.aeronomie.be/quality-assessment/>.

The monitored L2 is provided by DLR with predecessor version GDP 4.8 for GOME-2B and GDP 4.9 for GOME-2C.

#### *System developments:*

- The GOME-2 monitoring page shows time-series for Metop-B and Metop-C. Metop-A data is kept internally for comparison reasons.
- The current monitoring system, based on data storage in an SQL database, remains slow in use. As mentioned in the previous report, a new system has been under development and has shown to be much faster.

#### *Monitoring status:*

### SO<sub>2</sub>

In the case of SO<sub>2</sub>, the available geographical regions of interest are either locations with known outgassing volcanoes or locations with strong anthropogenic sources of SO<sub>2</sub>. The resulting graphs show a history of monthly average values over the selected region.

In Figure 7.18 and Figure 7.19, two relevant panels are presented for the time period 01/01/2024 – 30/06/2024. In the upper panels, the SO<sub>2</sub> fitting RMS is shown, an important parameter which acts as immediate indicator to the stability of the instruments/algorithms. In the bottom panels, the total vertical SO<sub>2</sub> column is presented, alongside other metrics, explained in the figure caption. Both panels include smaller subpanels which show the long-term behaviour of each sensor from the beginning of the satellite mission.





**Figure 7.18.** The behaviour of the GDP4.8 GOME-2B [blue curve] and GOME-2C [black curve] 6 km plume height SO<sub>2</sub> products between 01/01/2024 and 30/06/2024 over the region of Indonesian volcanoes. Upper panel, the SO<sub>2</sub> fitting RMS is shown and in the bottom panel, the total vertical SO<sub>2</sub> column. The equivalent long-term average is also provided [see insert legend].



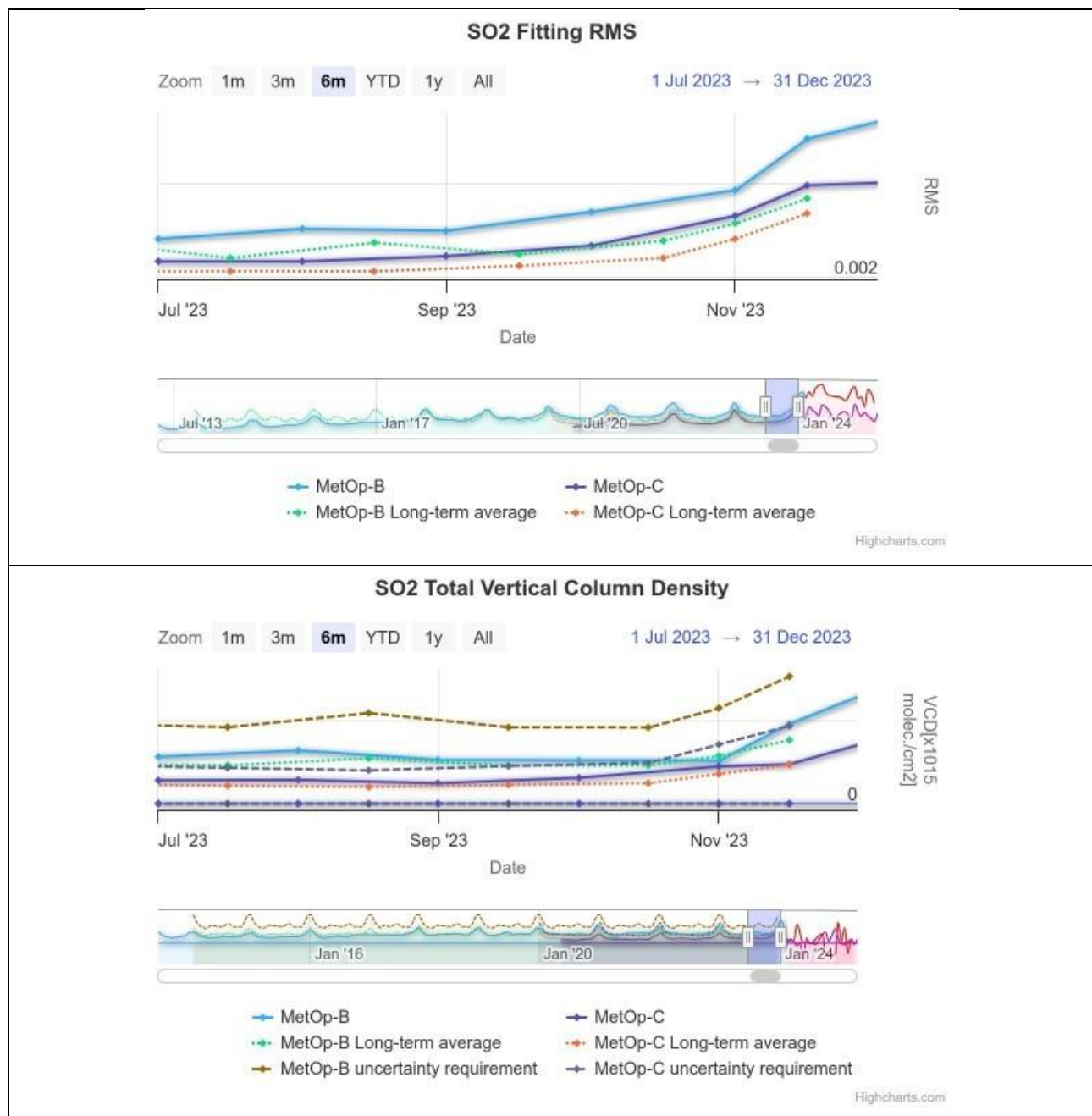


**Figure 7.19.** The behaviour of the GDP4.8 GOME-2B [blue curve] and GOME-2C [black curve] 6 km plume height SO<sub>2</sub> products between 01/07/2023 and 31/12/2023 over Indonesia. Upper panel, the SO<sub>2</sub> fitting RMS is shown and in the bottom panel, the total vertical SO<sub>2</sub> column. The equivalent long-term average is also provided [see insert legend].

From Figure 7.18 and Figure 7.19, upper panels, no spurious jumps or artefacts are observed during 2024 for either the anthropogenic or the volcanic locations in the SO<sub>2</sub> fitting RMS. However, not only it is said that RMS is ~20 – 25 % larger for GOME-2B than GOME-2C, but it is also equally larger from its long-term average. This points to a possible degradation effect in the GOME-2B L1b data which also affects the L2 data, as shown in Figure 7.18 and Figure 7.19, lower panels. GOME-2B has provided far larger (more than 50 %) SO<sub>2</sub> columnar estimates than GOME-2C and ~20 – 25 % larger than the long-term average.

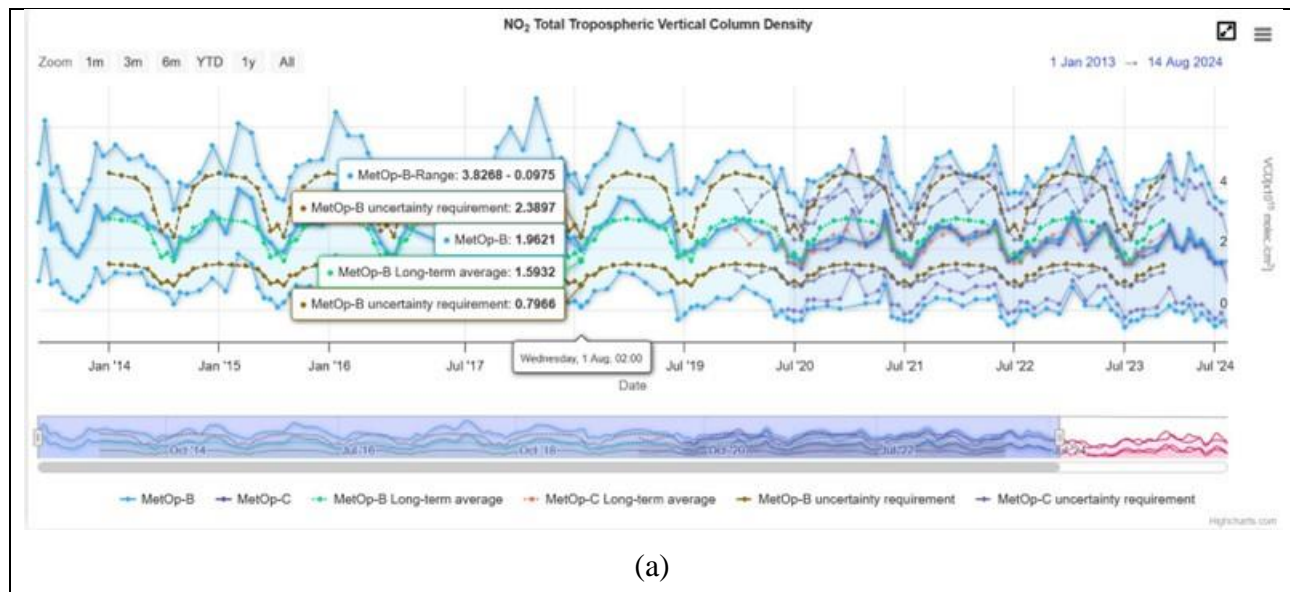
Both these issues are cause for concern and merit further investigation from the DLR L2 algorithm team. Currently, GOME-2 SO<sub>2</sub> retrieval uses a one fit-window approach with an improved fit-window for GOME-2C (which cannot be applied to GOME-2B due to L1b data degradation effects).

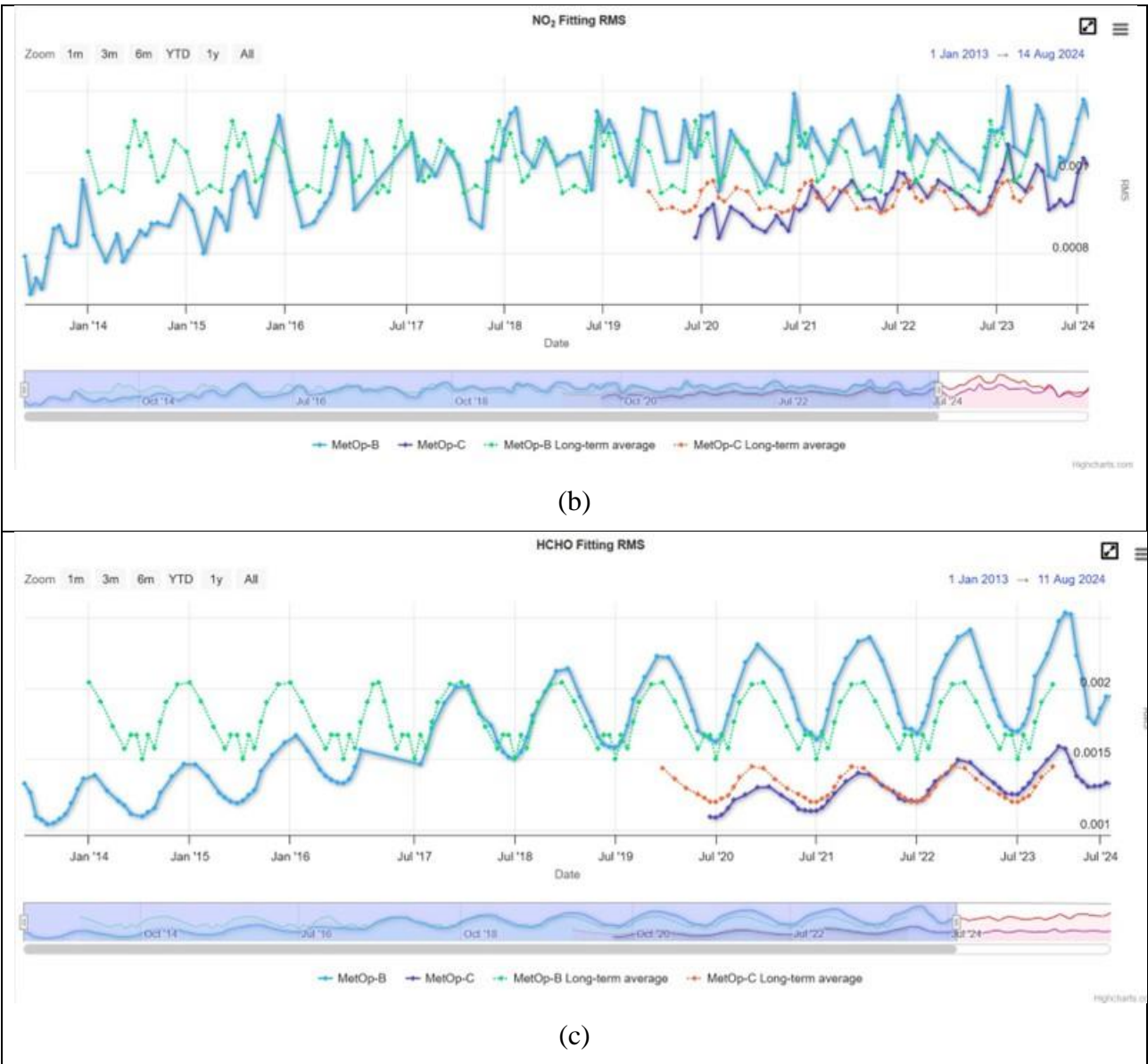
The overall quality of GOME-2B and GOME-2C SO<sub>2</sub> products can be improved with a 3-fit window retrieval approach (as for TROPOMI SO<sub>2</sub> retrieval), which is planned in the CDOP 4 for the NRT/offline products, as well as for the reprocessing.

### NO<sub>2</sub>, HCHO, and BrO

When observing the full time-series for the other monitored gases, column amounts between the two instruments agree quite well. Some examples are depicted in Figure 7.20. For NO<sub>2</sub>, the tropospheric column amounts of both sensors show the expected annual cycle and show no systematic mutual offset (panel a, situation over the Europe). If anything, the stratospheric column suggests a small negative trend. Indications of instrumental degradation are visible in the fit residual (RMS, panel b) of both instruments. On the other hand, the raise of GOME-2B RMS seems to flatten out over the last few years. For NO<sub>2</sub>, similar RMS patterns are observed over other geographical regions (not shown here).

Consistent patterns of total column amounts are also observed for HCHO (panel c, Equatorial Africa). There, however, the increase of the RMS signal for GOME-2B seems to continue also in recent years, something that is also observed for BrO (panel d), be it less pronounced and depending on the observed region.





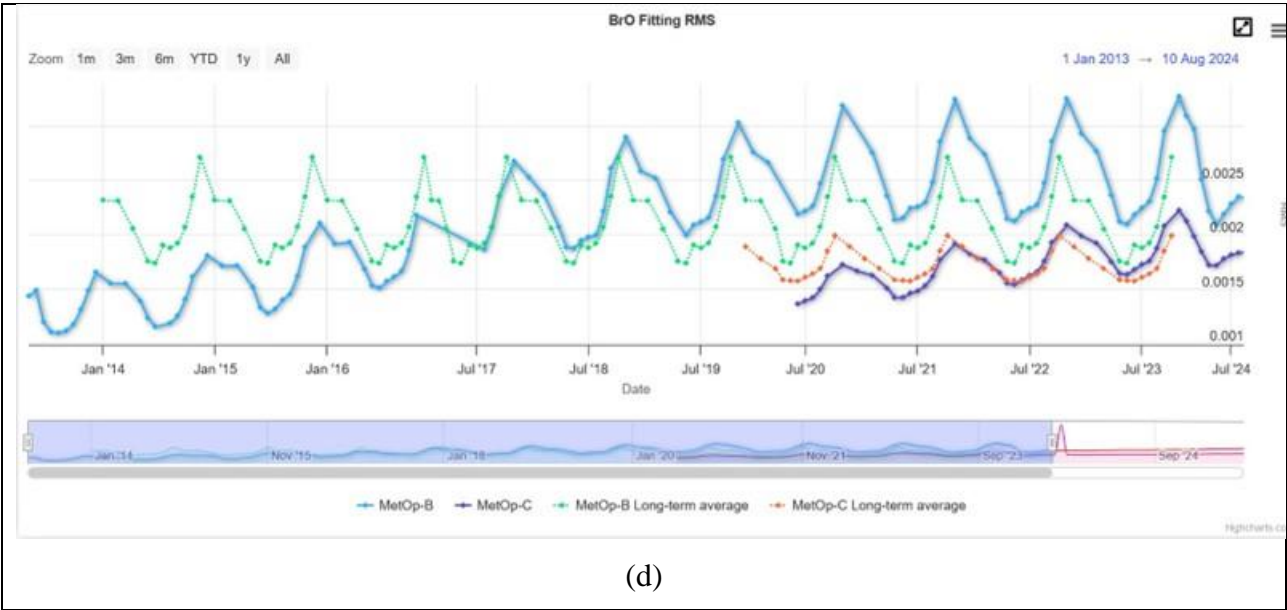


**Figure 7.20. Examples of time-series from the QA monitoring page: a) NO<sub>2</sub> tropospheric column over Europe, b) NO<sub>2</sub> fitting RMS over Europe, c) HCHO fitting RMS over the Southeastern US, and d) Fitting RMS for BrO, averaged over the 60°-90° Arctic latitude band.**

7.4. GOME-2 ozone profile products

**Table 7.13. Validation status of ozone profile products**

Product Identifier	Product Name	Accuracy	Reference	Validating Institute	Correlative data sources
O3M-47.1	NRT high-resolution ozone profile	Fulfil threshold accuracy requirements	RD7	KMI DWD	Ozonesonde data from <a href="#">SHADOZ</a> , <a href="#">NDACC</a> , <a href="#">NILU</a> and <a href="#">WOUDC</a> Lidar/microwave data from <a href="#">NDACC</a>
O3M-311			RD22		
O3M-39	Offline high-resolution ozone profile	Fulfil threshold accuracy requirements	RD6	KMI DWD	Ozonesonde data from <a href="#">SHADOZ</a> , <a href="#">NDACC</a> , <a href="#">NILU</a> and <a href="#">WOUDC</a> Lidar/microwave data from <a href="#">NDACC</a>
O3M-48			RD7		
O3M-312			RD22		

Validation results can be found in more detail on the at [AC SAF validation & quality assessment website](#).

**Validation activities summary:**

This summary contains validation results for the GOME-2B and GOME-2C high-resolution (HR) ozone profile products, retrieved by the Ozone Profile Retrieval Algorithm (OPERA) at KNMI.

This validation section focuses on the time period July 2023 – June 2024. For the ozone profiles, the time period considered is July 2023 – June 2024

The authors of this summary are Dr. Andy Delcloo from KMI and Dr. Peggy Achtert from DWD. More information on how these values are extracted is available in the [validation report](#).

There is no material difference in the content of the NRT vs. the offline vertical ozone profile data product, other than its size. The offline file is a concatenation of the NRT L2 PDUs for a particular orbit. While the validation partners are provided the L2 PDUs that were sent out in NRT for their validation, it makes no difference for the validation itself.

To report the skill scores of GOME-2 ozone profile products in a more condensed way, the statistics for the different output levels of GOME-2 are reduced to two layers: Lower Stratosphere (until an altitude of 30 km) and Upper Stratosphere (up to an altitude of 50 km).

The validation for the lower stratosphere is made with ozonesonde data, for the upper stratosphere with lidar, FTIR and/or microwave data. The stations used in this validation for the FTIR/lidar/microwave data are the Network for the Detection of Atmospheric Composition Change (NDACC) stations of Bern (microwave), Ny Ålesund (microwave, FTIR), Thule (FTIR), Payerne (microwave), Hohenpeissenberg (lidar), Table Mountain (lidar), Mauna Loa (microwave/lidar), Eureka (lidar), and Lauder (FTIR, lidar).

The collocation data used for the validation using ozonesonde data are shown in Figure 7.21.

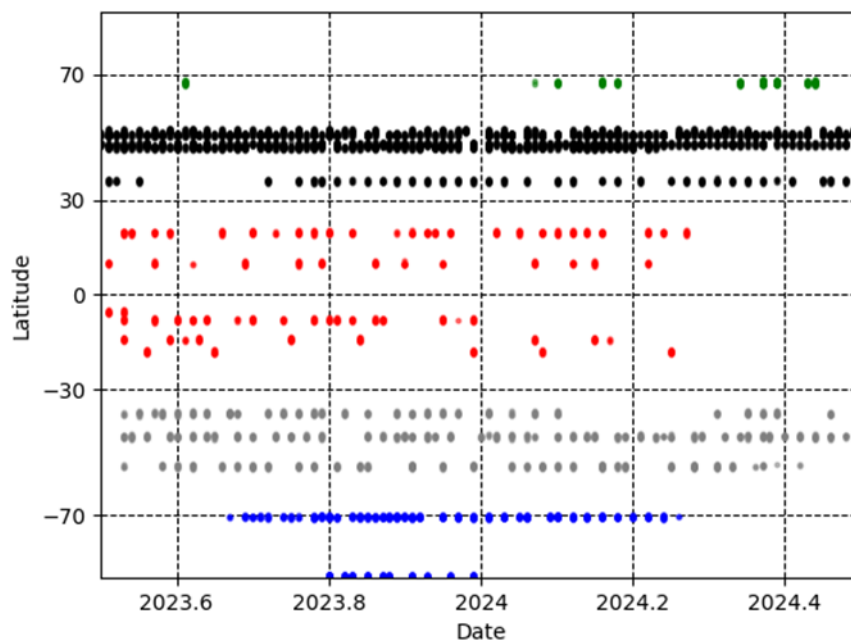


**Figure 7.21. Collocation data for the validation with ozonesonde data for the time period July 2023 – June 2024.**

Table 7.14 shows an overview of the obtained results for the time period July 2023 – June 2024 only for the lower and the higher stratosphere, not taking into account the tropospheric ozone column products since a dedicated product is discussed earlier in this report. The statistics for the lower stratosphere are obtained by KMI, the statistics for the higher stratosphere by DWD.



**Table 7.14. Absolute Differences (AD), Relative Differences (RD) and standard deviation (STDEV) are shown on the accuracy of GOME-2B/C HR ozone profile products for the lower and the higher stratosphere for five different latitude belts for the time period July 2023 – June 2024.**

<b>GOME-2B HR</b>						
	Lower Stratosphere			Upper Stratosphere		
	AD	RD	STDEV	AD	RD	STDEV
	(DU)	(%)	(%)	(DU)	(%)	(%)
<b>Northern Polar Region</b>	2.6	1.6	9.9			
<b>Northern Mid-Latitudes</b>	3.4	1.9	10.3	-5.6	-7-7	5.8
<b>Tropical Region</b>	7.5	5.6	5.4	-	-	-
<b>Southern Mid-Latitudes</b>	10.6	6.1	11.4	-3.9	-9.5	4.4
<b>Southern Polar Region</b>	12.2	29.6	80.9	-	-	-

<b>GOME-2C HR</b>						
	Lower Stratosphere			Upper Stratosphere		
	AD	RD	STDEV	AD	RD	STDEV
	(DU)	(%)	(%)	(DU)	(%)	(%)
<b>Northern Polar Region</b>	2.0	0.8	9.2			
<b>Northern Mid-Latitudes</b>	3.4	2.6	8.9	-3.1	-3.2	10.2
<b>Tropical Region</b>	5.0	6.2	7.1	-	-	-
<b>Southern Mid-Latitudes</b>	10.4	6.3	11.2	-4.3	-7.5	3.7
<b>Southern Polar Region</b>	6.8	22.0	61.9	-	-	-

The target value (15 % accuracy) is met in both lower and upper stratosphere for all belts under consideration for Metop-B and Metop-C, except for the Southern Polar Region. The discrepancy is highest at high-latitude.

More detailed ozone profile validation results can also be found on the AC SAF [ozone profile validation website](#).

#### 7.4.1. Online quality monitoring

Timeline of the vertically integrated Metop-B ozone profile with respect to time is presented in Figure 7.22.

More information and images at the following web addresses

<https://www.temis.nl/acsaf/timeseries.php?sat=metopb>

<https://www.temis.nl/acsaf/timeseries.php?sat=metopc>

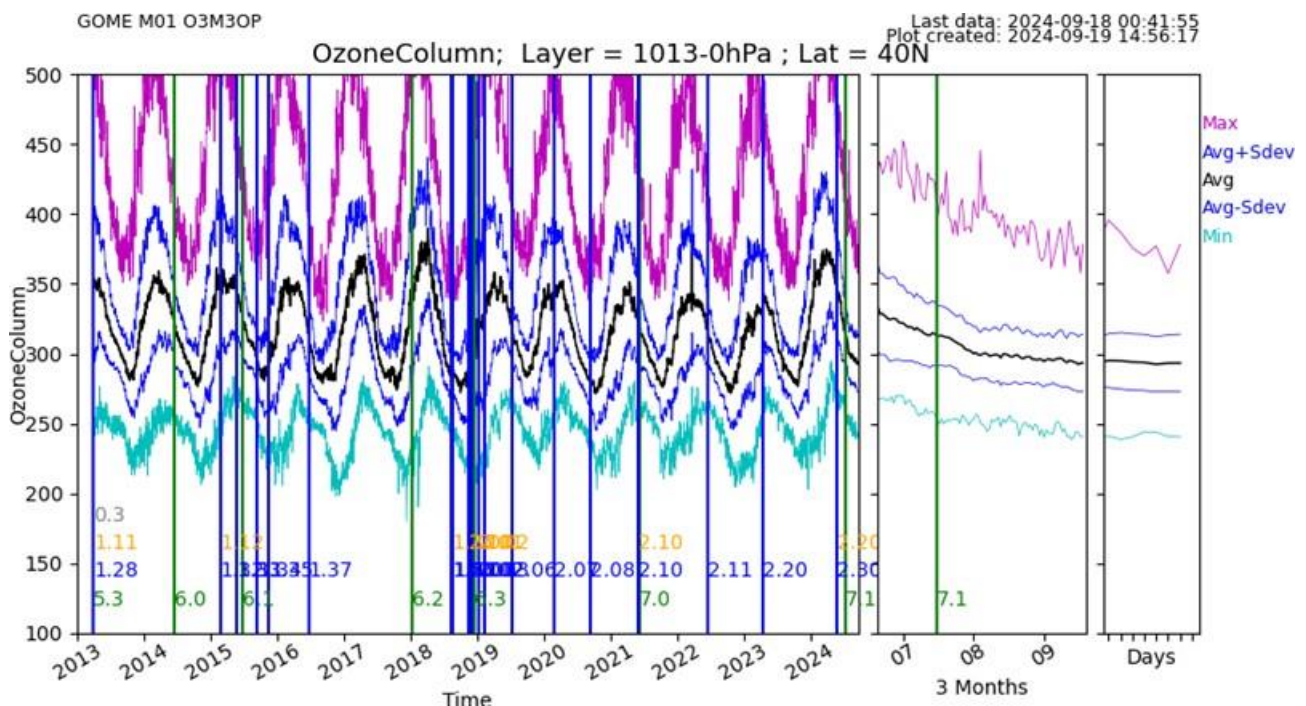


**Figure 7.22.** Timeline of vertically integrated Metop-B ozone profiles (=total ozone columns) and changes in data processor (vertical lines). The changes in late 2018 / early 2019, including the improved degradation correction, have resulted in much better ozone profiles and have also affected the total ozone columns shown here.

Legend of the coloured vertical lines:

- Green: PPF version
- Blue: Software version (PGE)
- Orange: Algorithm version
- Grey: Config version

## 7.5. GOME-2 aerosol products

**Table 7.15. Validation status of aerosol products**

Product Identifier	Product Name	Accuracy	Reference	Validating Institute	Correlative data sources	
O3M-78	NRT absorbing aerosol height	Fulfil threshold accuracy requirement	RD28	KMI, AUTH	CALIOP, EARLINET	
O3M-364						
O3M-72.1	NRT absorbing aerosol index from PMDs	Fulfil threshold accuracy requirement	RD13	KNMI	Comparisons with other satellite instruments: SCIAMACHY, OMI, and intercomparison of GOME-2A with GOME-2B	
O3M-362			RD29		Comparisons with the AAI products from GOME-2A and GOME-2B	
O3M-69	Offline absorbing aerosol height	Fulfil threshold accuracy requirements	RD28	KMI, AUTH	CALIOP, EARLINET	
O3M-79						
O3M-365						
O3M-63.1	Offline absorbing aerosol index from PMDs	Fulfil threshold accuracy requirements	RD13	KNMI	Comparisons with other satellite instruments: SCIAMACHY, OMI, and intercomparison of GOME-2A with GOME-2B	
O3M-73.1			RD29		Comparisons with the AAI products from GOME-2A and GOME-2B	
O3M-363						

### Validation activities summary:

This summary contains validation results for the GOME-2A, GOME-2B and GOME-2C Absorbing Aerosol Height (AAH) products and is made available by the validation teams of AUTH and KMI. More information on how these values are extracted is available in the validation report [validation report](#).

AAH is a new operational AC SAF product for aerosol layer height detection, developed by KNMI within the AC SAF. It uses the AAI as an indicator to derive the actual height of the absorbing aerosol layer in the O<sub>2</sub>-A band using the Fast Retrieval Scheme for Clouds from the Oxygen A band (FRESCO) algorithm (Wang *et al.*, 2012; Tilstra *et al.*, 2020). The AAH reported by GOME-2 onboard Metop-A, Metop-B and Metop-C, between 2007 and 2019, has been validated by AUTH against ground-based lidar data from the European Aerosol Research Lidar Network (EARLINET) database and by KMI against CALIOP aerosol layer height (De Bock, *et al.* 2020; Michailidis *et al.*, 2021).

### AUTH results:

A wide choice of lidar stations (first column of Table 7.17) was made to examine the behaviour of the comparisons for different common aerosol loads around Europe. The geographical distribution



of the selected EARLINET stations depicted in Figure 7.23 indicates the domain of applicability of the validation results. All participating stations (red circles) operate high-performance multi-wavelength lidar systems. The list of stations, along with their identification codes, surface elevation, and respective references, considered for the validation of the GOME2/Metop AAH product are shown in Table 7.16.

The total number of carefully screened collocations with the EARLINET lidar measurements was 385 for the three GOME-2 instruments, from the beginning of each mission to the reporting period. On average, the mean absolute bias (GOME-2 minus EARLINET lidar height) was found to be  $-0.56 \pm 2.01$  km, with a near-Gaussian distribution and minimum and maximum differences of  $\sim \pm 5$  km. On a per station basis, and with a couple of exceptions, their mean biases fall in the  $\pm 1$  km range, with an associated standard deviation between 0.6 – 2.4 km. The time period covered is January 2024 – June 2024 for the GOME-2B and GOME-2C offline AAH products.

**Table 7.16. Locations of EARLINET lidar stations and their geographical coordinates**

EARLINET Station	Code	Country	Coordinates	Elevation (m)
Antikythera	AKY	Greece	23.31E, 35.86N	193
Athens	ATZ	Greece	23.78E, 37.96N	212
Barcelona	BRC	Spain	2.12E, 41.39N	115
Bucharest	INO	Romania	26.03E, 44.34N	93
Dushanbe	DUS	Tajikistan	68.85E, 38.55N	864
Évora	EVO	Portugal	7.91W, 38.56N	293
Granada	GRA	Spain	3.60W, 37.16N	680
Lecce	SAL	Italy	18.10E, 40.33N	30
Leipzig	LEI	Germany	12.43E, 51.35N	125
Limassol <sup>1,2</sup>	LIM	Cyprus	33.04E, 34.67N	10
Minsk	MAS	Belarus	27.60E, 53.91N	200
Potenza	POT	Italy	15.72E, 40.60N	760
Sofia	SOF	Bulgaria	23.38E, 42.65N	550
Thessaloniki	THE	Greece	22.95E, 40.60N	50

<sup>1</sup> Cyprus University of Technology (CUT) [before Oct 2020]

<sup>2</sup> Leibniz Institute for Tropospheric Research and ERATOSTHENES Centre of Excellence [after Oct 2020]

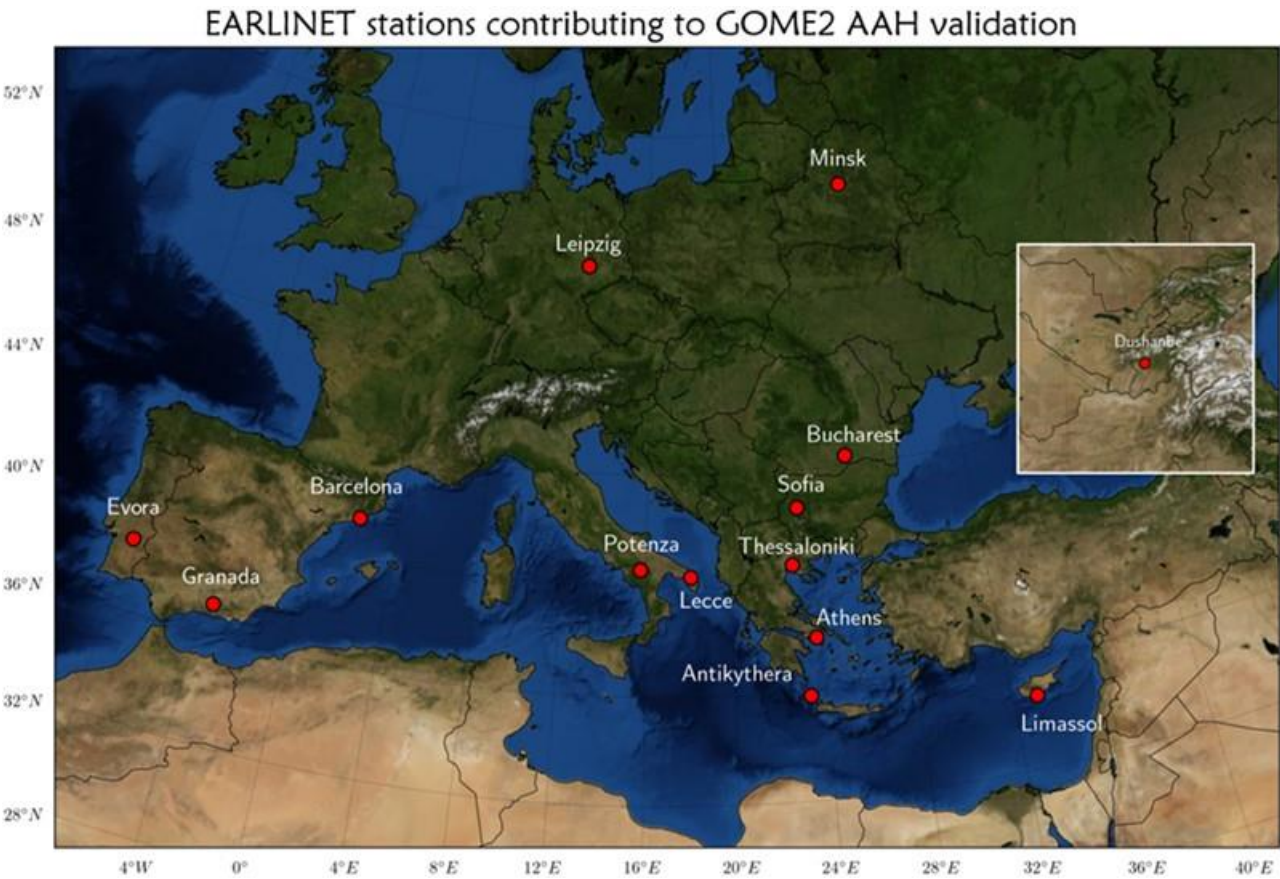


**Figure 7.23.** Geographical distribution of EARLINET ground-based stations for which co-locations with GOME-2 AAH data were used.

**Table 7.17. Summary of statistics for the comparisons between GOME-2 AAH and LIDAR ALH for all stations**

EARLINET Station	N	Statistical parameters (in km)			
		Mean absolute bias	Std	Min	Max
Athens, Greece	5	-1.98	0.78	-3.60	-1.06
Antikythera, Greece	33	-1.56	2.10	-6.77	3.66
Barcelona, Spain	36	-0.44	1.86	-4.66	2.86
Belsk, Poland	28	0.11	1.50	-3.11	3.24
Bucharest, Romania	19	-0.07	2.08	-4.81	3.37
Dushanbe, Tajikistan	36	-0.64	1.38	-3.81	1.78
Évora, Portugal	10	-0.09	1.98	-1.64	3.31
Granada, Spain	52	-0.49	2.00	-3.78	5.28
Lecce, Italy	18	-0.24	1.14	-3.47	2.05
Limassol, Cyprus	65	-1.03	2.42	-5.64	4.44
Minsk, Belarus	5	0.56	0.61	-0.05	1.51
Potenza, Italy	23	-1.25	1.68	-3.50	2.52
Thessaloniki, Greece	47	-0.03	2.19	-4.71	5.23
Warsaw, Poland	8	0.80	1.50	1.08	2.15
<b>Summary</b>	<b>385</b>	<b>-0.56</b>	<b>2.00</b>	<b>-6.77</b>	<b>5.28</b>

In Figure 7.24, the histogram of absolute differences between GOME-2 and EARLINET aerosol layer heights, calculated for all collocated cases is shown, with the associated statistics. The associated Absorbing Aerosol Index (AAI) value is color-coded. In the right panel, the scatter plot between GOME-2 AAH and aerosol layer height from EARLINET stations, for the totality of collocated cases is presented.

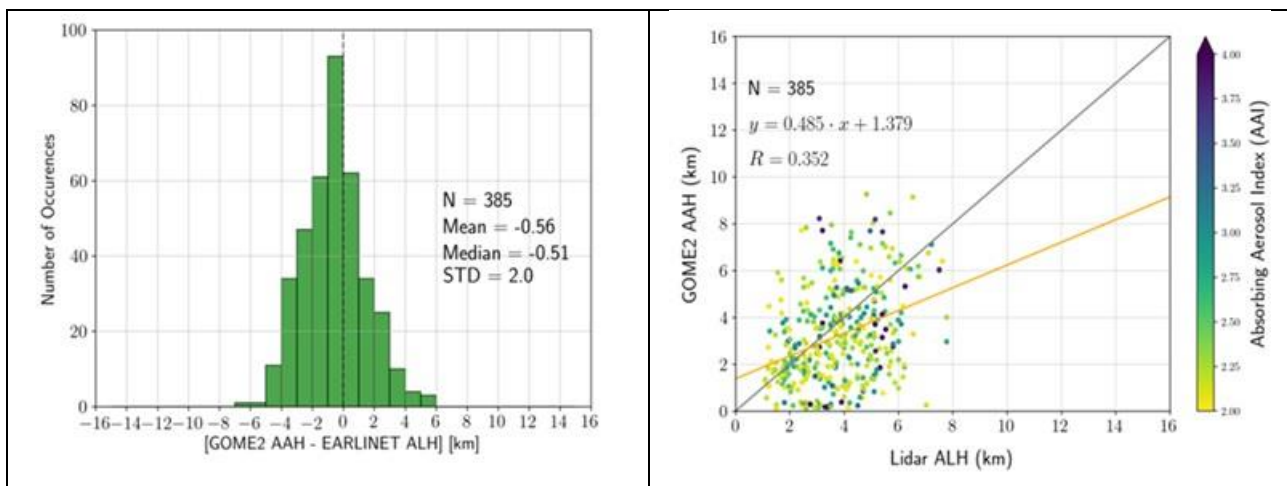


**Figure 7.24. Histogram of absolute differences between GOME-2 AAH and aerosol layer height obtained from EARLINET backscatter profiles (using the WCT method), calculated for all collocated cases. The associated AAI value is color-coded. Right: Scatter plot between GOME-2 AAH and aerosol layer height from EARLINET stations, for the total of collocated cases.**

Considering the possible temporal collocation mismatch and the spatial difference between the satellite pixel size and the point view of the ground-based observations, these results are quite promising and demonstrate that stable aerosol layers are well captured by the satellite sensors. The official AC SAF requirements for the accuracy of the GOME-2 AAH product state that, for heights < 10 km, the threshold accuracy is 3 km, the target accuracy is 2 km, and the optimal accuracy is 1 km. This validation effort shows that for all cases the target accuracy is met, see Table 7.18. For the different regimes, which relate to the degree of cloud cover, please refer to the [validation report](#) and Michailidis *et al.*, 2021.

**Table 7.18. Percentage of collocated lidar & GOME-2 AAH cases that fulfil the optimal accuracy criteria (first row), the target criteria (second row), the threshold criteria (third row) for Regime A in the first column, Regime B in the second, Regime C in the third and the totality of the collocations in the final column. The regimes are related to the degree of cloud cover.**

	Regime A (149 cases)	Regime B (136 cases)	Regime C (13 cases)	Total (298 cases)
<b>Optimal (1 km)</b>	30.7 %	48.8 %	48.5 %	40.1 %
<b>Target (2 km)</b>	53.8 %	75.0 %	71.4 %	64.7 %
<b>Threshold (3 km)</b>	77.4 %	88.5 %	88.5 %	83.4 %

#### KMI results:

At the time of writing this report, there was no updated AAH reference data available. Therefore, all the results are as in AC SAF Operations Report 1/2021.

KMI validated the AAH only for specific case studies related to volcanic eruptions. AAH values are only included in the analysis if the corresponding AAI is higher than 4. CALIOP and GOME data are compared when the distance between both overpasses is maximum 100 km. There is currently no constraint on the time difference between both overpasses.

Compared to the results shown in the [validation report](#), new data has been added to the study (i.e. Fournaise de la Piton 11-12 February 2020, Karymsky 1-2 April 2020, Kavachi 16 March 2020 and Kikai 29-30 April 2020) in this report. The updated results are summarized in Table 7.19.

Overall, just about 50-60 % of the AAH pixels from GOME-2A, GOME-2B and GOME-2C reach the threshold requirements (see Table 7.19 and Figure 7.25). The optimal requirement threshold is reached for GOME-2A, GOME-2B and GOME-2C in 18 %, 25 % and 24 % of the cases, respectively (when comparing the AAH with the minimum CALIOP layer height). If only the tropospheric aerosol species (as defined by CALIOP) are studied, the results improve. This can also be seen in Table 7.19 (values in brackets).

**Table 7.19. Percentage of data for each GOME-2 instrument that reached the threshold, target and optimal accuracy requirements. Values obtained when only considering the tropospheric aerosol species are shown in brackets**

GOME-2A				
		Layer height <10 km	Layer height >10 km	Total
<b>Threshold</b>	AAH-minC	56.0 % (69.6 %)	53.1 % (26.4 %)	55.9 % (68.9 %)
	AAH-maxC	56.4 % (69.5 %)	46.8 % (23.6 %)	56.2 % (68.7 %)

<b>Target</b>	<b>AAH-minC</b>	39.0 % (48.5 %)	43.5 % (19.1 %)	39.1 % (48.0 %)
	<b>AAH-maxC</b>	38.0 % (46.9 %)	32.4 % (23.6 %)	37.9 % (46.3 %)
<b>Optimal</b>	<b>AAH-minC</b>	17.3 % (21.5 %)	29.9 % (10.0 %)	17.6 % (21.3 %)
	<b>AAH-maxC</b>	18.1 % (22.3 %)	15.6 % (10.0 %)	18.1 % (22.1 %)
<b>GOME-2B</b>				
		<b>Layer height &lt;10 km</b>	<b>Layer height &gt;10 km</b>	<b>Total</b>
<b>Threshold</b>	<b>AAH-minC</b>	51.8 % (53.6 %)	22.9 % (11.7 %)	50.9 % (51.6 %)
	<b>AAH-maxC</b>	52.6 % (54.4 %)	20.6 % (10.2 %)	51.6 % (52.2 %)
<b>Target</b>	<b>AAH-minC</b>	42.9 % (44.5 %)	20.6 % (5.60 %)	42.2 % (42.6 %)
	<b>AAH-maxC</b>	37.0 % (38.3 %)	17.1 % (7.90 %)	36.4 % (36.8 %)
<b>Optimal</b>	<b>AAH-minC</b>	25.1 % (26.0 %)	17.1 % (3.40 %)	24.8 % (24.9 %)
	<b>AAH-maxC</b>	20.5 % (33.1 %)	16.5 % (3.00 %)	20.4 % (31.6 %)
<b>GOME-2C</b>				
		<b>Layer height &lt;10 km</b>	<b>Layer height &gt;10 km</b>	<b>Total</b>
<b>Threshold</b>	<b>AAH-minC</b>	50.8 % (50.8 %)	0.0 % (0.0 %)	46.8 % (46.8 %)
	<b>AAH-maxC</b>	57.1 % (57.1 %)	0.0 % (0.0 %)	52.9 % (52.9 %)
<b>Target</b>	<b>AAH-minC</b>	42.2 % (42.2 %)	0.0 % (0.0 %)	38.8 % (38.8 %)
	<b>AAH-maxC</b>	49.1 % (49.1 %)	0.0 % (0.0 %)	45.2 % (45.2 %)
<b>Optimal</b>	<b>AAH-minC</b>	26.3 % (26.3 %)	0.0 % (0.0 %)	24.1 % (24.1 %)
	<b>AAH-maxC</b>	34.5 % (34.5 %)	0.0 % (0.0 %)	31.6 % (31.6 %)

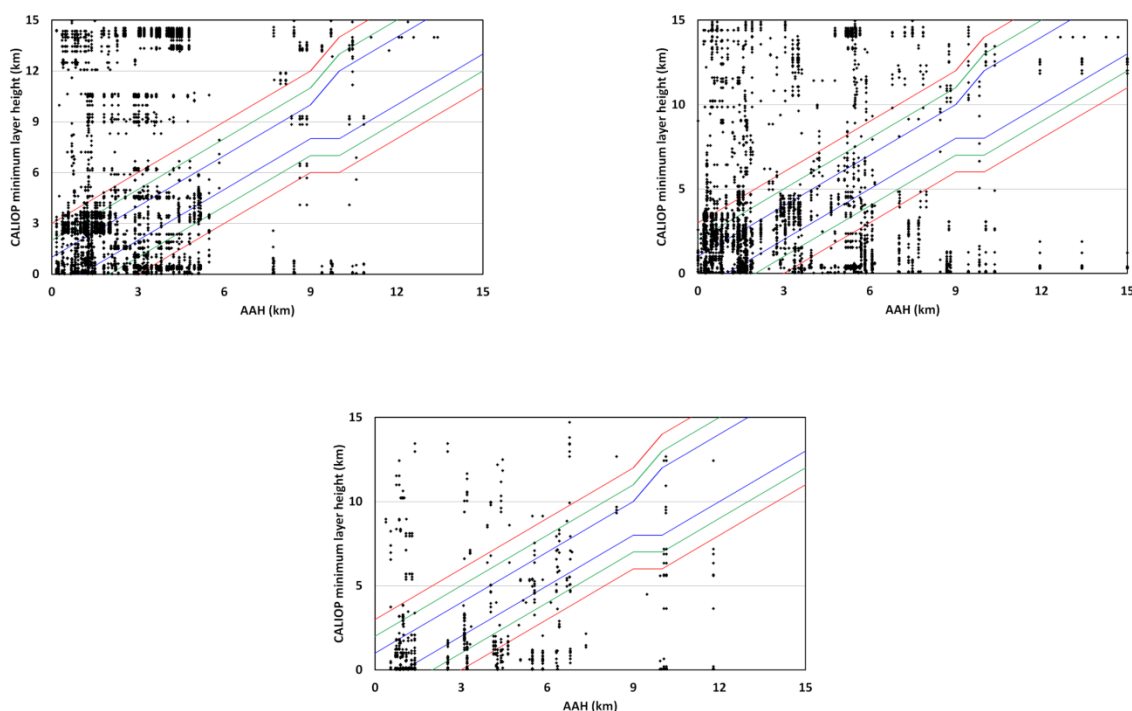


**Figure 7.25. Requirement plots for GOME-2A (upper left), GOME-2B (upper right) and GOME-2C (lower middle). The red, green and blue lines represent the threshold, target and optimal requirements. CALIOP pixels are only shown up to a height of 15 km, which is the detection limit of GOME-2.**

## References:

Michailidis, K., Koukouli, M.-E., Siomos, N., Balis, D., Tuinder, O., Tilstra, L. G., Mona, L., Pappalardo, G. and Bortoli, D.: First validation of GOME-2/MetOp absorbing aerosol height using EARLINET lidar observations, *Atmos. Chem. Phys.*, 21, 3193–3213, 2021.

<https://doi.org/10.5194/acp-21-3193-2021>

Tilstra, L. G., Tuinder, O., Wang, P. and Stammes, P.: ALGORITHM THEORETICAL BASIS DOCUMENT GOME-2 Absorbing Aerosol Height, SAF/AC//KNMI/ATBD/005, 1.4, Royal Netherlands Meteorological Institute, de Bilt, 2019.

[https://acsaf.org/docs/atbd/Algorithm\\_Theoretical\\_Basis\\_Document\\_AA\\_H\\_Apr\\_2019.pdf](https://acsaf.org/docs/atbd/Algorithm_Theoretical_Basis_Document_AA_H_Apr_2019.pdf), last access: 31 March 2021.

Wang, P., Tuinder, O. N. E., Tilstra, L. G., De Graaf, M. and Stammes, P.: Interpretation of FRESCO cloud retrievals in case of absorbing aerosol events, *Atmos. Chem. Phys.*, 12(19), 9057–9077, 2021.

<https://doi.org/10.5194/acp-12-9057-2012>

De Bock, V., A. Delcloo, K. Michailidis, M. Koukouli and D. Balis, ACSAF Absorbing Aerosol Height products validation report, SAF/AC/AUTH-RMI/VR/001, 1/2020, 3 July 2020.

[https://acsaf.org/docs/vr/Validation\\_Report\\_AA\\_H\\_Jul\\_2020.pdf](https://acsaf.org/docs/vr/Validation_Report_AA_H_Jul_2020.pdf), last access: 31 March 2021.

### 7.5.1. Online quality monitoring

The online quality monitoring of the AAI in this section shows (left duo-plot) the radiance corrections for the PMD-AAI at 340 and 380 nm, and (right duo-plot) the uncorrected residue, and the corrected residue. The rightmost plot is the result of all the corrections and should stay more or less flat when seasonal cycles and differences are removed.



The break in the curves of the latter plot in August 2018 is caused by the introduction of a combination of the ‘End-of-Orbit’ corrections and a flattening of the AAI across the swath.

The plots can also be found at: [TEMIS website](#).

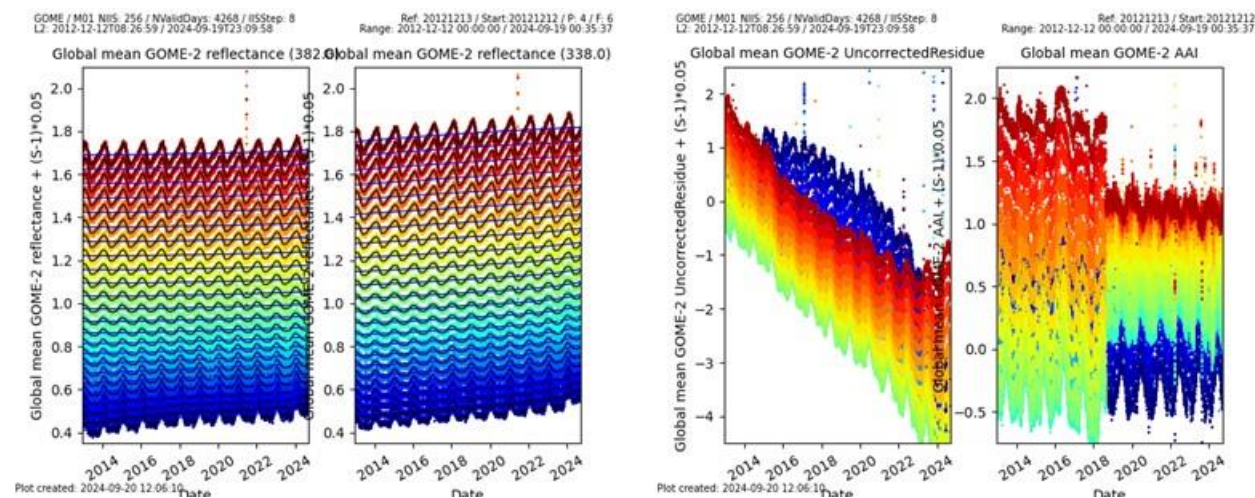


**Figure 7.26.** Timeline of global mean reflectances at 340 and 380 nm (left) and the uncorrected and corrected AAI from the PMDs of Metop-B.

## 7.6. GOME-2 UV products

**Table 7.20.** Validation status of UV products

Product Identifier	Product Name	Accuracy	Reference	Validating Institute	Correlative data sources
O3M-409	NRT UV index, clear-sky	Fulfils threshold accuracy requirements	RD8	DMI	<a href="#">WOUDC</a> , <a href="#">NEUBrew</a> , <a href="#">NSF</a>
O3M-410	NRT UV index, cloud-corrected				
O3M-450 – O3M-464	Offline surface UV	Fulfils target accuracy requirements	RD14	FMI	Brewers and SUV-spectroradiometers from <a href="#">WOUDC</a> , <a href="#">NEUBrew</a> , <a href="#">NSF</a> , <a href="#">NOAA</a> , <a href="#">AUTH</a> and <a href="#">FMI</a>

### 7.6.1. Online quality monitoring

NUV:

Online quality monitoring of the NRT UV index is found on [NUV web page](#). It can be traced that the quality of the NUV products is stable since the last validation. No problems with the data quality was found in the reporting period.

OUV:

[Online quality monitoring of offline surface UV](#) has not shown any unexpected, permanent changes in the monitoring value after the latest validation, indicating that the product accuracy has remained within requirements also during the reporting period. The latest OUV validation reports were published in February 2009 covering June 2007 – May 2008 (Metop-A data) and in February 2015 covering June 2012 – May 2013 (Metop-B data).

Figure 7.27 presents the long-term monitoring graph of OUV, which illustrates seasonal variation of **global average of erythemal daily dose** (yellow markers). Any sudden changes would indicate problems with data quality. Additionally, six-month average values (January – June and July – December) are represented by red markers.

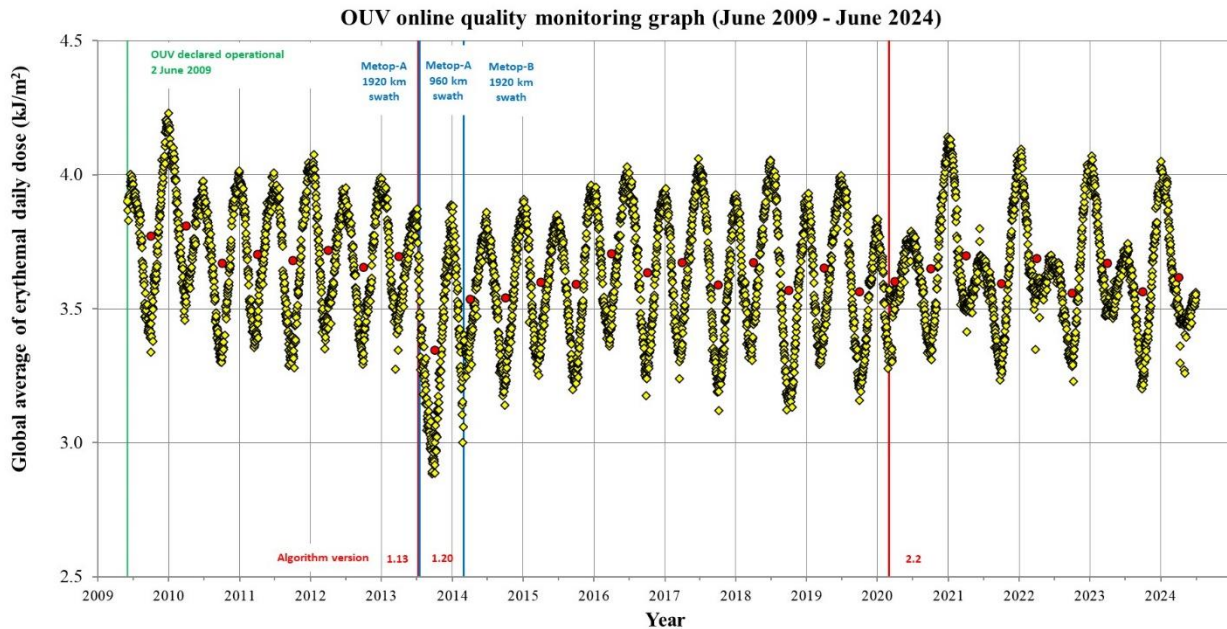


**Figure 7.27. OUV long-term monitoring graph.**

**NOTES:**

- GOME-2A was switched from nominal swath width (1920 km) to reduced swath width (960 km) 15 July 2013. The effect to OUV monitoring values can be clearly seen as more wide-spread global average values of erythemal daily dose. This is due to the dominance of lower EDD values in high latitudes when the satellite coverage near the equator is poor due to narrower swath width.
- OUV data processing was switched to use Metop-B data having nominal swath width of 1920 km 1 March 2014
- OUV data processing was switched to use Metop-B+C data 1 March 2020



## 7.7. IASI NRT products

**Table 7.21. Online quality monitoring of the IASI CO, SO<sub>2</sub>, O<sub>3</sub> and HNO<sub>3</sub> products**

Product Identifier	Product Name	Accuracy	Reference	Validating Institute	Correlative data sources
O3M-80	IASI NRT CO	Fulfils threshold accuracy requirement	RD18	LATMOS	FTIR NDACC, MOPITT
O3M-57	IASI NRT SO <sub>2</sub>	Fulfils threshold accuracy requirement	RD19	AUTH, BIRA-IASB, LATMOS, ULB	MAXDOAS
O3M-44 O3M-49	IASI NRT O <sub>3</sub>	Fulfils threshold accuracy requirement	RD31	AUTH, KMI, DWD	GOME-2, balloon sonde, lidar and microwave radiometer, Brewer and Dobson
O3M-81	IASI NRT HNO <sub>3</sub>	Fulfils threshold accuracy requirement	RD32	BIRA-IASB	FTIR NDACC (only available in 2021)

IASI NRT O<sub>3</sub> and IASI NRT HNO<sub>3</sub> products have been released by EUMETSAT as ‘operational’ on 18 May 2022.

IASI online quality monitoring is performed at ULB and LATMOS.

IASI NRT CO online monitoring:

[https://atmosphere.copernicus.eu/charts/packages/cams\\_monitoring/](https://atmosphere.copernicus.eu/charts/packages/cams_monitoring/)

### Dissemination monitoring activities summary:

#### IASI CO:

The IASI NRT CO product (v6.3) has been declared operational on 2 March 2017. Here we present statistical results when comparing the EUMETSAT product disseminated by EUMETCast in BUFR format (COX) with the native product produced at ULB (FORLI-CO v20191122) for 6 days representative of 6 months: January 15<sup>th</sup>, February 15<sup>th</sup>, March 16<sup>th</sup>, April 15<sup>th</sup>, May 15<sup>th</sup> and June 15<sup>th</sup>, 2024, for Metop-B and Metop-C. This allows monitoring if any discrepancy occurs between the two, EUMETSAT and native, products. So far, the discrepancies are found within the numerical errors inherent to the use of different IT infrastructure.

CO total column and profiles are investigated. Statistics between COX data and FORLI-CO data (v20191122) are presented in Table 7.22. Profiles correlation (“Correlation”) score is computed using the discreet cross correlation integral between two profiles, normalized by the square root of the product of their auto-correlation integral. Score of 1 is expected for perfectly matching profiles, 0 for unrelated ones. Absolute and relative differences are calculated for the total columns. These tables are extracted from the Daily Reports prepared by Daniel Hurtmans at ULB.

**Table 7.22. Statistics between COX data and FORLI-CO data for 6 days: January 15<sup>th</sup>, February 15<sup>th</sup>, March 16<sup>th</sup>, April 15<sup>th</sup>, May 15<sup>th</sup> and June 15<sup>th</sup>, 2024.****15/01/2024:**

		IASI-b		IASI-c	
		Native	COX	Native	COX
Individual Pixels		557321	556479	548850	548135
Common Pixels		555503 (99.67%)		547236 (99.71%)	
Correlation	Mean	0.9997±0.0008		0.9997±0.0007	
	Max	1.0000		1.0000	
	Min	0.8320		0.8439	
Total Column Differences	Mean (10 <sup>19</sup> mol/cm <sup>2</sup> )	0.0046±0.0044		0.0046±0.0041	
	Max (10 <sup>19</sup> mol/cm <sup>2</sup> )	0.7653		0.9244	
	Min (10 <sup>19</sup> mol/cm <sup>2</sup> )	-1.3304		-0.3307	
Total Column Relative Differences	Mean (%)	2.4126±1.4852		2.4158±1.4218	
	Max (%)	73.0177		42.5429	
	Min (%)	-196.6913		-55.3856	

**15/02/2024:**

		IASI-c		IASI-b	
		Native	COX	Native	COX
Individual Pixels		569210	568563	569831	569182
Common Pixels		567653 (99.73%)		568242 (99.72%)	
Correlation	Mean	0.9997±0.0009		0.9997±0.0007	
	Max	1.0000		1.0000	
	Min	0.7269		0.8869	
Total Column Differences	Mean (10 <sup>19</sup> mol/cm <sup>2</sup> )	0.0052±0.0124		0.0051±0.0085	
	Max (10 <sup>19</sup> mol/cm <sup>2</sup> )	4.4506		1.5582	
	Min (10 <sup>19</sup> mol/cm <sup>2</sup> )	-1.3381		-1.4604	
Total Column Relative Differences	Mean (%)	2.4849±1.4615		2.4938±1.4241	
	Max (%)	82.1277		61.7310	
	Min (%)	-66.8993		-68.3862	

**16/03/2024:**

		IASI-b		IASI-c	
		Native	COX	Native	COX
Individual Pixels		593401	592547	587173	586640
Common Pixels		591651 (99.71%)		585190 (99.66%)	
Correlation	Mean	0.9997±0.0007		0.9997±0.0006	
	Max	1.0000		1.0000	
	Min	0.8914		0.9271	
Total Column Differences	Mean ( $10^{19}$ mol/cm <sup>2</sup> )	0.0051±0.0050		0.0050±0.0043	
	Max ( $10^{19}$ mol/cm <sup>2</sup> )	1.1741		0.4986	
	Min ( $10^{19}$ mol/cm <sup>2</sup> )	-0.7915		-0.1447	
Total Column Relative Differences	Mean (%)	2.5470±1.3988		2.5521±1.3727	
	Max (%)	46.9075		37.2645	
	Min (%)	-43.5301		-55.8473	

**15/04/2024:**

		IASI-c		IASI-b	
		Native	COX	Native	COX
Individual Pixels		554307	553373	565972	569154
Common Pixels		552466 (99.67%)		559676 (98.33%)	
Correlation	Mean	0.9997±0.0010		0.9996±0.0012	
	Max	1.0000		1.0000	
	Min	0.5905		0.7447	
Total Column Differences	Mean ( $10^{19}$ mol/cm <sup>2</sup> )	0.0051±0.1100		0.0052±0.0060	
	Max ( $10^{19}$ mol/cm <sup>2</sup> )	8.8399		1.6323	
	Min ( $10^{19}$ mol/cm <sup>2</sup> )	-81.1198		-0.9721	
Total Column Relative Differences	Mean (%)	2.5984±9.3313		2.6032±1.4652	
	Max (%)	79.3728		84.2825	
	Min (%)	-6827.9051		-270.6928	

**15/05/2024:**

		IASI-b		IASI-c	
		Native	COX	Native	COX
Individual Pixels		537278	536238	520463	519576
Common Pixels		535431 (99.66%)		518724 (99.67%)	
Correlation	Mean	0.9996±0.0013		0.9996±0.0012	
	Max	1.0000		1.0000	
	Min	0.7810		0.8123	
Total Column Differences	Mean ( $10^{19}$ mol/cm <sup>2</sup> )	0.0053±0.0063		0.0054±0.0054	
	Max ( $10^{19}$ mol/cm <sup>2</sup> )	0.6163		0.4803	
	Min ( $10^{19}$ mol/cm <sup>2</sup> )	-2.1773		-1.8195	
Total Column Relative Differences	Mean (%)	2.6991±1.3829		2.7227±1.3224	
	Max (%)	62.4494		60.9178	
	Min (%)	-50.7226		-49.3443	

**15/06/2024:**

		IASI-c		IASI-b	
		Native	COX	Native	COX
Individual Pixels		588950	587927	594564	593353
Common Pixels		586914 (99.65%)		592359 (99.63%)	
Correlation	Mean	0.9995±0.0017		0.9995±0.0018	
	Max	1.0000		1.0000	
	Min	0.8001		0.7308	
Total Column Differences	Mean ( $10^{19}$ mol/cm <sup>2</sup> )	0.0048±0.0078		0.0048±0.0062	
	Max ( $10^{19}$ mol/cm <sup>2</sup> )	0.8813		0.7701	
	Min ( $10^{19}$ mol/cm <sup>2</sup> )	-4.9903		-2.5183	
Total Column Relative Differences	Mean (%)	2.6215±1.4083		2.6537±1.4360	
	Max (%)	65.9601		71.0028	
	Min (%)	-89.9671		-59.5958	

Figure 7.28 – Figure 7.33 show the correlation plots for total column between COX data and FORLI-CO for each platform. No critical deviation was found for these dates.

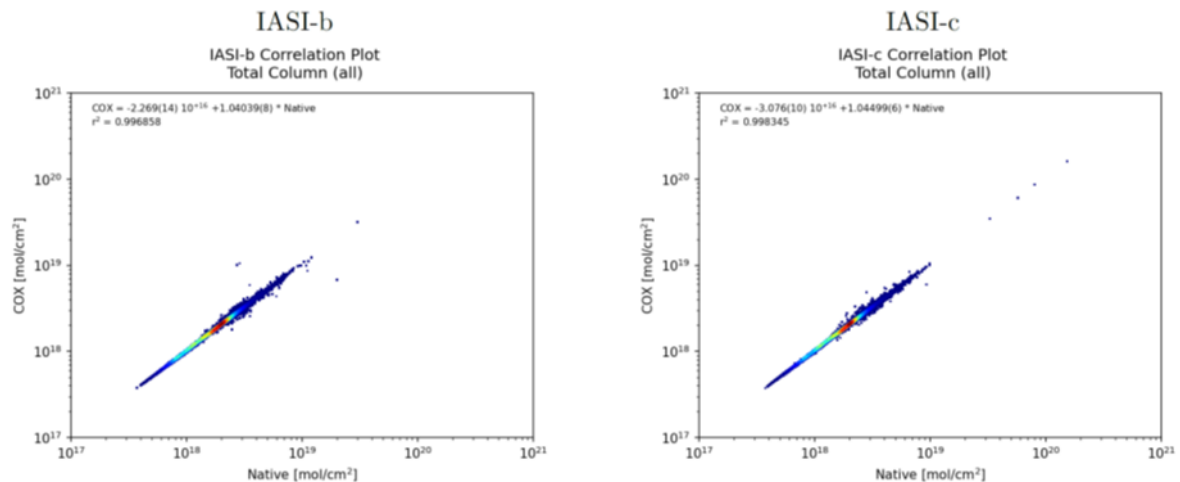


**Figure 7.28.** Correlation plots for total column between COX data and FORLI-CO for each platform for 15/01/2024. X-axis corresponds to native data (mol/cm<sup>2</sup>) and Y-axis corresponds to COX data (mol/cm<sup>2</sup>).

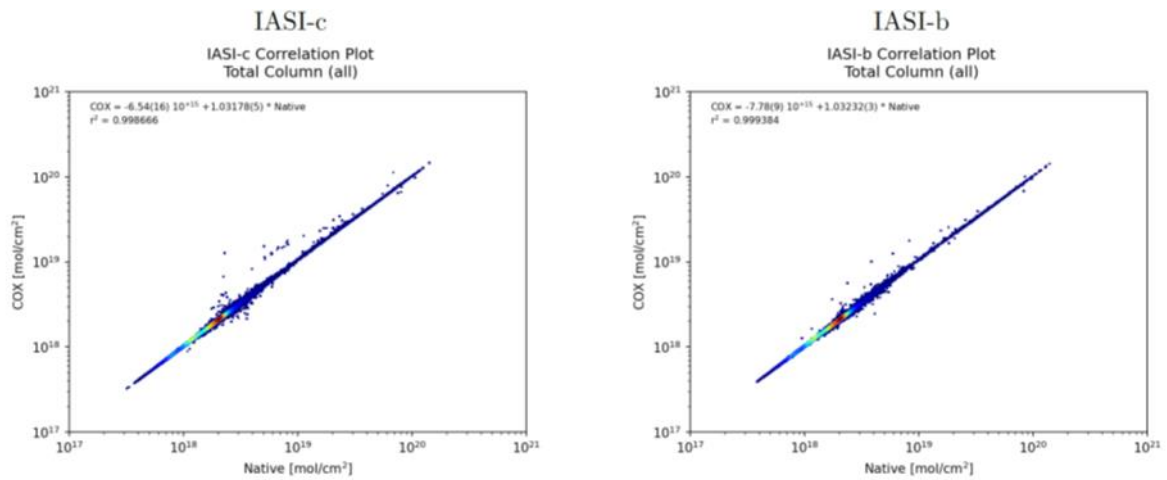


Figure 7.29. Same as Figure 7.28 but for 15/02/2024.

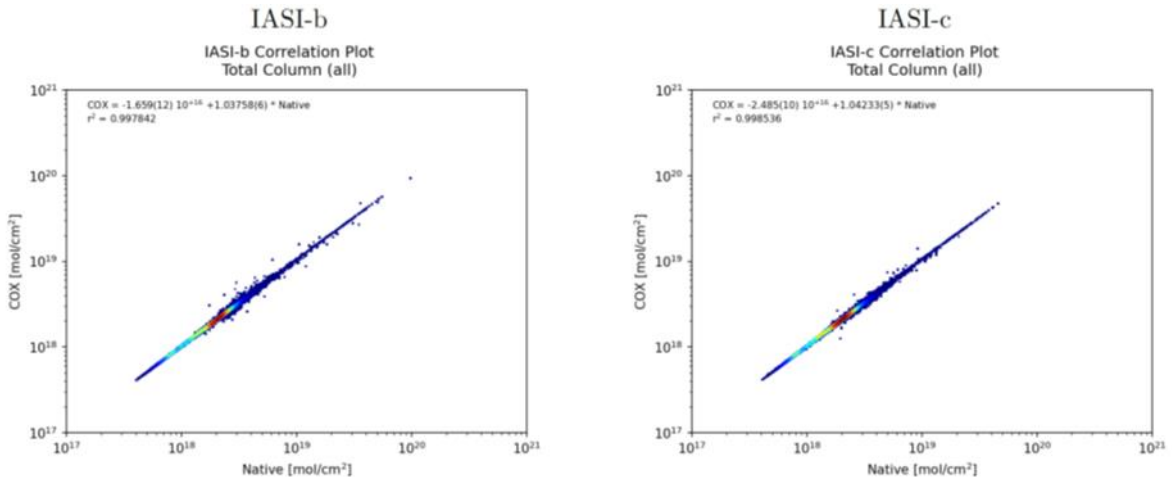


Figure 7.30. Same as Figure 7.28 but for 16/03/2024.

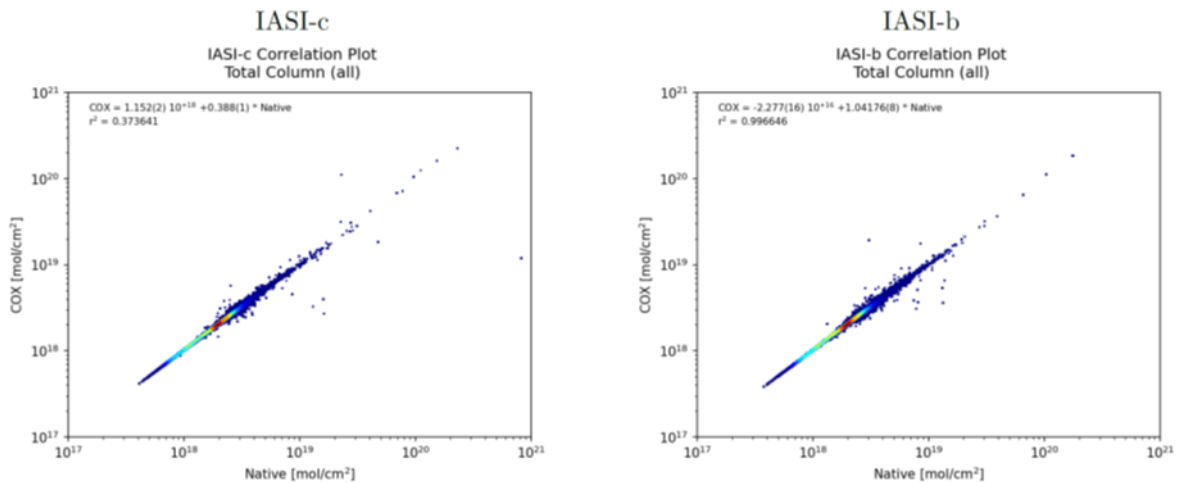


Figure 7.31. Same as Figure 7.28 but for 15/04/2024.



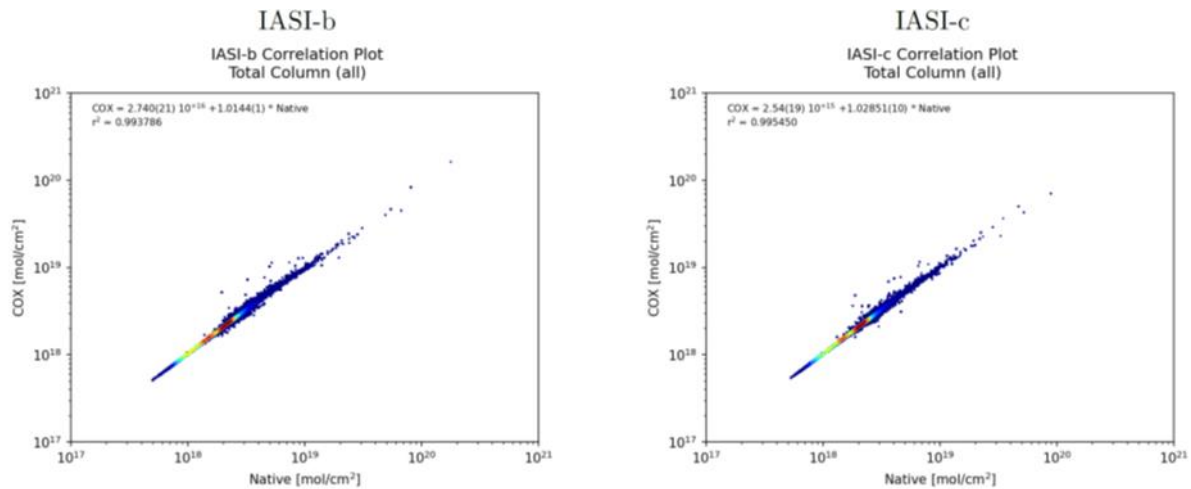


Figure 7.32. Same as Figure 7.28 but for 15/05/2024.

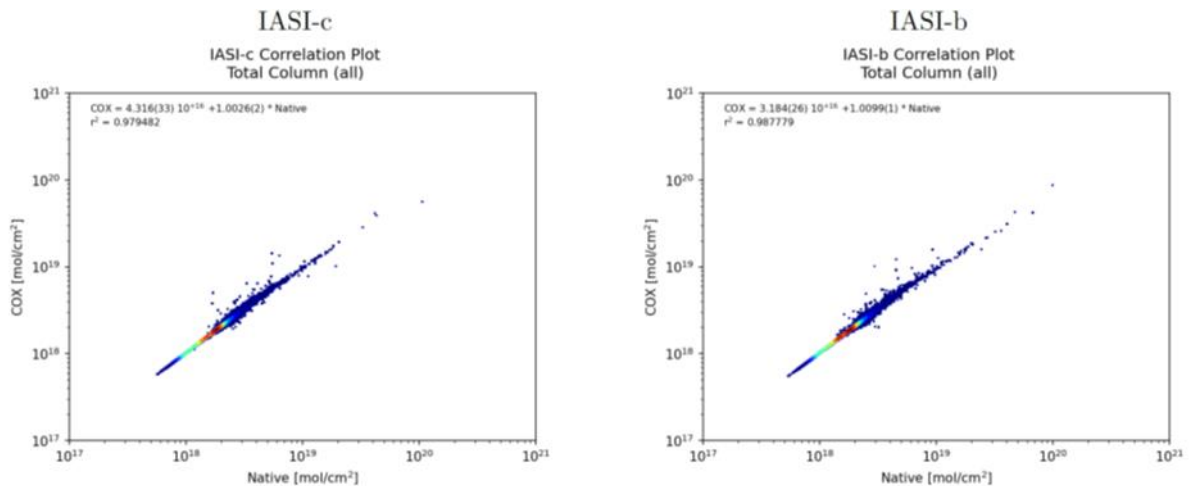


Figure 7.33. Same as Figure 7.28 but for 15/06/2024.

Note that a frequency distribution of the correlation coefficients (separated for each platform) will be provided when EUMETSAT will update the IASI CO retrieval algorithm at the EUMETSAT facilities. (In response to Action 3 (OR-9)).

### IASI SO<sub>2</sub>:

The IASI BRESCIA SO<sub>2</sub> retrieval algorithm has been implemented in the PPF v6.3 at EUMETSAT (operational release on 18/04/2018). Here we compare the EUMETSAT product disseminated by EUMETCast in BUFR format (SO<sub>2</sub> EUMET) with the native product produced at ULB (SO<sub>2</sub> ULB) for 5 days between March and May 2024, for Metop-B and Metop-C. We choose to study 17/03/2024, 18/03/2024, 23/04/2024, 30/04/2024 and 02/05/2024.

#### i) Online quality monitoring for SO<sub>2</sub> for five estimated altitudes:

For each of the five days, scatterplots for the different estimated altitudes (7, 10, 13, 16 and 25 km) are presented (Figure 7.34 – Figure 7.38). The data have been filtered following the recommendations of the Product User Manual (Section 5.2.2, i.e. we kept the pixels in the neighbourhood ( $\pm 10$  degrees) of SO<sub>2</sub>\_BT\_DIFFERENCE > 1K pixels, and did not use the pixels with a SO<sub>2</sub>\_BT\_DIFFERENCE < 0.4K.

We recall here that when the IASI L2 pressure and temperature profiles are not available, ECMWF forecasts (3h, interpolated in time and space) data are used in the EUMETSAT API. These pixels are flagged with  $SO_2\_QFLAG = 11$  and are not part of the comparison.

Correlation coefficients (in blue) are  $\sim 1$ .

So far, the discrepancies are found within the numerical errors inherent to the use of different IT infrastructure.

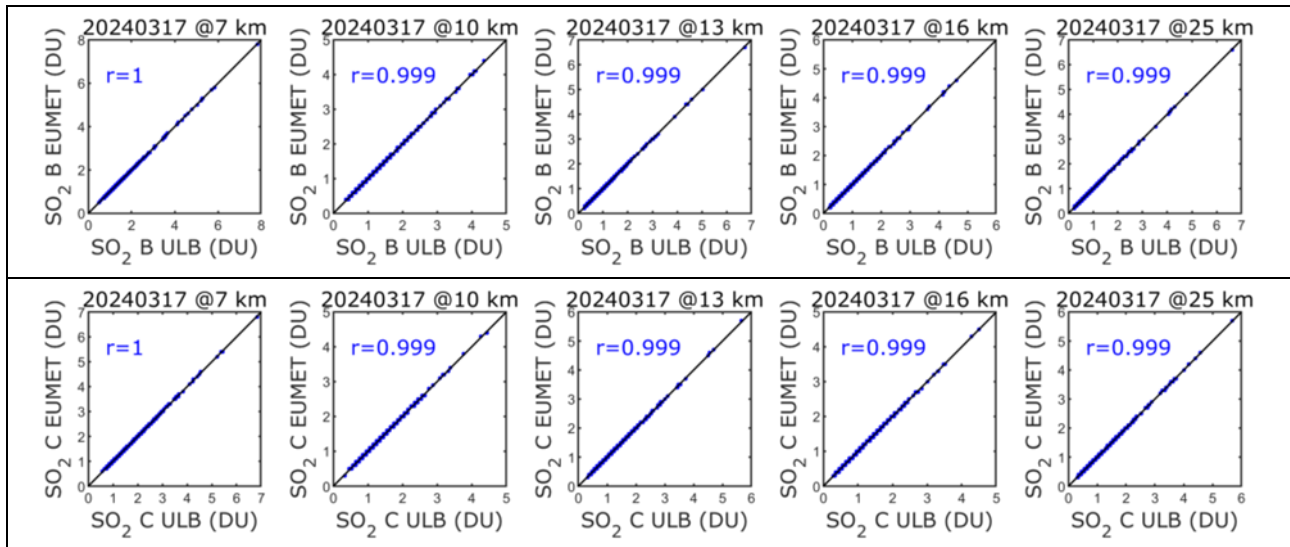


**Figure 7.34. Scatterplots for Metop-B (top) and Metop-C (bottom): SO<sub>2</sub> EUMET versus SO<sub>2</sub> ULB for 17/03/2024, for the five estimated altitudes (7, 10, 13, 16 and 25 km).**

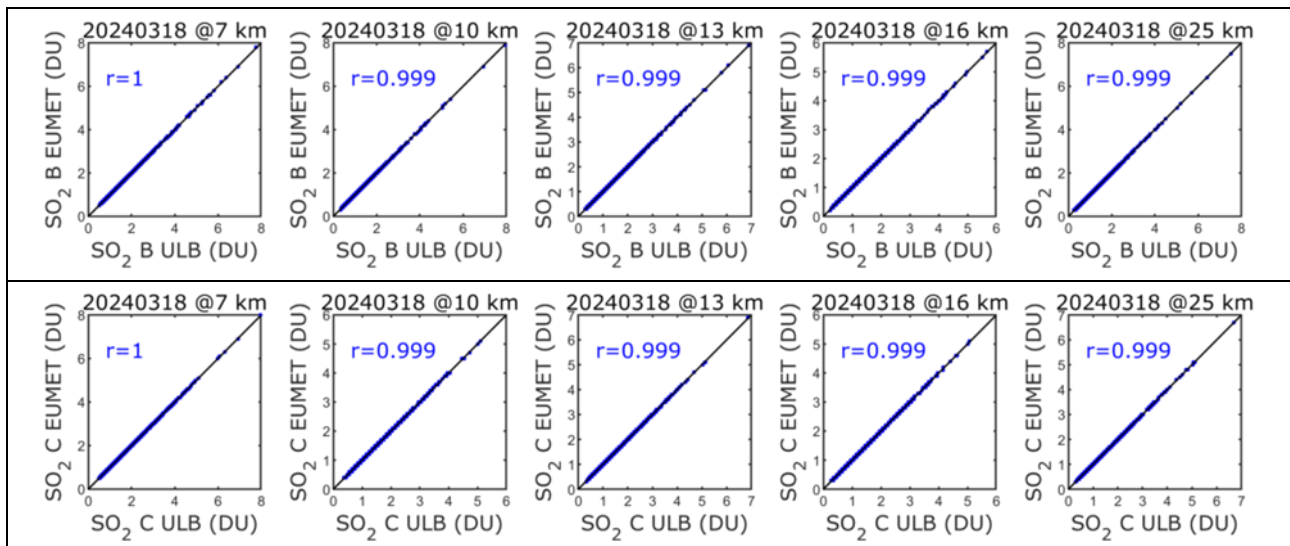


**Figure 7.35. Same as Figure 7.34 but for 18/03/2024.**



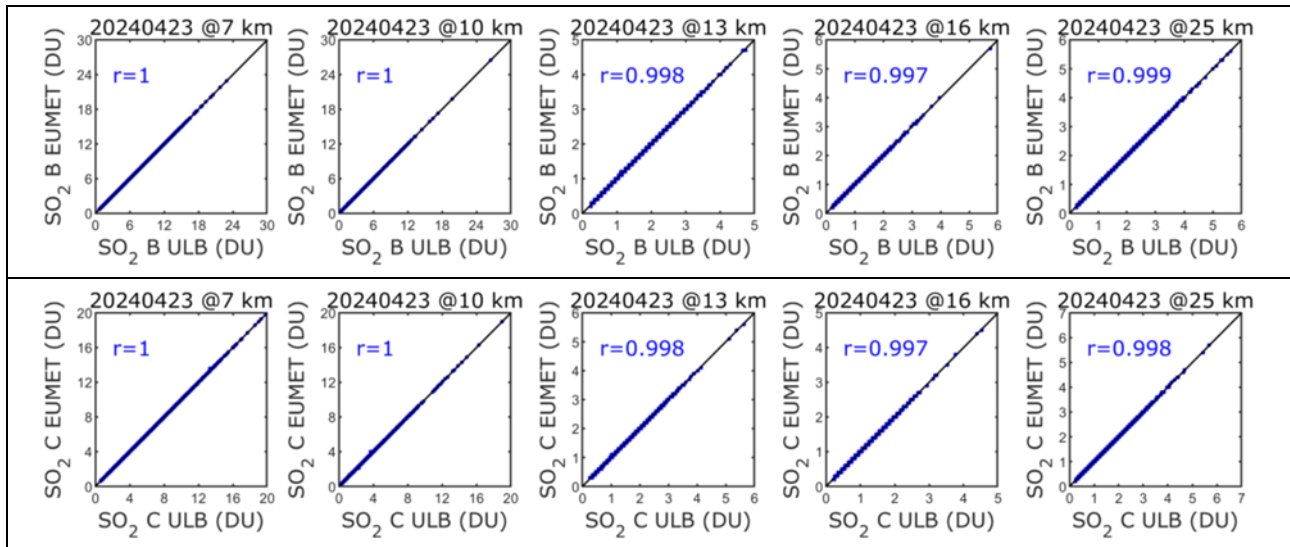


Figure 7.36. Same as Figure 7.34 but for 23/04/2024.

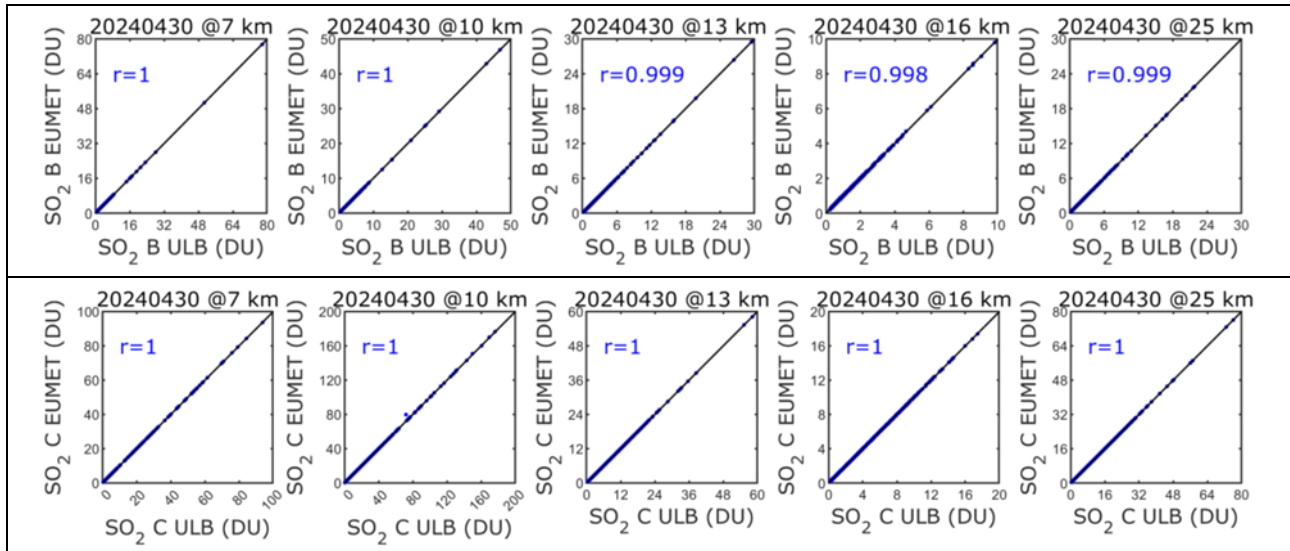


Figure 7.37. Same as Figure 7.34 but for 30/04/2024.

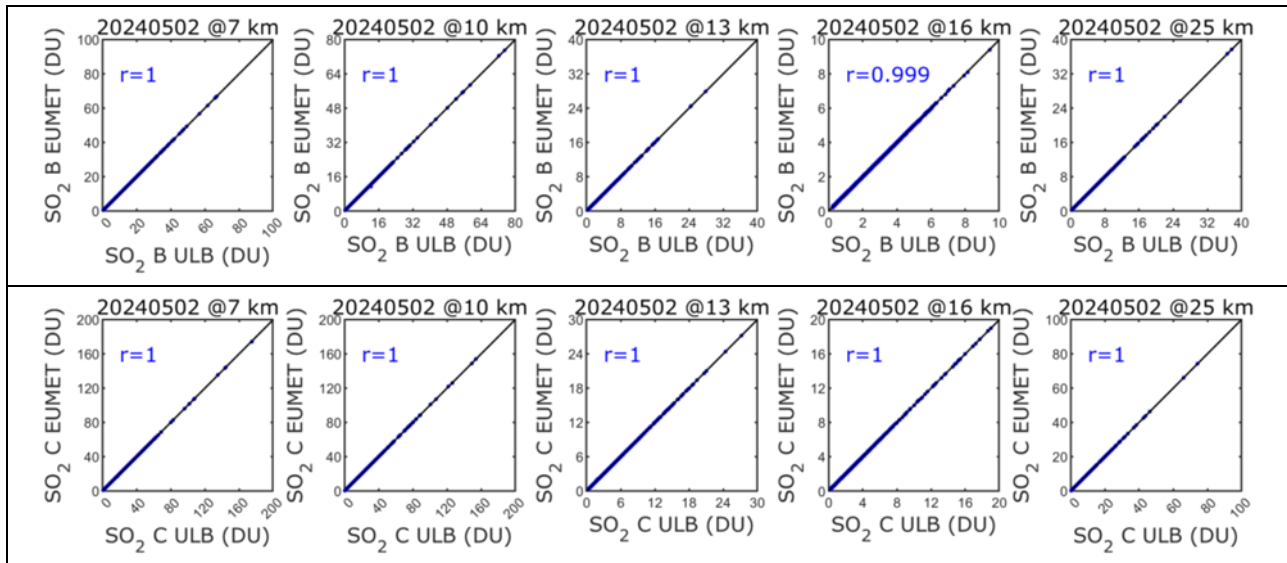


Figure 7.38. Same as Figure 7.34 but for 02/05/2024.

ii) Online quality monitoring for **SO2\_ALTITUDE** and **SO2\_COL**:

Although the two products **SO2\_ALTITUDE** (estimated altitude of the SO<sub>2</sub> plume) and **SO2\_COL** (SO<sub>2</sub> column at the estimated altitude) are operational since May 2021, **the EUMETSAT and the ULB algorithms versions are different**, with the ULB version being the latest version of the algorithm. **As said in the previous report, the EUMETSAT and ULB products are not the same and the comparison shows differences.** Scatterplots for five dates (17/03/2024, 18/03/2024, 23/04/2024, 30/04/2024 and 02/05/2024), for Metop-B and C are shown in Figure 7.39 – Figure 7.43. Daniel Hurtmans provided an updated version of the Brescia algorithm (including the SO<sub>2</sub> altitude) for implementation to EUMETSAT, in order for the two versions to be the same. We are waiting for an update from EUMETSAT.

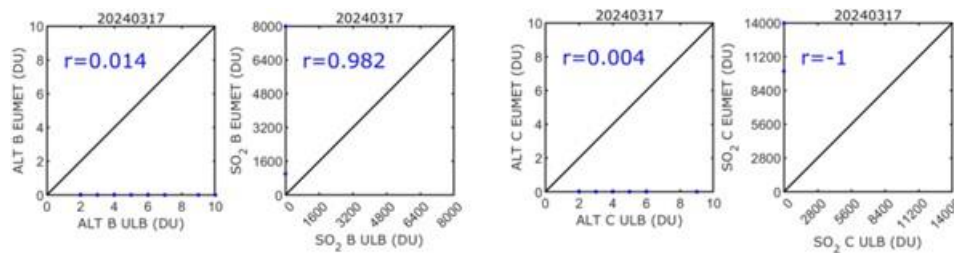


Figure 7.39. Scatter plots for Metop-B and Metop-C: **SO2\_ALTITUDE** EUMET versus **SO2\_ALTITUDE** ULB, as well as **SO2\_COL** EUMET versus **SO2\_COL** ULB, for 17/03/2024.

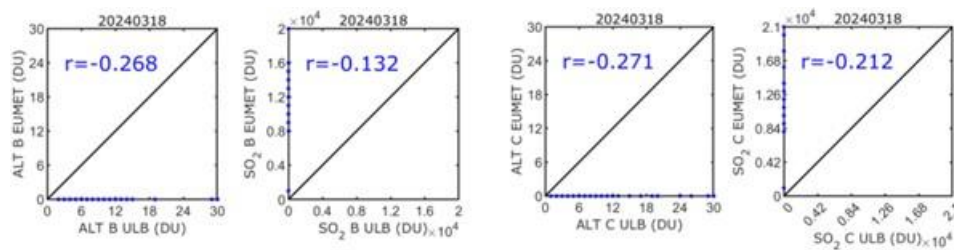


Figure 7.40. Same as Figure 7.39 but for 18/03/2024.

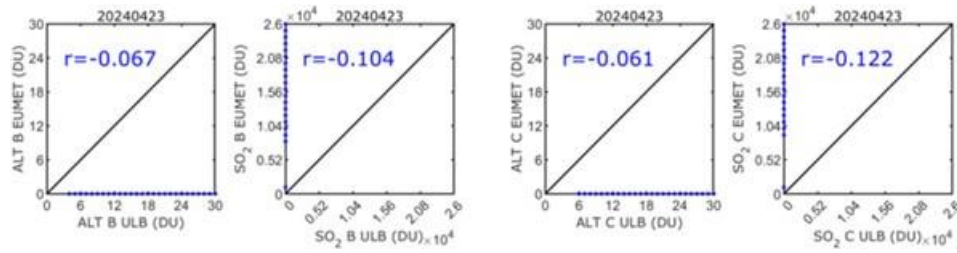


Figure 7.41. Same as Figure 7.39 but for 23/04/2024.

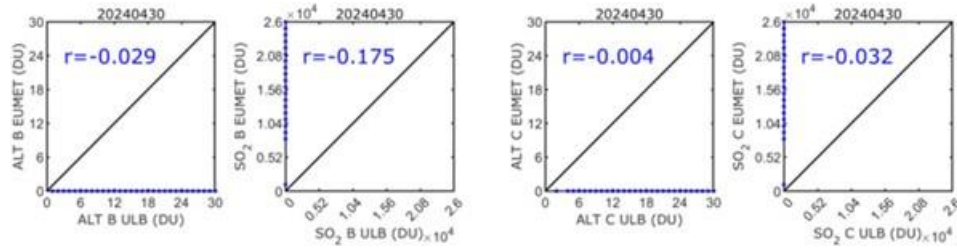


Figure 7.42. Same as Figure 7.39 but for 30/04/2024.

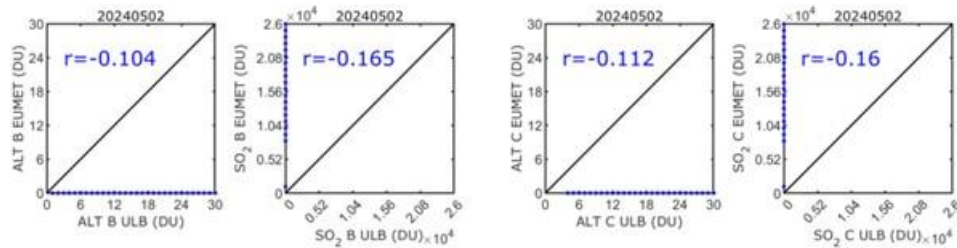


Figure 7.43. Same as Figure 7.39 but for 02/05/2024.

### IASI O3:

The IASI NRT O3 product (v6.5) has been released as operational product on 18 May 2022. Here we present statistical results when comparing the EUMETSAT product disseminated by EUMETCast in BUFR format (OZO) with the native product produced at ULB (FORLI-O3 v20191122) for six days representative of six months: January 15<sup>th</sup>, February 15<sup>th</sup>, March 15<sup>th</sup>, April 15<sup>th</sup>, May 15<sup>th</sup> and June 15<sup>th</sup>, 2024, for Metop-B and Metop-C. This allows monitoring if any discrepancy occurs between the two, EUMETSAT and native, products. The data have been filtered following the recommendations of the Product User Manual. Furthermore, data associated with DOFS>2 have also been filtered out.

O3 total and 0 – 6 km column are investigated. Detailed statistics for total column between OZO data and FORLI-O3 data (v20191122) for each of the six days are presented in Table 7.23. No critical deviation was found for these dates.

The difference between individual pixels in native and BUFR format is due to the fact that the NRT EUMETSAT version is the v2015, and only 1/10 pixels are treated to gain processing time, this means clearly a lower number of observations.

**Table 7.23. Statistics for total column between OZO data and FORLI-O3 data for six days: January 15<sup>th</sup>, February 15<sup>th</sup>, March 15<sup>th</sup>, April 15<sup>th</sup>, May 15<sup>th</sup> and June 15<sup>th</sup>, 2024.**

15 January 2024	IASI-C		IASI-B	
	Native	BUFR	Native	BUFR
Individual Pixels	381272	94817	389120	96331
Common Pixels	82818 (21.72%)		84392 (21.69%)	
Correlation	0.9994		0.9995	
Mean Total Column Differences (DU)	2.2794±2.2593		2.2928±2.1050	
Mean Total Column Relative Differences (%)	0.8154±0.7286		0.8199±0.6975	

15 February 2024	IASI-C		IASI-B	
	Native	BUFR	Native	BUFR
Individual Pixels	374849	92398	374925	92467
Common Pixels	81465 (21.73%)		81488 (21.73%)	
Correlation	0.9996		0.9996	
Mean Total Column Differences (DU)	2.3729±2.6849		2.3890±2.6645	
Mean Total Column Relative Differences (%)	0.8644±0.7495		0.8607±0.7367	

15 March 2024	IASI-C		IASI-B	
	Native	BUFR	Native	BUFR
Individual Pixels	342168	84456	342984	83767
Common Pixels	75050 (21.93%)		74418 (21.70%)	
Correlation	0.9998		0.9998	
Mean Total Column Differences (DU)	2.6932±1.9315		2.6897±1.9029	
Mean Total Column Relative Differences (%)	0.9513±0.5934		0.9422±0.5813	

15 April 2024	IASI-C		IASI-B	
	Native	BUFR	Native	BUFR
Individual Pixels	372281	92281	376537	93084
Common Pixels	81988 (22.02%)		81953 (21.76%)	
Correlation	0.9998		0.9998	
Mean Total Column Differences (DU)	2.9088±1.5561		2.8552±1.5882	
Mean Total Column Relative Differences (%)	0.9372±0.4880		0.9224±0.4966	

15 May 2024	IASI-C		IASI-B	
	Native	BUFR	Native	BUFR
Individual Pixels	351873	91986	359419	93293
Common Pixels	81805 (23.25%)		83165 (23.14%)	
Correlation	0.9998		0.9998	
Mean Total Column Differences (DU)	2.7082±1.4693		2.6101±1.4837	
Mean Total Column Relative Differences (%)	0.8844±0.4973		0.8571±0.5071	

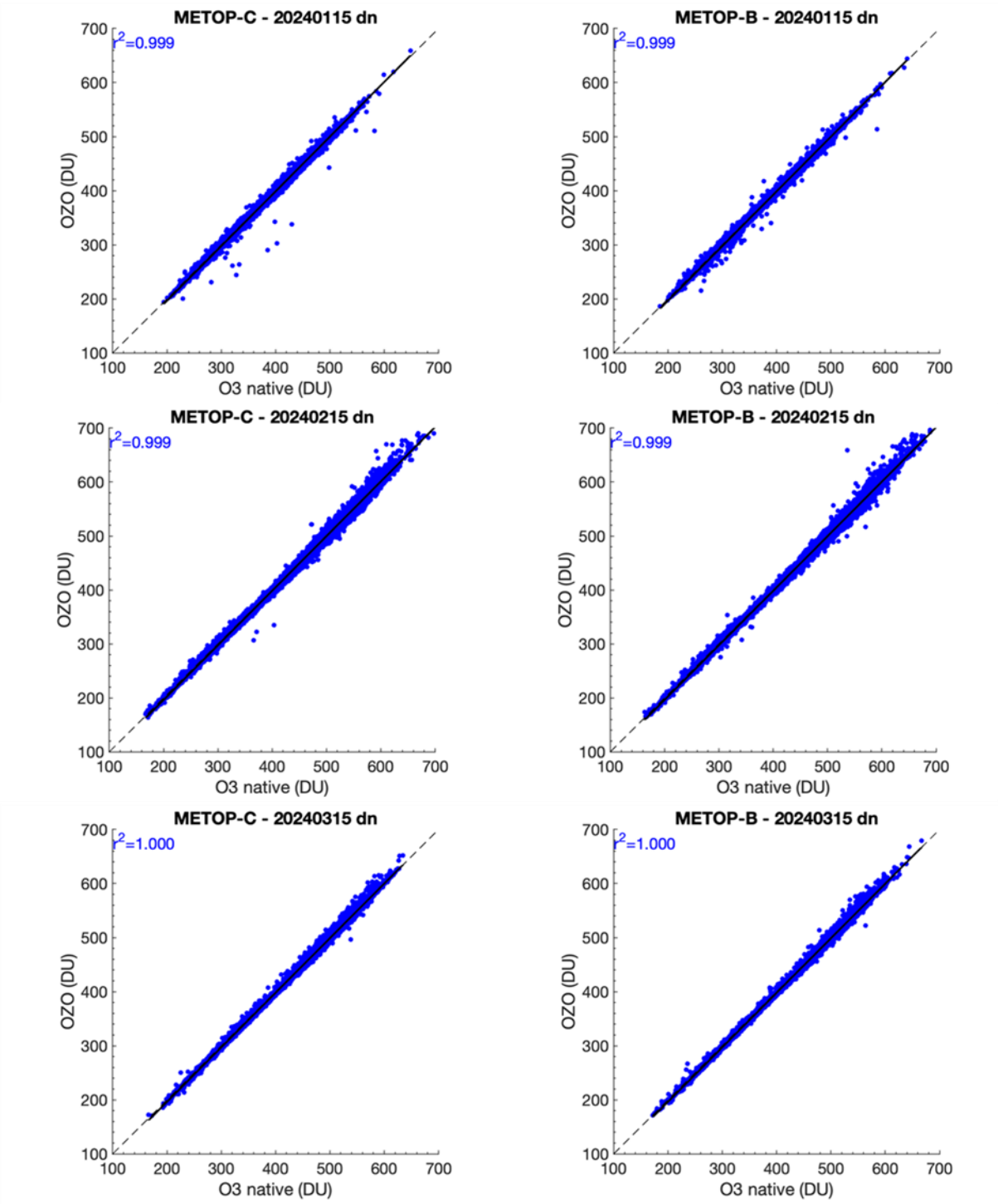
  

15 June 2024	IASI-C		IASI-B	
	Native	BUFR	Native	BUFR
Individual Pixels	396173	386994	402741	392421
Common Pixels	341751 (86.26%)		346539 (86.05%)	
Correlation	0.9995		0.9994	
Mean Total Column Differences (DU)	2.6387±1.6992		2.5357±1.8310	
Mean Total Column Relative Differences (%)	0.9051±0.5788		0.8706±0.6117	

Figure 7.44 and Figure 7.45 show the correlation plots for total and 0 – 6 km columns, respectively, between OZO data and FORLI-O3 for each platform. Correlation coefficients (in blue) are ~1.

So far, the discrepancies are found within the numerical errors inherent to the use of different IT infrastructure.





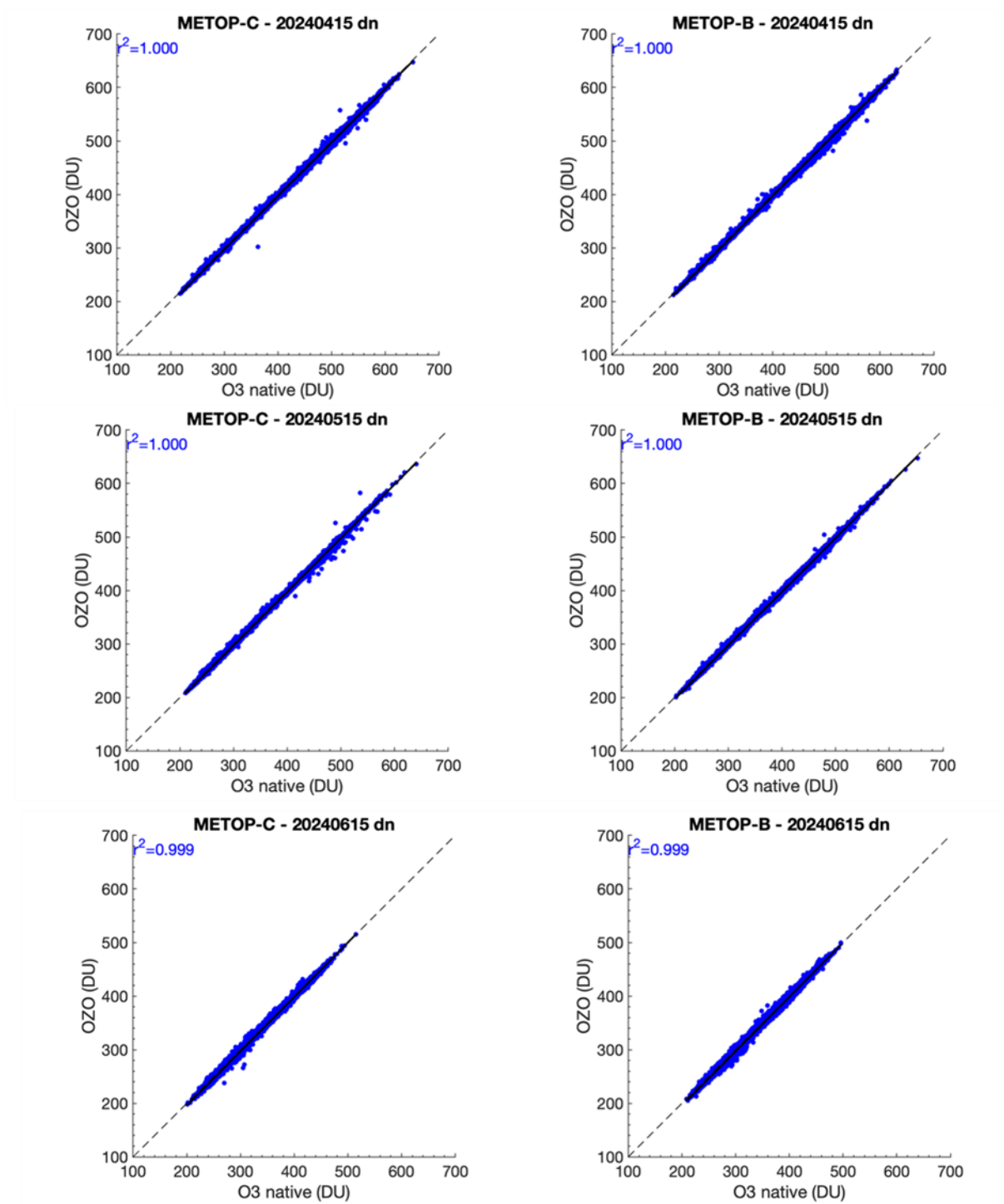
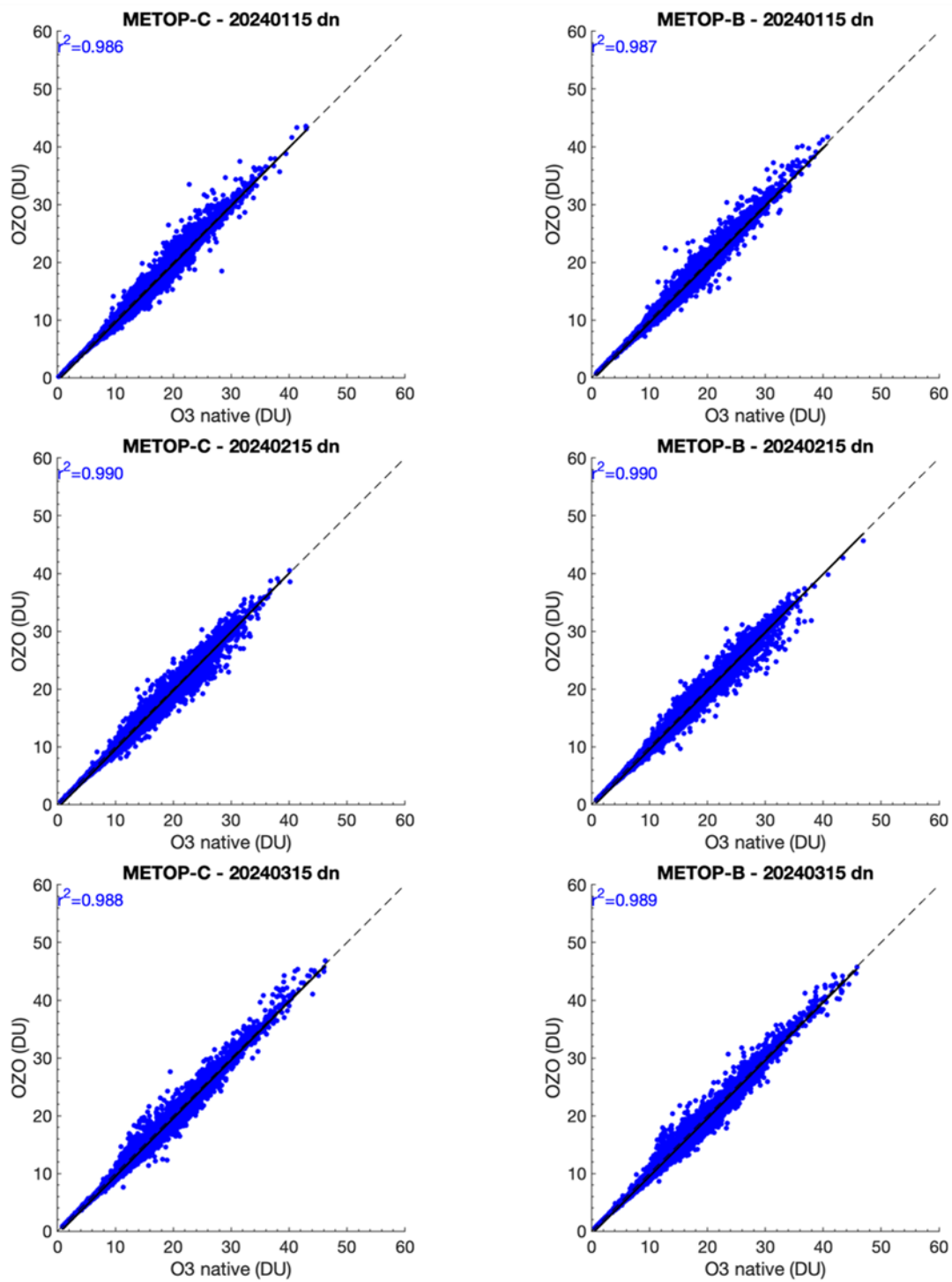
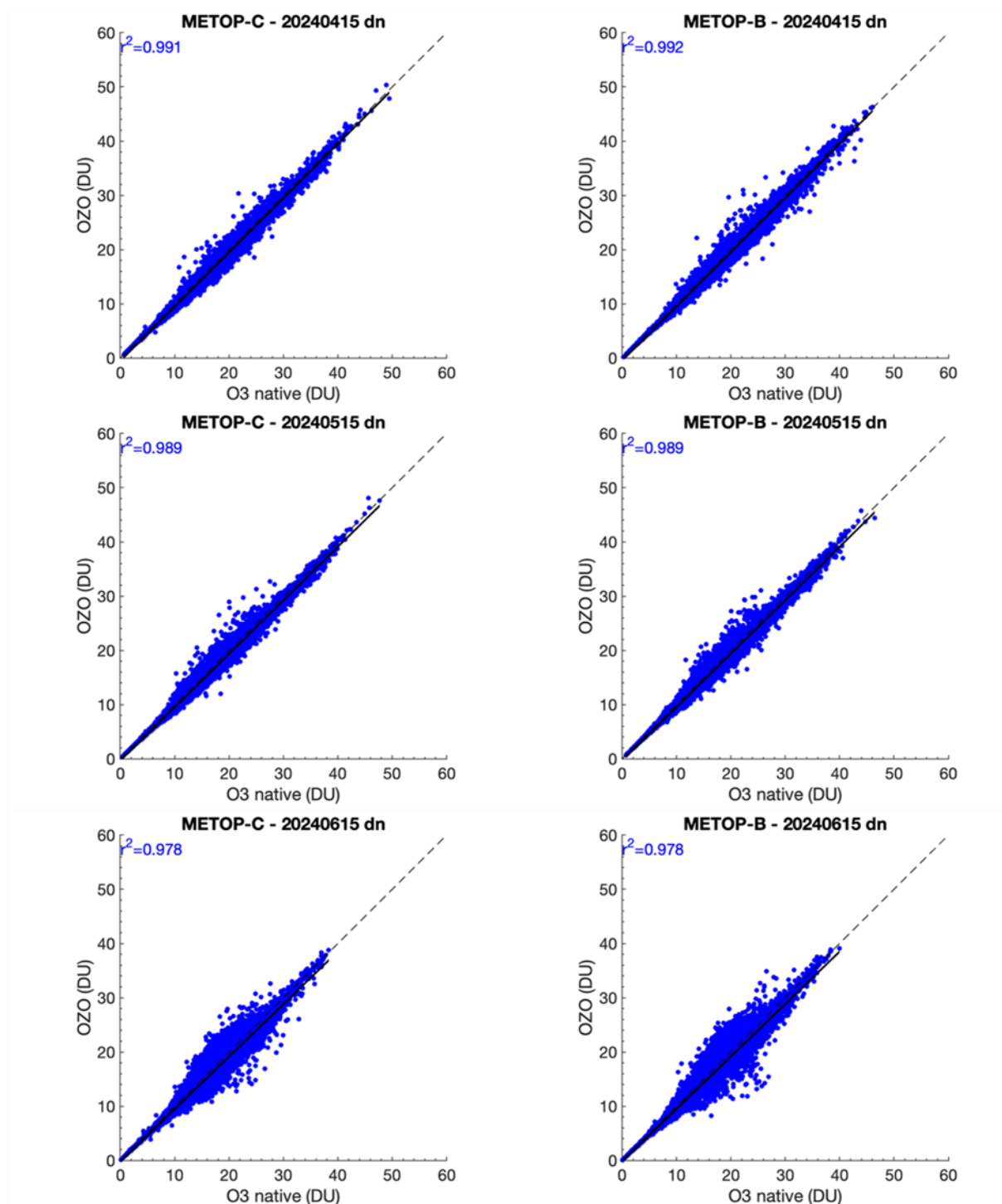


Figure 7.44. Correlation plots for total column between OZO and FORLI-O3 data for each platform for six days: January 15<sup>th</sup>, February 15<sup>th</sup>, March 15<sup>th</sup>, April 15<sup>th</sup>, May 15<sup>th</sup> and June 15<sup>th</sup>, 2024. X-axis corresponds to native data (DU) and Y-axis corresponds to OZO data (DU).







**Figure 7.45.** Correlation plots for 0 – 6 km column between OZO and FORLI-O3 data for each platform for six days: January 15<sup>th</sup>, February 15<sup>th</sup>, March 15<sup>th</sup>, April 15<sup>th</sup>, May 15<sup>th</sup> and June 15<sup>th</sup>, 2024. X-axis corresponds to native data (DU) and Y-axis corresponds to OZO data (DU).

### IASI HNO3:

The IASI NRT HNO3 product (v6.5) has been released as operational product on 18 May 2022. Here we present statistical results when comparing the EUMETSAT product disseminated by EUMETCast in BUFR format (NAC) with the native product produced at ULB (FORLI-HNO3 v20191122) for six days representative of six months: January 15<sup>th</sup>, February 15<sup>th</sup>, March 15<sup>th</sup>,

April 15<sup>th</sup>, May 15<sup>th</sup> and June 15<sup>th</sup>, 2024, for Metop-B and Metop-C. This allows monitoring if any discrepancy occurs between the two, EUMETSAT and native, products. The data have been filtered following the recommendations of the Product User Manual.

HNO<sub>3</sub> total column is investigated. Detailed statistics for total column between NAC data and FORLI-HNO<sub>3</sub> data (v20191122) for each of the six days are presented in Table 7.24. No critical deviation was found for these dates.

**Table 7.24. Statistics for total column between NAC data and FORLI-HNO<sub>3</sub> data for six days: January 15<sup>th</sup>, February 15<sup>th</sup>, March 15<sup>th</sup>, April 15<sup>th</sup>, May 15<sup>th</sup> and June 15<sup>th</sup>, 2024.**

15 January 2024	IASI-C		IASI-B	
	Native	BUFR	Native	BUFR
Individual Pixels	272840	57925	271434	58288
Common Pixels	51538 (18.89%)		51869 (19.11%)	
Correlation	0.9998		0.9997	
Mean Total Column Differences (x10 <sup>16</sup> molec cm <sup>-2</sup> )	0.0067±0.0171		0.0071±0.0214	
Mean Total Column Relative Differences (%)	0.8135±1.3411		0.8147±1.3541	

15 February 2024	IASI-C		IASI-B	
	Native	BUFR	Native	BUFR
Individual Pixels	265233	59722	264322	59337
Common Pixels	51950 (19.59%)		51788 (19.59%)	
Correlation	0.9999		0.9999	
Mean Total Column Differences (x10 <sup>16</sup> molec cm <sup>-2</sup> )	0.0077±0.0155		0.0077±0.0160	
Mean Total Column Relative Differences (%)	0.9243±1.3581		0.9027±1.3784	

15 March 2024	IASI-C		IASI-B	
	Native	BUFR	Native	BUFR
Individual Pixels	283982	58838	284088	57541
Common Pixels	53059 (18.68%)		51832 (18.25%)	
Correlation	0.9999		0.9999	
Mean Total Column Differences (x10 <sup>16</sup> molec cm <sup>-2</sup> )	0.0072±0.0146		0.0077±0.0148	
Mean Total Column Relative Differences (%)	0.8679±1.3217		0.8853±1.3300	

15 April 2024	IASI-C		IASI-B	
	Native	BUFR	Native	BUFR
Individual Pixels	297412	61130	309507	61550
Common Pixels	55158 (18.55%)		55514 (17.94%)	
0.999	0.999		0.9998	
Mean Total Column Differences ( $\times 10^{16}$ molec $\text{cm}^{-2}$ )	0.0062 $\pm$ 0.0167		0.0072 $\pm$ 0.0172	
Mean Total Column Relative Differences (%)	0.7623 $\pm$ 1.3282		0.8078 $\pm$ 1.3644	

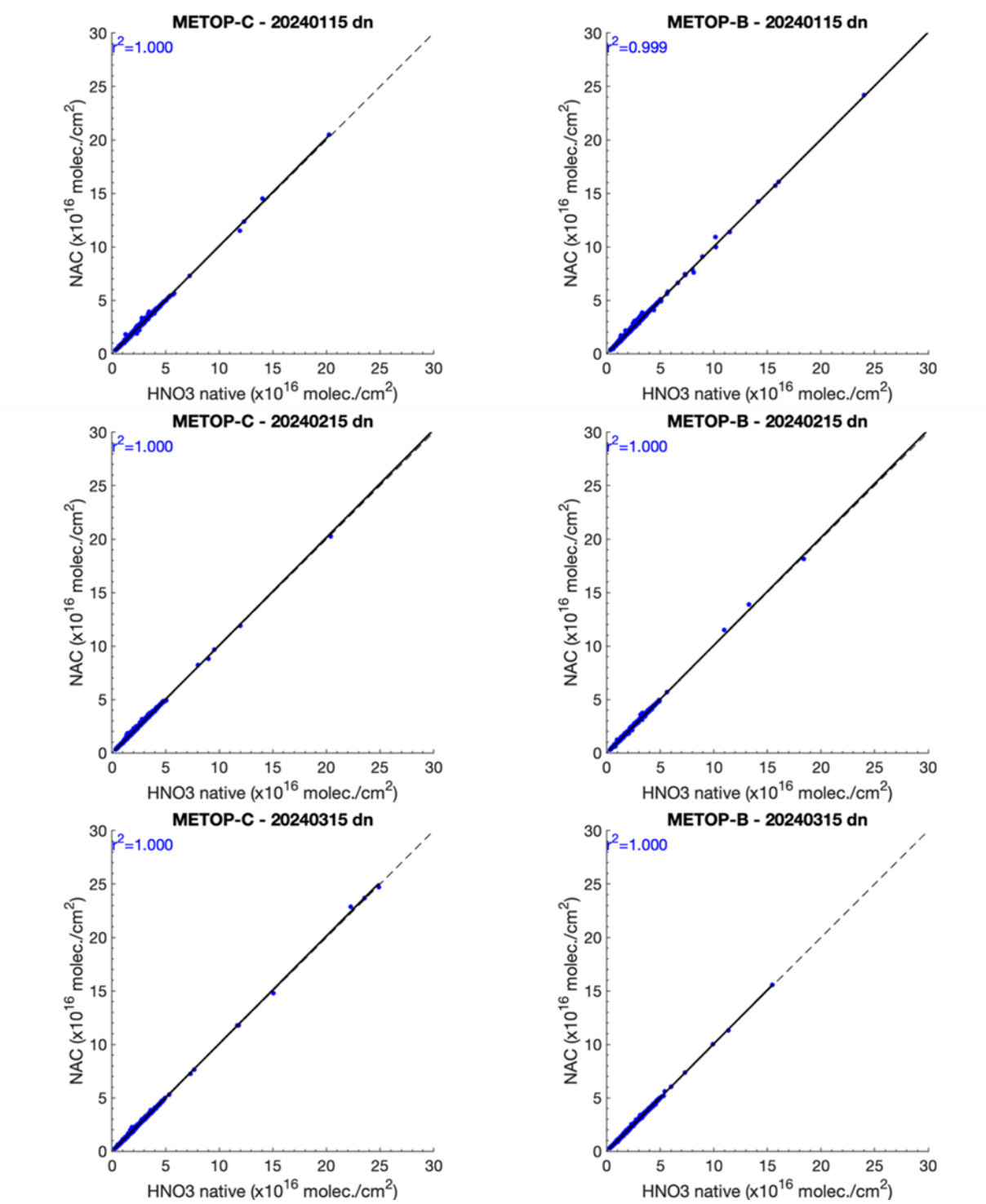
15 May 2024	IASI-C		IASI-B	
	Native	BUFR	Native	BUFR
Individual Pixels	270319	68565	282013	69027
Common Pixels	61921 (22.19%)		62291 (22.09%)	
Correlation	0.9998		0.9998	
Mean Total Column Differences ( $\times 10^{16}$ molec $\text{cm}^{-2}$ )	0.0053 $\pm$ 0.0175		0.5864 $\pm$ 1.2352	
Mean Total Column Relative Differences (%)	0.5864 $\pm$ 1.2352		0.6524 $\pm$ 1.2615	

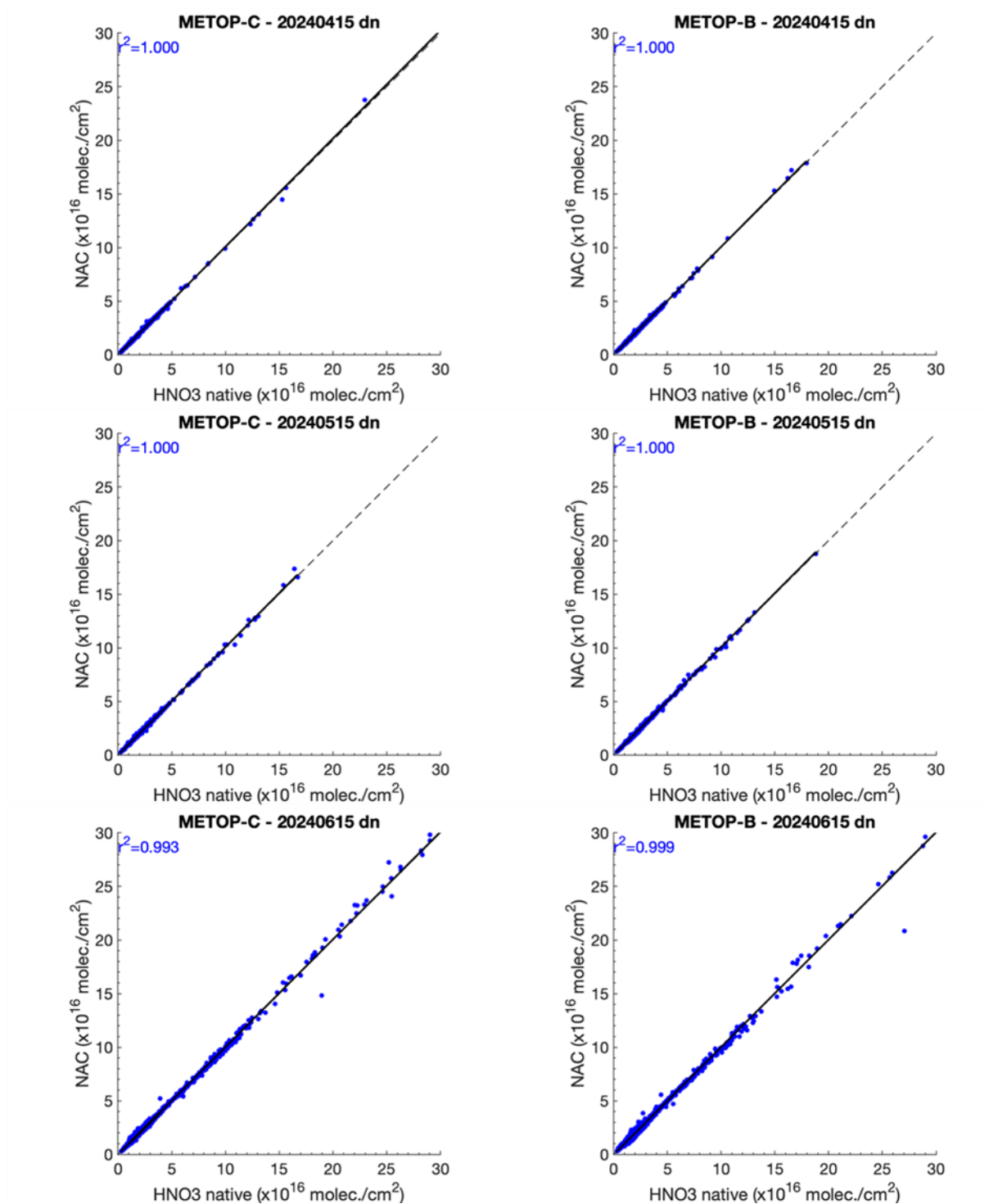
  

15 June 2024	IASI-C		IASI-B	
	Native	BUFR	Native	BUFR
Individual Pixels	305614	292718	313550	299770
Common Pixels	263446 (86.20%)		269357 (85.91%)	
Correlation	0.9964		0.9994	
Mean Total Column Differences ( $\times 10^{16}$ molec $\text{cm}^{-2}$ )	0.0096 $\pm$ 0.0751		0.0116 $\pm$ 0.0308	
Mean Total Column Relative Differences (%)	0.8187 $\pm$ 5.0413		0.9121 $\pm$ 1.5815	

Figure 7.46 shows the correlation plots for total column, respectively, between NAC data and FORLI-HNO<sub>3</sub> for each platform. Correlation coefficients (in blue) are  $\sim 1$ .

So far, the discrepancies are found within the numerical errors inherent to the use of different IT infrastructure.





**Figure 7.46.** Correlation plots for total column between NAC and FORLI-HNO3 data for each platform for six days: January 15<sup>th</sup>, February 15<sup>th</sup>, March 15<sup>th</sup>, April 15<sup>th</sup>, May 15<sup>th</sup> and June 15<sup>th</sup>, 2024. X-axis corresponds to native data (molec./cm<sup>2</sup>) and Y-axis corresponds to NAC data (molec./cm<sup>2</sup>).

### Validation with CO FTIR ground-based data

This section presents a comparison between the Metop-A/B/C IASI CO data and FTIR measurement data available from the NDACC (Network for the Detection of Atmospheric Composition Change) network. The Copernicus Atmosphere Monitoring Service (CAMS) projects



supports selected NDACC instruments and PIs for rapid delivery of quality measurements to the NDACC data host ([contract CAMS27](#)). Recent FTIR measurement data is now available for many more sites (in this study data from 24 sites is used).

These ground-based, remote-sensing instruments are sensitive to the CO abundance in the troposphere and lower stratosphere, i.e. between the surface and up to 20 km altitude. CO total columns are validated (from surface to 100 km). A description of the FTIR instruments and retrieval methodology can be found at <https://nors.aeronomie.be>. The typical uncertainty on the FTIR CO column is approximately 3 %, which is also used in the color scale in Figure 7.48.

In this comparison each FTIR measurement is co-located to all IASI measurements within a time difference of 3 hours and within a distance of 50 km to the effective location of the FTIR measurement (this effective location is calculated along the line of sight of the FTIR measurement). The IASI *a priori* is substituted in the FTIR retrieval and subsequently the FTIR retrieved profile with the IASI *a priori* is smoothed using the IASI averaging kernel, as described in Rodgers *et al.*, 2003. In the plots the relative differences are calculated using the latter FTIR columns (smoothed with the IASI averaging kernels). This validation methodology is described in more detail in Ronsmans *et al.*, 2016. All figures for the individual stations can be browsed on <https://cdop.aeronomie.be>.

**Table 7.25. Statistics between IASI-B/C and FTIR CO smoothed total columns for the entire time period January 2017 – June 2024 (the column “std” is the standard deviation of the local FTIR columns relative to the standard deviation of the IASI columns)**

	Metop-B					Metop-C				
	# meas.	Std.	R	rel. Diff.	Std. Rel. Diff.	# meas.	Std.	R	rel. Diff.	Std. Rel. Diff.
Eureka	928	0.7	0.87	18.2	16.3	33	0.3	-	12.3	21.2
Ny Ålesund	197	1.0	0.90	20.2	8.49	142	1.0	0.91	20.4	8.19
Thule	6517	0.8	0.84	5.81	11.7	3625	0.7	0.85	7.66	11.7
Kiruna	1176	1.1	0.82	-2.96	7.37	720	1.1	0.83	-2.61	6.96
Harestua	217	1.1	0.84	8.47	7.02	3	-	-	-	-
St. Petersburg	1329	0.8	0.88	8.45	7.42	652	0.8	0.92	9.44	6.55
Bremen	492	0.9	0.87	8.18	7.01	231	0.9	0.81	7.93	7.68
Garmisch	3028	0.9	0.86	2.35	7.44	1386	0.9	0.89	2.23	6.87
Zugspitze	3815	0.9	0.90	-1.16	6.44	2119	0.9	0.91	-1.36	6.10
Jungraujoch	1351	0.9	0.94	0.35	4.87	1053	0.9	0.93	-0.03	4.63
Toronto	1946	0.7	0.81	22.9	14.9	1416	0.6	0.84	23.6	14.7
Rikubetsu	85	0.9	0.87	5.01	7.13	49	1.0	0.82	1.43	7.11
Boulder	5928	0.9	0.87	-1.72	7.62	5371	0.9	0.85	-1.55	8.91
Xianghe	2298	0.6	0.85	12.5	14.7	1938	0.6	0.84	10.7	13.3
Tsukuba	449	0.8	0.83	7.65	9.51	280	0.9	0.90	5.24	6.41
Izana	1137	1.0	0.95	-0.47	4.21	573	0.9	0.96	0.80	4.41
Mauna Loa	1526	1.1	0.99	-0.80	2.81	632	1.1	0.99	-0.71	2.76
Altzomoni	1579	1.1	0.96	4.38	4.30	1027	1.1	0.96	4.17	4.53
Paramaribo	119	0.9	0.92	9.00	4.57	35	0.8	0.83	7.89	5.91
Porto Velho	278	0.9	0.98	9.82	6.64	0	-	-	-	-
La Reunion Mado	2601	1.0	0.99	4.96	3.30	704	1.0	0.99	6.15	3.49
Wollongong	2712	0.8	0.94	7.34	7.51	1842	0.8	0.93	6.86	7.47



Lauder	3638	0.9	0.95	9.81	6.25	2543	0.9	0.96	9.60	5.95
Arrival Heights	578	0.9	0.94	16.8	7.47	441	0.9	0.93	16.0	7.77
Average for all sites		0.9	0.90	7.30	7.71		0.9	0.86	6.64	7.84

The correlation coefficients of the Taylor diagrams (Figure 7.47 and Table 7.25) are generally ranging from ~0.8 to nearly 1, showing a very good agreement between the IASI and FTIR data, for Metop-B and Metop-C. However, some sites are special:

1. Rikubetsu, Ny Ålesund and Harestua have only a few co-located measurements and are statistically less relevant
2. Toronto has a lower correlation although the site has many co-locations. This may be due to some co-locations where the IASI concentration is much higher than observed by the FTIR and probably related to false co-locations during fire events. The FTIR time-series seems to suffer from outliers being too low.
3. At Kiruna, Thule and Eureka the satellite underestimates the CO columns by up to 30 % during the early spring weeks and is related to a reduced sensitivity of the IASI CO product during local spring.

The Taylor diagrams in Figure 7.47 and statistics in Table 7.25 also show that the standard deviations of the FTIR columns values are smaller compared the satellite standard deviation probably due to higher noise on the satellite time-series. Almost all site points are shifted left of the satellite reference, typically with a factor of 0.8 to 1 of the standard deviation of the satellite CO columns.

Figure 7.48 shows the time-series of bi-weekly mean relative differences for the time period January 2017 – June 2024. Red indicates a positive bias (IASI > NDACC) while blue indicates an underestimation of the satellite retrievals. The chosen color scale is based on the FTIR typical uncertainty. The IASI retrieval uncertainty should be added (typically around 4 %), so only biases above 5 % are to be considered significant. In the Northern Hemisphere a seasonal changing bias is observed: overestimation during summer and underestimation during winter months. A similar seasonal dependence but less pronounced is observed in the Southern Hemisphere. A longer time period is required to study this seasonal dependence in more detail.

We can conclude that for most of the 24 stations included in the comparison, mean relative differences, or biases, are less than 10 % (see the individual station plots at <https://cdop.aeronomie.be> under Validation Results). For the Eureka, Ny Ålesund and Arrival Heights stations, located at high latitudes, biases are larger. A similar bias is found by Buchholz *et al.* (2017) when comparing with MOPITT data. When looking at the stations between -60° and 60°, the Toronto station shows the largest biases (mean bias  $\pm 20$  %) which seems to be due to outliers.

The IASI data are generally overestimating with the overall bias of approx. 7 % being off the same order as the reported combined total uncertainty of 5 % (Table 7.25).

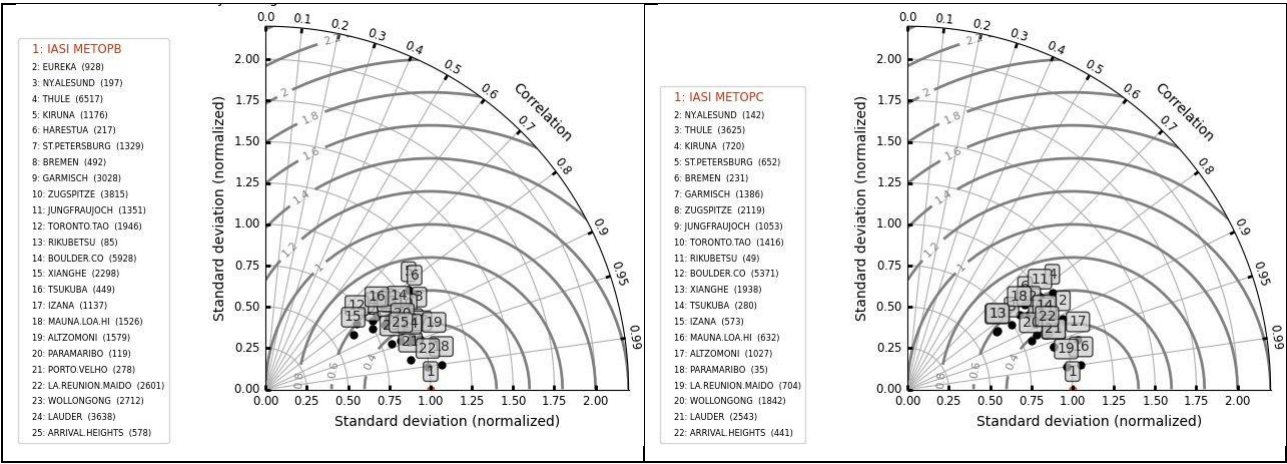


**Figure 7.47. Correlation plots for IASI-B (left) and IASI-C (right) CO total columns against 24 NDACC FTIR sites. The stations are slightly shifted to the left, indicating that the satellite time-series has a higher standard deviation (more noisy).**

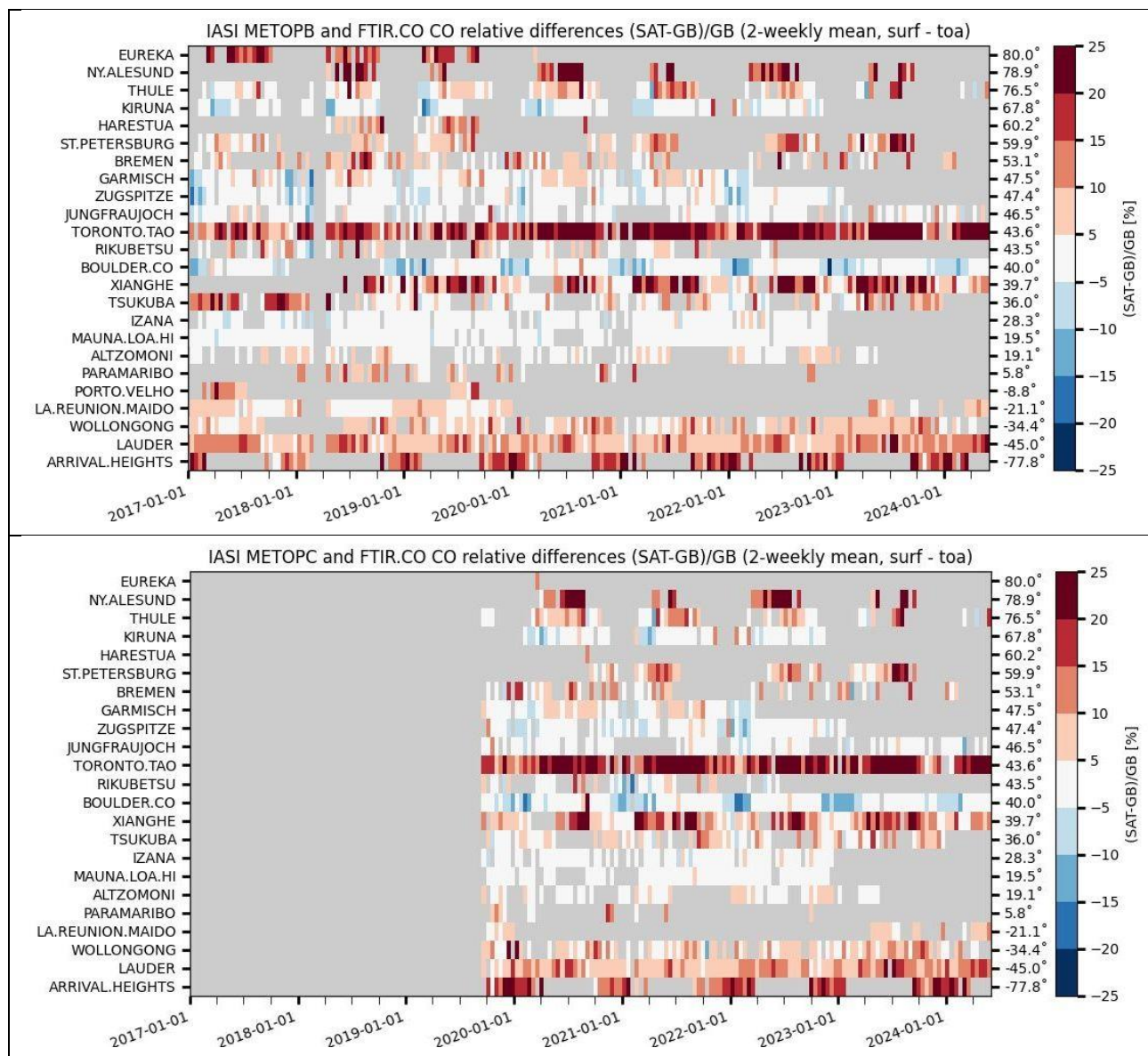


**Figure 7.48. Time-series of bi-weekly relative difference for IASI-B (top) and IASI-C (bottom). The Metop-C relative bias time-series seems to correspond closely to the Metop-B time-series.**

**Acknowledgements:** The data used in this publication were obtained as part of the Network for the Detection of Atmospheric Composition Change ([NDACC](#)) and are publicly available. Rapid delivery of NDACC data is partly supported by the CAMS-27 data procurement service contracted by ECMWF for the validation of the Copernicus Atmospheric Monitoring Service ([CAMS](#)).

#### References:

Buchholz, R. R., Deeter, M. N., Worden, H. M., Gille, J., Edwards, D. P., Hannigan, J. W., Jones, N. B., Paton-Walsh, C., Griffith, D. W. T., Smale, D., Robinson, J., Strong, K., Conway, S., Sussmann, R., Hase, F., Blumenstock, T., Mahieu, E., and Langerock, B.: Validation of MOPITT carbon monoxide using ground-based Fourier transform infrared spectrometer data from NDACC, *Atmos. Meas. Tech.*, 10, 1927-1956, 2017.

<https://doi.org/10.5194/amt-10-1927-2017>

Rodgers, C. D., and Connor, B. J.: Intercomparison of remote sounding instruments, *J. Geophys. Res.*, 108, 4116-4129, 2003.

<https://doi.org/10.1029/2002JD002299>

Ronsmans, G., Langerock, B., Wespes, C., Hannigan, J. W., Hase, F., Kerzenmacher, T., Mahieu, E., Schneider, M., Smale, D., Hurtmans, D., De Mazière, M., Clerbaux, C., and Coheur, P.-F.: First characterization and validation of FORLI-HNO<sub>3</sub> vertical profiles retrieved from IASI/Metop, *Atmos. Meas. Tech.*, 9, 4783-4801, 2016.

<https://doi.org/10.5194/amt-9-4783-2016>

## 8. List of AC SAF users

The institutes of registered users of AC SAF products are listed below.

### 8.1. FMI archive

#### Europe:

Armenia:

- ICHD

Austria:

- Central Institute for Meteorology and Geodynamics
- Private individual
- Sistema GmbH
- University of Veterinary Medicine
- University of Vienna (2 users)

Belarus:

- National Academy of Sciences
- State University

Belgium:

- BIRA-IASB
- Flanders Marine Institute
- Ghent University (15 users)
- Karel de Grote University College
- KMI (4 users)
- KU Leuven
- Novigo+
- ULB (3 users)

Bulgaria:

- Bulgarian Academy of Science
- Space Research and Technology Institute (2 users)

Croatia:

- J. J. Strossmayer University of Osijek

Czech Republic:

- Czech Hydrometeorological Institute (4 users)
- Global Change Research Institute

Denmark:

- Aarhus University (2 users)
- DMI (3 users)
- DTU Compute

Estonia:

- Estonian Environment Agency
- Intertrust

Finland:

- FMI (11 users)
- Häme University of Applied Sciences
- University of Helsinki (2 users)

France:

- AERIS/ICARE
- Aix-Marseille University
- CNRS (3 users)
- Grenoble Alpes University
- Laboratory of Atmospheric Optics
- Lasem
- LATMOS
- LISA (2 users)
- LISA-CNRS
- LSCE-IPSL-CNRS
- Météo France (5 users)
- Mines Paristech
- ONERA
- Open University
- Private Individual (2 users)
- Reuniwatt
- Sistema
- Sorbonne University
- Université Claude Bernard
- University of Reunion (2 users)
- University of Lille
- University of Paris Est Creteil

Germany:

- Brandenburg University of Technology
- Dataperti
- DLR (3 users)
- DWD (4 users)
- EUMETSAT (21 users)
- Federal Office for Radiation Protection
- Forschungszentrum Jülich GmbH (5 users)
- Fraunhofer Institute
- Fraunhofer IOSB
- Gymnasium Olching
- Oldenburg University
- Private Individual (2 users)
- Max Planck Institute for Chemistry (5 users)
- Sabrina Szeto Consulting
- Synwer GmbH
- Technical University of Munich
- University of Bremen (5 users)

- University of Cologne
- University of Hildesheim
- University of Konstanz
- University of Münster
- University of Potsdam

Greece:

- AUTH (5 users)
- Eratosthenes Centre of Excellence
- Hellenic Centre for Marine Research
- IESL/FORTH
- National and Kapodistrian University of Athens
- National Technical University of Athens (2 users)
- Private Individual
- Technical University of Crete
- University of Athens (2 users)
- University of the Aegean
- University of Crete (2 users)

Hungary:

- Eötvös Loránd University (2 users)
- Hungarian Academy of Sciences
- Hungarian Meteorological Service (2 users)
- Individual
- University of Szeged

Ireland:

- Trinity College Dublin

Italy:

- ARPA Valle d'Aosta
- B-Open Solutions S.r.l. (2 users)
- CNR-ISAC
- European Space Agency
- fabbricadigitale
- IFAC-CNR (2 users)
- Julia Wagemann Consulting
- LaMMA Consortium (2 users)
- MEE0
- National Institute for Astrophysics
- Private Individual (2 users)
- Regional Environmental Protection Agency Calabria
- University of Bologna (2 users)
- University of Milan
- University of Modena and Reggio Emilia
- University of Venice

Latvia:

- Latvian Environment, Geology and Meteorology Centre



Lithuania:

- Lithuanian National Meteorological Service
- Vilnius University

Malta:

- University of Malta

The Netherlands:

- BESSR
- Delft University of Technology
- ESA
- KNMI (6 users)
- Leiden University
- S[&]T Corporation
- Wageningen University & Research (2 users)

Norway:

- Norwegian Institute for Air Research (2 users)
- UiT The Arctic University of Norway

Poland:

- CloudFerro
- IMGW
- Institute of Environmental Protection (2 users)
- Institute of Geodesy and Cartography
- Military University of Technology
- O3Lab
- University of Warsaw

Portugal:

- Instituto Dom Luiz
- Instituto Português do Mar e da Atmosfera (4 users)
- University of Aveiro
- University of Lisbon
- University of Trás-os-Montes and Alto Douro (2 users)

Republic of North Macedonia:

- Hydrometeorological Service

Romania:

- Babes-Bolyai University (3 users)
- Global Top Systems
- INCAS
- INOE (2 users)
- National Meteorological Administration (2 users)
- University of Galați (3 users)
- Politehnica University of Bucharest

Russia:

- Altai State University
- Daghestan Scientific Centre of Russian Academy of Sciences

- Federal Research Center Krasnoyarsk Scientific Center of the Siberian Branch of the RAS (2 users)
- Fedorov Institute of Applied Geophysics
- IG RAS
- Institute of Atmospheric Physics
- Institute of Computational Modeling of the Siberian Branch of the RAS
- Institute of Global Climate and Ecology
- Irkutsk State Transport University
- Moscow State University
- Planeta (3 users)
- Research Center of Ecological Safety
- Roscosmos
- St. Petersburg State University
- Tomsk State University of Control Systems and Radioelectronics
- V.E. Zuev Institute of Atmospheric Optics

Serbia:

- Geographical institute “Jovan Cvijic”, SASA

Slovakia:

- Private Individual

Slovenia:

- Bide-san, s.p.

Spain:

- Autonomous University of Barcelona
- Barcelona Supercomputing Center
- Basque Meteorology Agency
- Complutense University of Madrid
- CREAM-CSIC-UAB
- GREA
- I.E.S. Punta del Verde
- Modeliza
- NAITEC (2 users)
- Pablo de Olavide University
- Polytechnic University of Catalonia (2 users)
- Private Individual
- State Meteorological Agency (2 users)
- University of Alicante
- University of Barcelona (3 users)
- University of the Basque Country
- University of Extremadura
- University of Granada (2 users)
- University of Málaga
- University of Oviedo
- University of Valencia (3 users)
- University of Valladolid (2 users)

Sweden:

- Blackebergs Gymnasium
- NBI/Handelsakademin
- SMHI (5 users)

Turkey:

- Cukurova University
- Hacettepe University
- Istanbul University
- Middle East Technical University
- Turkish State Meteorological Service (2 users)
- Van Yüzüncü Yıl University

Ukraine:

- Batata LLC
- Scientific Centre for Aerospace Research of the Earth
- Taras Shevchenko National University of Kyiv
- UHE LED LLC
- UHMC
- Ukrainian Hydrometeorological Institute (2 users)

United Kingdom:

- Aggreko
- Atheras Analytics
- ECMWF (2 users)
- ESA
- IDEMS International
- London School of Economics and Political Science
- Office of National Statistics
- Private individual
- Rutherford Appleton Lab (2 users)
- Satavia Ltd.
- Satellite Applications Catapult
- Science and Technology Facilities Council (2 users)
- siHealth Ltd.
- University College London
- University of Edinburgh
- University of Hertfordshire
- University of Leeds (2 users)
- University of Leicester
- University of Manchester
- University of Oxford
- University of Sheffield
- University of York

**Asia:**

Afghanistan:

- Vortil Co. Ltd.

Bangladesh:

- Institute of Forestry and Environmental Sciences
- Stamford University
- University of Dhaka

China:

- Anhui Institute of Optics and Fine Mechanics
- Anhui Institute of Meteorological Sciences
- Anhui Normal University
- Beijing Municipal Environmental Monitoring Center
- Beijing Normal University (3 users)
- Beijing Zhixin Remote Sensing Geographic Information Co., Ltd
- Chengdu University of Information Technology
- China Academy of Sciences (7 users)
- China Meteorological Administration
- China University of Geosciences
- China University of Mining and Technology (6 users)
- Chinese Academy of Meteorological Sciences (3 users)
- East China University of Science and Technology
- Fudan University
- Guangzhou University
- HTHJ
- Institute of Atmospheric Physics (3 users)
- Institute of Desert Meteorology
- Institute of Earthquake Forecasting
- Institute of Remote Sensing and Digital Earth (3 users)
- Jiangsu Meteorological Observatory
- Jiangsu Normal University (2 users)
- Jilin University
- Lanzhou University (2 users)
- Lanzhou Jiaotong University
- Nanjing University
- Nanjing University of Information Science & Technology (7 users)
- National Satellite Meteorological Center
- National University of Defense Technology
- Northeast Normal University
- Northwest Normal University
- Peking University (3 users)
- Private Individual
- “School”
- Shandong University
- Shanghai University (2 users)
- Shenzhen University
- Southern University of Science and Technology (4 users)
- State Environmental Protection Key Lab of Satellite Remote Sensing
- Sun Yat-Sen University (2 users)
- The Chinese University of Hong Kong (2 users)

- The Institute of Atmospheric Physics (3 users)
- Tsinghua University (2 users)
- (unknown) (4 users)
- University of Science and Technology (4 users)
- Wuhan University (7 users)
- Xiamen University
- Zhejiang University (3 users)

India:

- Anna University
- Aryabhata Research Institute of Observational Sciences
- Banaras Hindu University
- Birla Institute of Technology
- Bose Institute
- Council of Scientific and Industrial Research
- CSIR-NIO
- CSIR-NPL
- Dibrugarh University
- “Education”
- IIT KGP
- Indian Institute of Remote Sensing
- Indian Institute of Science
- Indian Institute of Technology Delhi
- Indian Institute of Technology Kharagpur (4 users)
- Indian Institute of Technology Roorkee (2 users)
- Indian Institute of Tropical Meteorology (3 users)
- Indian Space Research Organization (3 users)
- Jawaharlal Nehru Technological University, Kakinada
- Jawaharlal Nehru University
- Malaviya National Institute of Technology Jaipur
- Mangalore University
- MSRIT
- National Atmospheric Research Laboratory (2 users)
- National Centre for Medium Range Weather Forecasting
- National Institute of Technology
- National Remote Sensing Centre
- Savitribai Phule Pune University (2 users)
- School of Planning and Architecture, Bhubaneswar
- SIG
- SRM Institute of Science and Technology
- University of Calcutta
- University of Hyderabad
- University of Kalyani
- Vikram Sarabhai Space Centre (2 users)
- Vindhyachal Ecology and Natural History Foundation

Indonesia:

- Bandung Institute of Technology
- Meteorological, Climatological, and Geophysical Agency (3 users)
- National Institute for Aeronautics and Space
- Sumatera Institute of Technology

Iran:

- Sepehr Payesh

Japan:

- Chiba University
- Ibaraki University
- Japan Meteorological Agency
- Kyushu University
- National Institute for Environmental Studies
- Waseda University

Malaysia:

- Malaysian Meteorological Department
- Malaysian Space Agency
- National University of Malaysia (5 users)

Myanmar:

- Yangon Technological University

Nepal:

- International Centre for Integrated Mountain Development (2 users)
- Institute for Advanced Sustainability Studies
- Institute of Tibetan Plateau Research
- Institute of Engineering

Pakistan:

- University of the Punjab
- National University of Sciences & Technology

Philippines:

- Manila Observatory

Singapore:

- National University of Singapore (2 users)

South Korea:

- Chungnam National University (3 users)
- Gwangju Institute of Science and Technology (4 users)
- Hankuk University of Foreign Studies
- Korea Meteorological Administration (2 users)
- Korea Polar Research Institute
- National Institute of Environmental Research (2 users)
- National Meteorological Satellite Center (4 users)
- Pukyong National University
- Yonsei University (3 users)
- Kongju National University

- Seoul National University

Sri Lanka:

- Central Environmental Authority
- Private Individual

Taiwan:

- Academia Sinica
- Garmin
- National Central University (3 users)
- National Taipei University
- National Taiwan University
- Research Center for Environmental Changes

Thailand:

- Asian Institute of Technology
- King Mongkut's Institute of Technology Ladkrabang

Vietnam:

- University of Science (2 users)

**Middle East:**

Iran:

- Atmospheric Science & Meteorological Research Center
- Islamic Azad University
- Tabriz University
- "University"
- University of Tehran
- Unknown

Iraq:

- Al Iraqia University
- Mustansiriyah University

Israel:

- Israel Institute for Biological Research
- University of Tel Aviv (2 users)

Oman:

- Sultan Qaboos University

Saudi Arabia:

- King Abdullah University of Science and Technology (2 users)
- Private individual

United Arab Emirates:

- Amity University
- Khalifa University
- Uruk Engineering & Contracting



**North America:**

Canada:

- Canadian Space Agency
- Dalhousie University
- Environment and Climate Change Canada
- Environment Canada
- University of Saskatchewan

United States of America:

- Caltech
- Colorado State University
- Department of Defence
- EMDO Lab
- Florida State University
- Harvard-Smithsonian Center for Astrophysics
- Intertek
- Joint Center for Satellite Data Assimilation
- Michigan Technological University (5 users)
- Mote Marine Laboratory
- NASA (2 users)
- Naval Research Laboratory
- NOAA
- Northeastern University
- Princeton University
- Private Individual
- SpaceKnow Inc.
- Texas A&M University
- The Aerospace Corporation
- Trinity Consultants Inc.
- University of Alabama in Huntsville
- University of Alaska (2 users)
- University of Arizona
- University of California (3 users)
- University of Central Florida
- University of Colorado Boulder
- University of Kansas
- University of Maryland (2 users)
- University of Tennessee
- University of Washington
- Unknown
- USGS
- U.S. Environmental Protection Agency

**South America:**

Argentina:

- National Space Activities Commission
- Universidad Nacional de Córdoba

- Universidad Nacional de Rosario

Brazil:

- APAC
- LAPIS
- Universidade Federal de Alagoas

Chile:

- University of the Americas

Colombia:

- Universidad EAFIT

Ecuador:

- Universidad San Francisco de Quito (2 users)

Guatemala:

- ASEFOR
- INSIVUMEH

Mexico:

- Ibero Puebla
- Instituto Politecnico Nacional

Paraguay:

- Universidad San Carlos

Peru:

- Servicio Nacional de Meteorología e Hidrología del Perú

Uruguay:

- Universidad de la República

**Australia / New Zealand:**

- Bureau of Meteorology
- University of Canterbury (3 users)
- University of Melbourne (2 users)
- University of Southern Queensland (2 users)
- University of Sydney

**Africa:**

Algeria:

- CTS/ASAL
- Meteo Algeria

Cameroon:

- African Institute for Mathematical Sciences

Democratic Republic of the Congo:

- University of Kinshasa

Egypt:

- Egyptian Meteorological Authority (3 users)
- National Research Institute of Astronomy and Geophysics

Eritrea:

- Department of Environment

Ethiopia:

- Addis Ababa University

Ghana:

- Ghana Meteorological Agency
- Kwame Nkrumah University of Science and Technology
- University of Energy and Natural Resources

Morocco:

- Abdelmalek Essaadi University
- EM5D
- Maroc Météo
- University of Hassan II Casablanca

Nigeria:

- Abdou Moumouni University
- Federal University Lafia

South Africa:

- National Chemical Emergency Centre
- South African Weather Service (2 users)
- Stellenbosch University
- University of KwaZulu-Natal
- University of Pretoria
- University of the Witwatersrand

Registered users: **689**

## **8.2. DLR archive**

### **Europe:**

Austria:

- University of Veterinary Medicine
- University of Vienna

Belarus:

- National Academy of Sciences

Belgium:

- Antea Group
- BIRA-IASB (5 users)
- Flanders Marine Institute
- Ghent University (11 users)
- KMI (3 users)
- Novigo+
- ULB (4 users)

Bulgaria:

- Space Research and Technology Institute (2 users)

Cyprus:

- The Cyprus Institute

Czech Republic:

- Charles University
- Czech Hydrometeorological Institute (5 users)
- Global Change Research Institute

Denmark:

- Aarhus University (2 users)
- DTU Compute

Estonia:

- Estonian Environment Agency
- Intertrust

Finland:

- FMI (10 users)
- Häme University of Applied Sciences

France:

- AERIS/ICARE
- Aix-Marseille University
- CNRS (3 users)
- Grenoble Alpes University
- Institute of Environmental Geosciences
- Laboratory of Atmospheric Optics
- Lasem
- LATMOS (3 users)
- LISA
- LISA-CNRS
- LSCE-IPSL-CNRS
- Météo France (4 users)
- Mines Paristech
- Open University
- Reuniwatt
- Sistema
- Sorbonne University
- Université Claude Bernard
- University of Reunion (2 users)

Germany:

- Brandenburg University of Technology
- Dataperti
- DLR (4 users)
- DWD (2 users)
- EUMETSAT (19 users)
- Forschungszentrum Jülich GmbH (3 users)

- Fraunhofer Institute
- Gymnasium Olching
- Heidelberg University
- Karlsruhe Institute of Technology (3 users)
- Max Planck Institute for Chemistry (4 users)
- Private Individual (2 users)
- Sabrina Szeto Consulting
- Technical University of Munich
- University of Augsburg
- University of Bremen (8 users)
- University of Cologne (2 users)
- University of Hildesheim
- University of Münster

Greece:

- AUTH (4 users)
- Eratosthenes Centre of Excellence
- Hellenic Centre for Marine Research
- IESL/FORTH
- National and Kapodistrian University of Athens
- National Technical University of Athens (2 users)
- Private Individual
- Technical University of Crete
- University of Athens (2 users)
- University of Crete (2 users)

Hungary:

- Hungarian Meteorological Service (3 users)
- Individual
- University of Szeged

Ireland:

- Trinity College Dublin

Italy:

- B-open Solutions S.r.l. (2 users)
- CNR-ISAC
- fabbricadigitale
- IFAC-CNR
- Italian National Research Council
- Julia Wagemann Consulting
- LaMMA Consortium
- MEEO
- National Institute of Geophysics and Volcanology
- Private Individual
- Regional Environmental Protection Agency Calabria
- University of Bologna
- University of Modena and Reggio Emilia
- University of Venice

Latvia:

- Latvian Environment, Geology and Meteorology Centre

Lithuania:

- Lithuanian National Meteorological Service

Malta:

- University of Malta

The Netherlands:

- BESSR
- Delft University of Technology
- KNMI (7 users)
- Leiden University
- S[&]T Corporation
- Wageningen University & Research (2 users)

Norway:

- UiT The Arctic University of Norway

Poland:

- CloudFerro
- Institute of Environmental Protection (2 users)
- Institute of Geodesy and Cartography
- Institute of Meteorology and Water Management-NRI
- Military University of Technology
- O3Lab
- University of Warsaw

Portugal:

- Instituto Dom Luiz (2 users)
- Instituto Português do Mar e da Atmosfera (3 users)
- University of Tras-os-Montes and Alto Douro

Romania:

- Babes-Bolyai University (3 users)
- Global Top Systems
- INOE (3 users)
- University of Galați (3 users)
- Politehnica University of Bucharest

Russia:

- Altai State University
- Institute of Computational Modeling of the Siberian Branch of the RAS
- Institute of Global Climate and Ecology
- Irkutsk State Transport University
- Planeta

Serbia:

- Geographical institute “Jovan Cvijic”, SASA

Slovakia:

- Private Individual

Slovenia:

- Bide-san, s.p.

Spain:

- Autonomous University of Barcelona
- Complutense University of Madrid
- GREA
- Modeliza
- NAITEC
- Pablo de Olavide University
- Polytechnic University of Catalonia (2 users)
- Private Individual
- State Meteorological Agency (2 users)
- Universitat Politècnica de València
- University of Alicante
- University of Barcelona (3 users)
- University of Granada (3 users)
- University of Extremadura (2 users)
- University of Oviedo (2 users)
- University of Valencia (3 users)
- University of Valladolid

Sweden:

- SMHI (4 users)
- The Swedish Defence Research Agency (2 users)

Turkey:

- Cukurova University
- Hacettepe University
- Kastamony University
- Middle East Technical University
- Turkish State Meteorological Service (2 users)
- Van Yüzüncü Yıl University

Ukraine:

- Batata LLC
- Scientific Centre for Aerospace Research of the Earth
- UHE LED LLC
- UHMC
- Ukrainian Hydrometeorological Institute

United Kingdom:

- Aggreko
- ECMWF (4 users)
- ESA
- IDEMS International
- Hibarcus



- London School of Economics and Political Science
- Private individual
- Rutherford Appleton Lab
- Satavia Ltd.
- Satellite Applications Catapult
- Science and Technology Facilities Council (2 users)
- siHealth Ltd.
- University of Hertfordshire
- University of Leeds (2 users)
- University of Leicester (2 users)
- University of Manchester
- University of York (2 users)

**Asia:**

Bangladesh:

- Institute of Forestry and Environmental Sciences
- University of Dhaka

China:

- Anhui Normal University
- Anhui Institute of Meteorological Sciences University of Dhaka
- Anhui Institute of Optics and Fine Mechanics (2 users)
- Anhui University (3 users)
- Beijing Municipal Environmental Monitoring Center
- Beijing Normal University
- Beijing Zhixin Remote Sensing Geographic Information Co., Ltd
- Chinese Academy of Meteorological Sciences (2 users)
- China Academy of Sciences (7 users)
- China Meteorological Administration
- China University of Mining and Technology (7 users)
- Chinese University of Hong Kong
- East China Normal University
- East China University of Science and Technology
- Fudan University
- Guangzhou University
- Hong Kong University of Science and Technology
- HTHJ
- Institute of Atmospheric Physics
- Institute of Geographic Sciences and Natural Resources Research, China Academy of Sciences
- Institute of Remote Sensing and Digital Earth
- Jiangsu Meteorological Observatory
- Jiangsu Normal University (2 users)
- Jinan University
- Lanzhou University
- Nanjing University (3 users)
- Nanjing University of Information Science & Technology (6 users)
- National Satellite Meteorological Center

- Northeast Normal University
- Northwest Normal University
- Ocean University of China
- Peking University (4 users)
- PIE
- Piesat Information Technology Co. ,Ltd.
- Private Invidual
- “School”
- Shandong University (2 users)
- Shanghai University
- Shenzhen University
- South China Agricultural University
- Southern University of Science and Technology (3 users)
- State Environmental Protection Key Lab of Satellite Remote Sensing
- The Chinese University of Hong Kong (2 users)
- The Institute of Atmospheric Physics (2 users)
- Tsinghua University (3 users)
- University of Science and Technology (7 users)
- (unknown) (5 users)
- Wuhan University (8 users)
- Wuhan University of Technology
- Zhejiang Academy of Agricultural Sciences
- Zhejiang University (2 users)

India:

- Anna University
- Aryabhatta Research Institute of Observational Sciences
- Banaras Hindu University
- Birla Institute of Technology
- Bose Institute
- Central University of Hyderabad
- Central University of Rajasthan
- CSIR-NIO
- Dibrugarh University (2 users)
- “Education”
- IIT KGP
- Indian Institute of Remote Sensing
- Indian Institute of Science
- Indian Institute of Technology Delhi
- Indian Institute of Technology Kharagpur (3 users)
- Indian Institute of Technology Roorkee (2 users)
- Indian Institute of Tropical Meteorology (3 users)
- Indian Space Research Organization (3 users)
- Jawaharlal Nehru University
- Malaviya National Institute of Technology Jaipur
- MSRIT
- National Atmospheric Research Laboratory

- National Centre for Medium Range Weather Forecasting
- National Institute of Technology
- Savitribai Phule Pune University (2 users)
- School of Planning and Architecture, Bhopal
- SIG
- SRM Institute of Science and Technology
- University of Calcutta
- University of Hyderabad
- University of Kalyani
- Vikram Sarabhai Space Centre

Indonesia:

- Bandung Institute of Technology
- Meteorological, Climatological, and Geophysical Agency (3 users)
- National Institute for Aeronautics and Space
- Sumatera Institute of Technology

Japan:

- Chiba University
- Fukuoka University
- Ibaraki University
- Japan Meteorological Agency
- Kyushu University (2 users)
- Nagoya University
- National Institute for Environmental Studies
- Remote Sensing Technology Center of Japan
- Waseda University

Malaysia:

- Malaysian Meteorological Department
- Malaysian Space Agency
- National University of Malaysia (4 users)

Myanmar:

- Yangon Technological University

Nepal:

- Institute for Advanced Sustainability Studies
- Institute of Engineering
- International Centre for Integrated Mountain Development (2 users)

Pakistan:

- National University of Sciences and Technology
- University of the Punjab

Singapore:

- National University of Singapore (2 users)

South Korea:

- Chungnam National University (3 users)
- Gwangju Institute of Science and Technology (4 users)

- Korea Meteorological Administration
- Korea Polar Research Institute
- National Institute of Environmental Research (2 users)
- National Meteorological Satellite Center (3 users)
- Seoul National University (4 users)
- Ulsan National Institute of Science and Technology
- University of Suwon
- Yonsei University (6 users)

Sri Lanka:

- Central Environmental Authority

Taiwan:

- National Central University (2 users)

Thailand:

- King Mongkut's Institute of Technology Ladkrabang

Vietnam:

- University of Science (2 users)

#### **Middle East:**

Iran:

- Khavaran Institute of Higher Education
- Sepehr Payesh
- Tabriz University
- "University"
- University of Tehran (2 users)

Iraq:

- Al Iraqia University
- Mustansiriyah University

Saudi Arabia:

- King Abdulaziz City for Science and Technology
- King Abdullah University of Science and Technology
- Private individual

United Arab Emirates:

- Amity University (2 users)
- Khalifa University
- Uruk Engineering & Contracting

#### **North America:**

Canada:

- Environment and Climate Change Canada (5 users)
- Environment Canada
- University of Saskatchewan

USA:

- Arizona State University

- Caltech (2 users)
- Colorado State University
- Department of Defence
- Florida State University
- Johns Hopkins University
- Harvard University (3 users)
- Intertek
- Joint Center for Satellite Data Assimilation
- Michigan Technological University (3 users)
- NASA (6 users)
- NOAA (4 users)
- Princeton University
- Private Individual
- Smithsonian Astrophysical Observatory
- SpaceKnow Inc.
- Texas A&M University
- Trinity Consultants Inc.
- University of Alabama in Huntsville
- University of Alaska (2 users)
- University of Arizona
- University of California (4 users)
- University of Central Florida
- University of Colorado Boulder
- University of Houston
- University of Illinois
- University of Maryland (3 users)
- University of North Carolina at Chapel Hill
- University of Washington (2 users)
- University of Wisconsin-Madison
- Unknown
- USGS
- U.S. Environmental Protection Agency
- Utah State University

**South America:**

Argentina:

- Argentine Air Force
- National Space Activities Commission
- Universidad Nacional de Rosario

Brazil:

- APAC
- LAPIS
- Universidade Federal de Alagoas
- University of São Paulo

Chile:

- University of the Americas

Colombia:

- Universidad EAFIT

Ecuador:

- Universidad San Francisco de Quito

Guatemala:

- INSIVUMEH

Mexico:

- Ibero Puebla
- Instituto Politecnico Nacional

Paraguay:

- Universidad San Carlos

Peru:

- Servicio Nacional de Meteorología e Hidrología del Perú

Uruguay:

- Universidad de la República

**Australia / New Zealand:**

- Environmental Systems & Services
- University of Canterbury (2 users)
- University of Melbourne (2 users)
- University of Southern Queensland

**Africa:**

Algeria:

- CTS/ASAL
- Meteo Algeria

Cameroon:

- African Institute for Mathematical Sciences

Democratic Republic of the Congo:

- University of Kinshasa

Egypt:

- Egyptian Meteorological Authority (3 users)
- National Research Institute of Astronomy and Geophysics

Eritrea:

- Department of Environment

Ghana:

- Ghana Meteorological Agency
- Kwame Nkrumah University of Science and Technology

Morocco:

- Abdelmalek Essaadi University
- EM5D
- Maroc Météo

- National Center for Meteorological Research
- University of Hassan II Casablanca

Nigeria:

- Federal University Lafia

South Africa:

- South African Weather Service
- Stellenbosch University
- University of Pretoria
- University of the Witwatersrand
- Ware Jacob Enterprises

Registered users: **623**

### **8.3. DMI (NUV product via FTP)**

- Meteorological Institute of Romania  
⇒ Several commercial companies obtain the data from MIR
- Danish Meteorological Institute, Denmark
- TrygFonden, Denmark
- Department for Health, Greenland Homerule
- The Danish Cancer Society, Denmark
- Libraries of Hjørring Community
- SunSense AS, Norway
- Richard McKenzie, New Zealand
- Elian Wolfram, Laser Research Center and Applications, Argentina
- KMI, Belgium
- By & Havn I/S, Denmark

Registered users: **11**

### **8.4. KNMI (unofficial NRT AAI via FTP)**

- FMI, Finland
- William B. Hanson Center for Space Science, USA
- University of Leicester, UK

Registered users: **3**

### **8.5. Known international projects that use EUMETCast or WMO/GTS**

- MACC project
- SACS service
- Temis WWW service
- ESA GlobVapour
- ESA CCI Ozone project



**8.6. EUMETCast**

Albania	6	Hungary	13	Poland	14
Algeria	4	Iceland	1	Portugal	6
Angola	1	India	2	Qatar	3
Armenia	1	Iran, Islamic Republic of	34	Reunion	2
Austria	20	Iraq	2	Romania	10
Azerbaijan	3	Ireland	8	Russian Federation	7
Belgium	11	Israel	5	Rwanda	2
Benin	1	Italy	282	San Marino	1
Bosnia and Herzegovina	1	Jordan	1	Saudi Arabia	2
Botswana	4	Kazakhstan	6	Senegal	6
Brazil	3	Kenya	6	Serbia	2
Bulgaria	6	Kuwait	2	Seychelles	1
Burkina Faso	1	Kyrgyzstan	1	Slovakia	7
Cameroon	3	Latvia	1	Slovenia	2
Canada	1	Lebanon	3	South Africa	6
Cape Verde	1	Lesotho	2	South Sudan	1
China	4	Liberia	1	Spain	43
Congo	1	Libya	1	Sudan	1
Congo, Democratic Republic of	1	Lithuania	2	Sweden	5
Croatia	1	Luxembourg	2	Switzerland	15
Cyprus	1	Madagascar	3	Tajikistan	1
Czech Republic	21	Malawi	2	Tanzania, United Republic of	3
Denmark	6	Mali	1	Togo	1
Egypt	3	Malta	2	Tunisia	3
Equatorial Guinea	1	Mauritania	3	Türkiye	7
Estonia	3	Mauritius	2	Turkmenistan	1
Eswatini	2	Moldova, Republic of	1	Uganda	3
Ethiopia	6	Morocco	5	Ukraine	3
Finland	4	Mozambique	2	United Arab Emirates	3
France	64	Namibia	1	United Kingdom	115
Gabon	1	The Netherlands	23	United States	2
Georgia	1	Niger	2	Uzbekistan	1
Germany	111	Nigeria	7	Vietnam	1
Ghana	5	Norway	4	Yemen	1
Greece	20	Oman	1	Zambia	3
Guinea-Bissau	2	Pakistan	2	Zimbabwe	2
Hong Kong	1	Palestine	1		
<b>TOTAL (June 2024)</b>	<b>1051</b>				

## 9. Updates during the reporting period

Listed below are the major configuration updates concerning operational data processing and archiving. If new versions of relevant AC SAF documents are released during the reporting period, they should be listed here also.

### 9.1. Software updates

- |         |  |
|---------|--|
| 1 March | FMI: Operating system of the OUV processing server updated to Red Hat Enterprise Linux release 9.2   |
| 14 May  | KNMI: Operating system and PGE upgrade of the operational processors for the ozone profile, aerosol and SIF products, and derived L3 grids (software version 2.40) |

### 9.2. Hardware updates

*Nothing to report.*

### 9.3. Documentation updates

- |            |  |
|------------|--|
| 25 January | ULB, LATMOS: Product User Manual for IASI NRT SO <sub>2</sub> columns and altitude (issue 1.6) |
| 18 April   | FMI: AC SAF Operations Report 2/2023 (revision 1)  |
| 30 April   | KNMI: OPERA Software Release Note (issue 2.30)   |
| 6 May      | FMI: Software Version Document (issue 1.15)  |
| 15 May     | FMI: AC SAF Service Specification (issue 1.8)  |

## 10. Changes in appearance and content of the web portal

Listed below are the major changes in the appearance and content on the [AC SAF main web pages](#).

**Table 10.1. Changes in appearance and content of the main AC SAF web pages during the reporting period**

Date	Description
25 June	Demonstrational products grouped together under ‘Product info’ menu item Pages <i>products/euv_demo.php</i> and <i>euv_validation/index.php</i> published
26 June	Page <i>top_stories.html</i> published, closes OR-13 Action 001

In addition to updates above, following routine updates are conducted whenever necessary:

- The links to public AC SAF user documents are updated whenever new documents or new versions of existing documents become available
- The “top story” on the front page is updated
- News list on the front page is updated

## APPENDIX 1

Table A.1 presents the overall summary of orders from AC SAF archive at FMI, sorted by product types, during the reporting period

Table A.2 presents a detailed summary of product orders from AC SAF archive at FMI during the reporting period.

**Table A.1. Overall summary of product orders, by product type, during the reporting period**

Product type	Number of orders	Number of users	Number of products	Total size
OHP-A	7	5	75	25.4 GB
OHP-B	6	3	35	12.2 GB
OHP-C	6	6	2009	504 GB
ARS-A	1	1	2	1.85 MB
ARS-B	13	5	15676	16.2 GB
ARS-C	13	3	16106	16.6 GB
ARP-A	3	3	5632	35.2 GB
ARP-B	12	8	22053	152 GB
ARP-C	11	6	16449	117 GB
OUV-A	4	4	4411	8.07 GB
OUV-B	3	3	2068	649 MB
OUV-AB	3	2	1801	232 MB
OUV-BC	19	7	4497	484 MB
LER-MSC-AB	0	0	0	-
LER-MSC-ABC	0	0	0	-
LER-PMD-AB	0	0	0	-
LER-PMD-ABC	0	0	0	-

**Table A.2. More detailed summary of product orders during the reporting period**

JANUARY			
Product type	Number of products	Order size	Institute / company
OUV-BC	Time series for 32 days Selected subset: UVADD, UVBDD, UVADR, UVBDR Location: 18.06E, 59.33N (3.64 kB in total)		Blackebergs Gymnasium, Sweden
OUV-BC	Time series for 123 days Selected subset: UVADD, UVBDD, UVADR, UVBDR Location: 18.06E, 59.33N (12.1 kB in total)		Blackebergs Gymnasium, Sweden

OUV-BC	Time series for 89 days Selected subset: UVADD, UVBDD, UVADR, UVBDR Location: 18.06E, 59.33N (17.0 kB in total)		Blackebergs Gymnasium, Sweden
OUV-BC	Time series for 89 days Selected subset: UVADD, UVBDD, UVADR, UVBDR Location: 18.06E, 59.33N (8.94 kB in total)		Blackebergs Gymnasium, Sweden
OUV-BC	Time series for 365 days Selected subset: UVADD, UVBDD, UVADR, UVBDR Location: 18.06E, 59.33N (34.6 kB in total)		Blackebergs Gymnasium, Sweden
OUV-BC	Time series for 364 days Selected subset: UVADD, UVBDD, UVADR, UVBDR Location: 80.19W, 25.76N (34.5 kB in total)		Blackebergs Gymnasium, Sweden
OUV-BC	Time series for 365 days Selected subset: UVADD, UVBDD, UVADR, UVBDR Location: 174.8E, 41.30S (34.6 kB in total)		Blackebergs Gymnasium, Sweden
OUV-B OUV-BC	Time series for 366 days Selected subset: UVADD, UVBDD Location: 4.42E, 36.71N (26.6 kB in total)		Blackebergs Gymnasium, Sweden
OUV-BC	92 Selected subset: UVADD, UVBDD, UVI Region: 18.0E – 29.0E, 53.0N – 61.0N (2.64 MB in total)		Latvian Environment, Geology and Meteorology Centre
OUV-BC	92 Selected subset: UVADD, UVBDD, UVI Region: 18.0E – 29.0E, 53.0N – 61.0N (10.9 MB in total)		Latvian Environment, Geology and Meteorology Centre
OHP-A	1	248 MB	Sepehr Payesh, Iran
OHP-C	1	252 MB	National Space Activities Commission, Argentina
OUV-A	1 Selected subset: ERYDD Region: global (626 kB in total)		O3Lab, Poland
OHP-C	1724	432 GB	University of Science and Technology, China

ARS-B ARS-C	850	875 MB	AUTH, Greece
ARS-B ARS-C	877	904 MB	AUTH, Greece
ARS-B ARS-C	877	903 MB	AUTH, Greece
ARS-B ARS-C	4217	30.7 GB	AUTH, Greece
<b>FEBRUARY</b>			
<b>Product type</b>	<b>Number of products</b>	<b>Order size</b>	<b>Institute / company</b>
ARP-A ARP-B	5604 5605	70.1 GB	FMI, Finland
OHP-A	26	9.70 GB	IFAC-CNR, France
OUV-BC	Time series for 3 days Selected subset: DNADD Location: 24.90E, 60.30N (0.76 kB in total)		FMI, Finland
OHP-B	2	502 MB	Chengdu University of Information Technology, China
<b>MARCH</b>			
<b>Product type</b>	<b>Number of products</b>	<b>Order size</b>	<b>Institute / company</b>
OHP-C	1	250 MB	Private Individual, Italy
OUV-BC	Time series for 1 day Selected subset: UVADD, UVBDD Location: 43.00E, 11.00N (0.67 kB in total)		LaMMA Consortium, Italy
OUV-BC	Time series for 6 days Selected subset: UVADD, UVBDD Location: 11.00E, 43.00N (0.67 kB in total)		LaMMA Consortium, Italy
OUV-BC	Time series for 3 days Selected subset: UVADD, UVBDD, JO1D, JNO2 Location: 121.00E, 25.00N (0.93 kB in total)		National Taiwan University
OUV-BC	Time series for 5 days Selected subset: UVADD, UVBDD, JO1D, JNO2 Location: 5.20E, 52.10N (1.11 kB in total)		National Taiwan University
ARS-C	439	453 MB	AUTH, Greece
ARS-B ARS-C	438 439	904 MB	AUTH, Greece
ARS-B ARS-C	433 437	903 MB	AUTH, Greece

ARP-B	2	14.3 MB	Institute of Atmospheric Physics, China
OUV-A	366 Selected subset: UVADD, UVBDD Region: 73.5E – 135.0E, 18.0N – 53.5N (27.1 MB in total)		China University of Geosciences
APRIL			
Product type	Number of products	Order size	Institute / company
ARP-B ARP-C	56 57	825 MB	FMI, Finland
ARP-B ARP-C	57 57	833 MB	FMI, Finland
ARP-B ARP-C	43 43	629 MB	FMI, Finland
ARP-B ARP-C	57 56	811 MB	FMI, Finland
OHP-C	7	1.74 GB	Wuhan University, China
ARP-A ARP-B	14 14	163 MB	FMI, Finland
OUV-A OUV-AB	2041 Selected subset: ERYDD, DNADD, PLADD, VITDD, UVADD, UVBDD, UVI Region: global (8.04 GB in total)		Wuhan University, China
ARS-B ARS-C	440 439	905 MB	AUTH, Greece
ARS-B ARS-C	240 235	492 MB	AUTH, Greece
OHP-B	1	248 MB	Forschungszentrum Jülich, Germany
OHP-A	1	370 MB	Ghent University, Belgium
OHP-A	1	370 MB	Ghent University, Belgium
ARS-B	14	14.4 MB	Indian Institute of Science
OHP-B	1	252 MB	Forschungszentrum Jülich, Germany
OHP-A	15	3.57 GB	Forschungszentrum Jülich, Germany
OHP-B	1	249 MB	Forschungszentrum Jülich, Germany
OHP-A	2	487 MB	Forschungszentrum Jülich, Germany
MAY			
Product type	Number of products	Order size	Institute / company
OUV-BC	61 Selected subset: UVADD, UVBDD, UVI Region: 18.0E – 29.0E, 53.0N – 61.0N (1.87 MB in total)		Latvian Environment, Geology and Meteorology Centre

OUV-AB OUV-B OUV-BC	1826 Selected subset: ERYDD Region: global (1.11 GB in total)		Wuhan University, China
OUV-A OUV-AB OUV-B OUV-BC	6183 Selected subset: ERYDD, UVBDD Region: 24.0W – 10.0E, 22.0N – 42.0N (248 MB in total)		University of Manchester, UK
ARP-B ARP-C	156 156	2.26 GB	FMI, Finland
OHP-C	273	68.3 GB	East China University of Science and Technology
OHP-A OHP-B	29 29	21.2 GB	University of Tehran, Iran
OHP-B	1	375 MB	University of Tehran, Iran
OHP-C	3	752 MB	University of Tehran, Iran
ARS-B ARS-C	12040 12049	24.8 GB	NAITEC, Spain
ARP-B ARP-C	12040 12049	171 GB	NAITEC, Spain
<b>JUNE</b>			
<b>Product type</b>	<b>Number of products</b>	<b>Order size</b>	<b>Institute / company</b>
ARS-B ARS-C	441 438	913 MB	AUTH, Greece
ARS-B ARS-C	185 185	384 MB	AUTH, Greece
ARP-B	1772	12.9 GB	AUTH, Greece
ARP-C	1766	12.9 GB	AUTH, Greece
OUV-BC	31 Selected subset: UVADD, UVBDD, UVI Region: 18.0E – 29.0E, 53.0N – 61.0N (964 kB in total)		Latvian Environment, Geology and Meteorology Centre
ARP-A ARP-C	14 14	188 MB	AUTH, Greece
ARP-C	1	6.97 MB	AUTH, Greece
ARS-C	1	1.03 MB	AUTH, Greece
ARP-B ARP-C	142 142	1.95 GB	AUTH, Greece
ARS-B ARS-C	142 142	294 MB	AUTH, Greece
ARS-A ARS-B	2 1	2.77 MB	Private Individual, France



**APPENDIX 2**

Table A.3 presents a detailed summary of failed product orders from AC SAF archive at FMI during the reporting period. The middle column indicates whether the failure was related to problems with AC SAF archive and/or ordering system or was the problem on the user’s side.

**Table A.3. Summary of failed product orders during the reporting period**

Date	Error type	Failure description and details
		Order ID: User institute: Order contents: Ordering log error message: Failure description: Corrective action: Final outcome: